University of Miami
Scholarly Repository

Open Access Theses | Electronic Theses and Dissertations

2008-01-01

Experimental Evaluation of Full Scale I-Section Reinforced Concrete Beams with CFRP-Shear Reinforcement

Christian Aquino
University of Miami, c.aquino@umiami.edu

Follow this and additional works at: https://scholarlyrepository.miami.edu/oa_theses

Recommended Citation
Aquino, Christian, "Experimental Evaluation of Full Scale I-Section Reinforced Concrete Beams with CFRP-Shear Reinforcement" (2008). *Open Access Theses*. 162.
https://scholarlyrepository.miami.edu/oa_theses/162

This Open access is brought to you for free and open access by the Electronic Theses and Dissertations at Scholarly Repository. It has been accepted for inclusion in Open Access Theses by an authorized administrator of Scholarly Repository. For more information, please contact repository.library@miami.edu.

www.manaraa.com

UNIVERSITY OF MIAMI

EXPERIMENTAL EVALUATION OF FULL SCALE I-SECTION REINFORCED CONCRETE BEAMS WITH CFRP-SHEAR REINFORCEMENT

By

Christian Aquino

A THESIS

Submitted to the Faculty
of the University of Miami
in partial fulfillment of the requirements for
the degree of Master of Science

Coral Gables, Florida

December 2008

www.manaraa.com

©2008
Christian Aquino
All Rights Reserved

www.manaraa.com

UNIVERSITY OF MIAMI

A thesis submitted in partial fulfillment of
the requirements for the degree of
Master of Science

EXPERIMENTAL EVALUATION OF FULL SCALE I-SECTION REINFORCED CONCRETE BEAMS WITH CFRP-SHEAR REINFORCEMENT

Christian Aquino

Approved:

Antonio Nanni, Ph.D., P.E. Professor and Chair of the Civil Architectural and Environmental Engineering Department	Terri A. Scandura, Ph.D. Dean of the Graduate School
Ronald F. Zollo, Ph.D., P.E. Professor of the Civil, Architectural and Environmental Engineering Department	Fabio Matta, Ph.D. Research Assist. Professor of the Civil, Architectural and Environmental Engineering Department
Carol DiLaurenzio Hays, Ph.D., P.E. Engineering Analytics, Inc.	

www.manaraa.com

AQUINO, CHRISTIAN (M.S., Civil Engineering)

Experimental Evaluation Of Full Scale
I-Section Reinforced Concrete Beams
With CFRP-Shear Reinforcement

(December 2008)

Abstract of a thesis at the University of Miami.

Thesis supervised by Professor Antonio Nanni.
No. of pages in text. (110)

Fiber reinforced polymer (FRP) systems have shown great promise in strengthening reinforced concrete structures. These systems are a viable option for use as external reinforcement because of their light weight, resistance to corrosion, and high strength. These systems, externally bonded in the form of sheets or laminates, have shown to increase the flexural and more recently the shear capacity of members. Major concerns of the system are issues related to the bond strength and premature peeling especially when reentrant corners are present. The objectives of this study were to verify the effectiveness of carbon FRP (CFRP) laminates on an I-section beam with no anchorage and to determine the feasibility of using an anchorage system to prevent premature debonding. The two types of anchorage systems used were a horizontal CFRP laminate and glass FRP (GFRP) spikes. These anchorage systems verified that the use of anchorage on I-shaped beams can prevent premature debonding of the laminate and allow the specimens to achieve a higher shear capacity. Recommendations for future research of such systems are also presented.

www.manaraa.com

ACKNOWLEDGMENTS

I would like to express my gratitude to all those who helped me in fulfilling the tasks of this project. I would like to thank my professor and advisor Dr. Antonio Nanni for providing me with knowledge and advice throughout the duration of the project. I would like to thank the other members of the committee: Dr. Fabio Matta for helping me with the experimental tests and providing advice throughout the project; Dr. Ronald Zollo for providing his advice, knowledge, and support in the lab; and Dr. Carol Hays for helping me with the experimental tests and providing her advice.

I would like to thank BASF for providing the materials used for testing and Mr. Walter Hanford for providing his knowledge and expertise.

I would also like to thank Mr. Candido Hernandez for providing support during delivery of the beams.

Finally, I would like to thank the graduate and undergraduate students of the Civil, Architectural, and Environmental Engineering Department for providing support throughout the project.

www.manaraa.com

TABLE OF CONTENTS

www.manaraa.com

www.manaraa.com

LIST OF FIGURES

www.manaraa.com

www.manaraa.com

www.manaraa.com

LIST OF TABLES

www.manaraa.com

CHAPTER 1

INTRODUCTION

1.1 GENERAL

Over the years, externally bonded Carbon Fiber Reinforced Polymer (CFRP) Laminates have become an effective alternative to repairing damaged and deficient concrete structures. In many cases, rehabilitating with CFRP systems provides a more economical and technically superior alternative to traditional techniques, such as steel and cementitious materials, due to less labor and equipment requirements. In addition, CFRPs have become a viable choice due to their resistance to corrosion and high strength to weight ratio. Today, CFRPs have become increasingly popular within the transportation infrastructure (Bakis et al. 2002).

Numerous research studies have shown that the use of externally bonded CFRP laminates can substantially increase the flexural, shear, and compressive strength of concrete members. In Chapter 2, the literature review summarizes a selection of research studies on the use of CFRP in shear for strengthening of concrete beams as well as a summary of available design standards that are relevant in justifying this research project. However, there is a lack of knowledge on the use of CFRP laminates for shear strengthening of I-shaped concrete beams. Based on the information presented in Chapter 2, the intent of this research project is defined.

1.2 SIGNIFICANCE

This research project intends to investigate the behavior of a full-scale flexural member requiring shear strengthening, which has the shape of a bulb-T girder. Because

www.manaraa.com

of the presence of the bulb (Figure 1.2), the CFRP laminates that are externally bonded need to be investigated. In order to better understand this behavior, reinforced concrete (RC) beams that present shear failure prior to bending failure will be tested. Since bulb-T girders are typically made of prestressed concrete (PC) and the beams being tested are RC for ease of fabrication, differences in the shear response between RC and PC beams must be noted so that a meaningful extrapolation can be made.

The primary differences between RC and PC beams are the shear capacity that can be achieved and the crack pattern. In the case of a PC beam, the combined action of axial load, flexure, and prestressing are taken into account in the shear design (NCHRP Report 549). The use of prestressed strands allows for a higher capacity and longer spans by adding an axial force that offsets the tensile stress in the beam. Also, in PC beams, higher strength concrete is generally used. These factors contribute to the crack pattern of the beam. In a PC beam, there is a significantly larger amount of shear cracks that form in the web and the widths of the cracks are generally small. Also, the cracks form at an angle of about 60 degrees (Nilson et al. 2004). In the case of RC beams, the capacity and span lengths are considerably lower than what can be achieved through a PC beam. The crack pattern is also significantly different. RC beams tend to have fewer cracks, however, crack widths are wider than that of a PC beam and the cracks tend to form at an angle of about 45 degrees (Nilson et al. 2004). Flexure cracks are also much more evident in RC beams because they do not have an axial force that is resisting the tensile stress like a PC beam does. It must be kept in mind that the crack patterns are affected by the amount of tensile and shear reinforcement used. Differences in crack pattern can affect the behavior of the CFRP system.

www.manaraa.com

An RC beam was chosen because it was not the intent of this research project to study methods of increasing the beam's strength. The main area of study was on determining an anchorage scheme that can prevent premature debonding of the CFRP laminates. RC beams were used because they presented a worst case scenario for the laminates due to wider cracks and the 45 degree angle at which they form. This allows for a greater contribution from of the CFRP laminate to be engaged whereas in a PC beam the cracks are smaller and less of the laminate is engaged. Premature debonding should occur sooner in a RC beam because the laminate has to bridge a wider crack. Therefore, the results obtained for an RC beam can be applied to a PC beam due to the fact that an RC beam presents the worst case scenario in terms of CFRP laminate debonding. However, it is recognized that the 60 degree angle in a PC beam decreases the effectiveness of the CFRP laminate because the direction of the principal stress is not the same as in an RC beam. The contribution of the FRP system to the shear strength of a member is based on the fiber orientation and an assumed crack pattern (Khalifa et al. 1998). Therefore, the ideal fiber orientation of the laminate should be perpendicular to the crack so that the fiber direction is in the same direction as the principal stress. As the angle of the principal stress changes from being parallel to the fiber orientation, the effectiveness of the laminate decreases. The laminate no longer experiences a principal stress in one direction but a stress that has two components (directions). This is illustrated in Figure 1.1.

www.manaraa.com

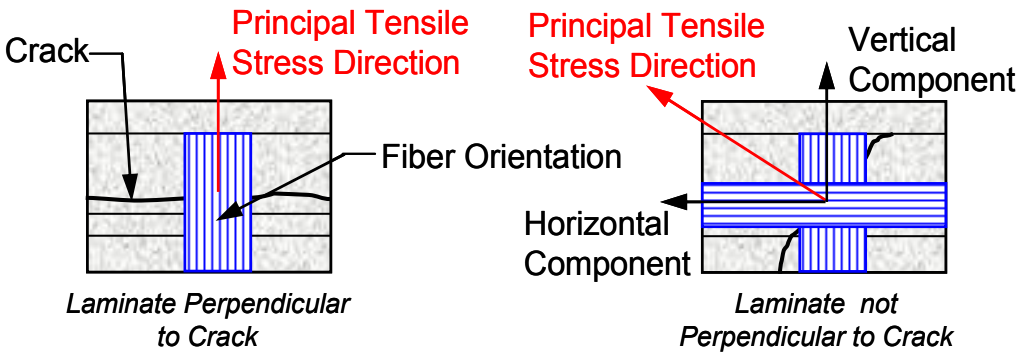

Figure 1.1 – Stress Direction at Location of a Crack

The laminate has no tensile strength perpendicular to the fiber orientation. Therefore, an RC beam will be tested with both a horizontal and vertical laminate in order to address the issue of a crack that forms at about 60 degrees in a PC beam that further reduces the effectiveness of the laminates. The combination of a horizontal and vertical laminate is used to address the issue of a two component stress, as shown in Figure 1.1, for a laminate not perpendicular to the crack. The horizontal laminate will also provide anchorage of the vertical laminate.

The use of an RC beam allows for the development of shear cracks at a lower load than that of a PC beam and allows the use of a lower capacity testing frame.

In previous research aimed at determining the efficiency of shear strengthening with CFRP laminates, failure often occurred due to debonding of the CFRP laminates. This mode of failure of the laminate has been observed to occur due to the loss of aggregate interlock in the concrete which results in a large shear crack. When a crack forms, high tensile stresses are developed in the portion of the CFRP laminate that bridges the crack. As the crack continues to grow, stress in the laminate continues to increase. These tensile stresses must be transferred to the concrete through the bond

www.manaraa.com

interface (Khalifa et al. 1998). Debonding of the laminate occurs when failure of the bond between the laminate and concrete substrate occurs before CFRP rupture. This occurs due to the fact that since the laminate has a high modulus of elasticity, the stress in the laminate can not increase indefinitely and must be released or transferred somewhere else. This stress is released by debonding that occurs at the crack edge and propagates throughout the laminate causing failure of the system. In the case of an I-section beam, failure due to debonding has been observed to occur where the bulb meets the web (Hutchinson et at. 1999). This type of debonding is illustrated in Figure 1.2.

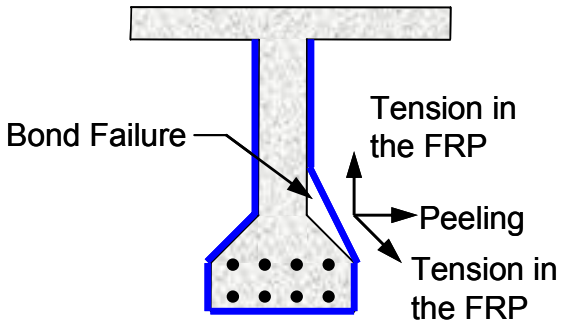

Figure 1.2 – Failure Mode

As illustrated in the figure, the laminate experiences two different types of stresses that cause debonding. The tension (axial stress) in the CFRP, due to shear in the concrete, results in the peeling stress due to the straightening effect the laminate is experiencing that is caused by the reentrant corner in the bulb shape. It is this additional stress component that causes the bond strength to be exceeded resulting in premature failure of the system. This type of failure mechanism has not been studied thoroughly and characterized, nor have practical mitigation measures been devised and validated. Due to the anticipation of debonding, it is important to study the use of anchorage as a means to prevent premature debonding of the CFRP laminates.

www.manaraa.com

1.3 OBJECTIVES OF THE RESEARCH

The objectives of this research project are as follows:

a) Verify the effectiveness of externally bonded CFRP laminates for shear strengthening applied onto a bulb-shaped beam with no anchorage.

b) Determine the constructability and structural efficiency of different anchorage systems that allow the bonded CFRP laminates to be better utilized.

1.4 METHODOLOGY OF THE RESEARCH

The methodology for the research stated is as follows:

1. **Design of the Specimens and Test Matrix.** This first task required the design of the specimens to be used in the research. Once a design was complete, the test matrix could be developed. This matrix was based on how each beam was going to be externally reinforced with CFRP laminates and anchorage.
2. **Manufacturing and Prepping of the Specimens.** A local pre-cast concrete manufacturer was enlisted for construction of the beams. Logistics were planned for the delivery of the specimens to the testing facility. Once the specimens arrived to the testing facility a plan was developed for application of the external CFRP reinforcement.
3. **Testing of Full-Scale Beams.** Testing was carried out in the Civil, Architectural, and Environmental Engineering Department's structural lab at the University of Miami in Coral Gables, Florida. The specimens were tested, in four-point bending, under displacement control using a 200 kip (890 kN) actuator. Data collected included applied load, displacement via direct current

www.manaraa.com

displacement variable transformer (DCVT) sensors, and strain in the concrete and external CFRP reinforcement via strain gauges and pi-gauges.

4. **Analysis of Test Results.** Analysis of the data collected during testing consisted of comparing strengthened specimens to the un-strengthened (control) specimen. In order to establish and compare the effectiveness of each test, moment capacities, strain in the concrete and CFRP laminates at chosen locations, and midspan deflections were used as key indicators. Based on the analysis of the data collected design recommendations and further research needs are presented.

www.manaraa.com

CHAPTER 2

LITERATURE REVIEW

2.1 OVERVIEW

This chapter discusses current methods used in strengthening RC beams in the shear region using external CFRP reinforcement. The literature review examines the relevant aspects of the methods used in strengthening RC beams in shear. Furthermore, it presents results of past research of strengthened beams that includes behavior and failure modes of the strengthening system. Based on these results and by also identifying gaps in the research, conclusions can be made on the effectiveness of the research project being undertaken. Also, a review of available design codes and their use in this project is discussed.

2.2 SHEAR STRENGTHING OF BEAMS

2.2.1 BACKGROUND

Numerous research projects have been undertaken to study the behavior of RC beams strengthened in shear using externally bonded CFRP laminates. The research projects presented in this section are divided into two sub-sections: General and Relevant. The research projects presented in the "General" section were chosen to provide a general background, overview of the different types of external shear reinforcement schemes devised, and to understand the failure mechanism of such systems. These research projects considered several different configurations for the externally bonded laminates. These configurations ranged from fully wrapping of CFRP laminates on all four faces of a rectangular beam to bonding CFRP onto the sides of the beam.

www.manaraa.com

The research projects presented in the "Relevant" section pertain to projects that are similar to the current research project being undertaken in regards to geometry and the use of anchorage. The projects chosen are also samples of research projects that are considered as pioneering by providing the basis for future projects and design standards. These research projects focus on the behavior of externally reinforcing RC flexural members, such as T-beams, in shear and the use of anchorage to prevent straightening of the laminate and debonding. Most of the specimens in each research study were tested using four-point loading.

2.2.2 RESEARCH PROJECTS: GENERAL

Chaallal et al. (1998) investigated the use of unidirectional CFRP laminate strips, which had a width of 2 inches (50 mm), in different angles to strengthen rectangular RC beams in shear. Three groups of specimens were tested. The first set of beams had internal shear reinforcement and were the control specimens, the second set was under-reinforced with internal shear reinforcement, and the third set was also under-reinforced with internal shear reinforcement but were retrofitted with the external CFRP laminate strips at 90 and 45 degrees to the horizontal. The CFRP laminates were only applied to the two vertical faces of the beams. The tests showed an increase in strength of 70% and increased stiffness for the retrofitted specimens. Failure of the retrofitted specimens occurred due to shear cracking, which produced severe delamination of the CFRP laminates. The investigation also concluded that the diagonal CFRP laminates outperformed the vertical side laminates for shear strengthening. However, diagonal laminates may produce premature failure as a result of delamination starting from the

www.manaraa.com

tension stress region. Therefore, CFRP U laminates should be used in cases of extreme loading because U laminates minimize the effect of stress concentrations.

Triantafillou (1998) also investigated the use of CFRP laminate strips in different angles to strengthen rectangular RC beams. Three groups of specimens were tested. The first set of beams were used as the control specimens, the second set had the CFRP strips applied at 45 degrees to the horizontal, and the third set had the CFRP strips applied at 90 degrees to the horizontal. Internal steel reinforcement was not included in the three groups in order to force shear failure. The investigation concluded that retrofitted specimens had an increase in shear strength that ranged from 65 to 95% compared to the control specimen. Failure of the specimens was due to shear cracking which caused delamination of the CFRP strips. Furthermore, the investigation concluded that CFRP strips applied at 45 degrees to the horizontal were more effective than the vertical strips because the fibers were almost nearly perpendicular to the shear cracks.

Khalifa et al. (1998) reviewed current research on shear strengthening with FRP so that design algorithms can be proposed for computing the contribution of FRP to the shear capacity of an RC member. The research proposed two design approaches for determining the shear contribution. The first was based on effective FRP stress because previous research by Triantafillou (1998) showed that CFRP rupture occurs at a stress level below the ultimate strength of the CFRP due to stress concentrations. This design approach is similar to the approach used for steel shear reinforcement and is a function of FRP stiffness and ultimate strain. This approach is governed by a rupture point and fracture of the CFRP sheet instead of a yield point as in steel. The second approach was

www.manaraa.com

based on bond mechanism. This approach considers the effects of concrete strength and the bonded surface configuration due to the delamination failure mode. As stated earlier, delamination occurs due to failure of the bond interface between the laminate and concrete. These two design approaches are combined and result in a method that is consistent with design procedures of the American Concrete Institute 318 (ACI 318). Also, these approaches have been used to formulate the shear contribution due to FRP, V_f, that is presented in the ACI 440 design guidelines.

2.2.3 RESEARCH PROJECTS: RELEVANT

Hutchinson et al. (1999) investigated the use of CFRP laminates to strengthen AASHTO bridge girders in shear. Various types of configurations were used for strengthening the beams. Beams were strengthened by applying the CFRP vertically and diagonally at 45 degrees to the horizontal, diagonally with a horizontal sheet on top for anchorage, and diagonally with clamps for anchorage. The clamping scheme was in the form of a tubular steel section that ran along where the stem of the beam met the bulb. This was then bolted to the beam with a thru-bolt. This is illustrated in Figure 2.1.

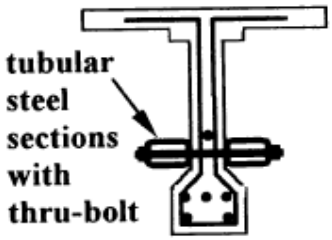

Figure 2.1 – Clamping Scheme (Hutchinson et al. 1999)

The beams were also strengthened in flexure in order to increase the flexural capacity. The investigation concluded that all beams failed in shear with inclined shear

www.manaraa.com

cracks occurring typically at 30 degrees. For all the beams retrofitted with CFRP sheets, the concrete remained bonded to the sheets over most of the beam at failure. This indicated that shear failure occurred in the concrete substrate rather than debonding of the sheets. The beams with the diagonal configuration showed straightening of the sheets due to the shape of the girder. As a result of this, the diagonal sheets were not very effective and the increase in ultimate shear capacity was only 9 to 10%. For the diagonal with horizontal sheet configuration, an increase of 16% was seen in shear capacity. Also, straightening of the CFRP sheets was not as extensive as the beams that were just strengthened with diagonal sheets. For the diagonal sheets with clamps, an increase of 28% in ultimate shear capacity was achieved but this does not represent the full potential of the configuration since failure of the beam occurred outside of the strengthened zone. Furthermore, the clamping scheme used effectively controlled the straightening of the diagonal sheets.

Deniaud et al. (2001) investigated the effect externally bonded FRP laminates had on RC T-beams. The research tested a total of four full-scale T-beams that had a length of 12 feet (3.7 m), a depth of 23-5/8 inches (600 mm), and had internal shear reinforcement in the form of closed steel stirrups. However, two tests were conducted per beam by only testing one shear span at a time, making a total of eight beams tested. This was done by providing external steel stirrups to strengthen the shear span that was not being tested ensuring that only the tested shear span would fail. The beams were designed to provide a flexural capacity much greater (between 2.0 and 3.5 times) than the shear capacity before being externally reinforced. The experimental program consisted

www.manaraa.com

of three control specimens and five externally reinforced specimens. This matrix is shown in Figure 2.2 along with the test setup in Figure 2.3.

Table 2—Test matrix of T600 series

Specimen	Stirrup spacing, mm	External FRP reinforcement
T6NS	None	None
T6NS-C45	None	Carbon sheets Replark Type 20 at 45 degrees (50 mm wide, 50 mm gap)
T6S4	400	None
T6S4-C90	400	Carbon sheets Replark Type 20 at 90 degrees (50 mm wide, 50 mm gap)
T6S4-G90	400	Glass fibers SEH51 at 90 degrees (no gap)
T6S4-Tri	400	Triaxial glass fibers (no gap)
T6S2	200	None
T6S2-Tri	200	Carbon sheets Replark Type 20 at 90 degrees (50 mm wide, 50 mm gap)

Figure 2.2 – Test Matrix (Deniaud et al. 2001)

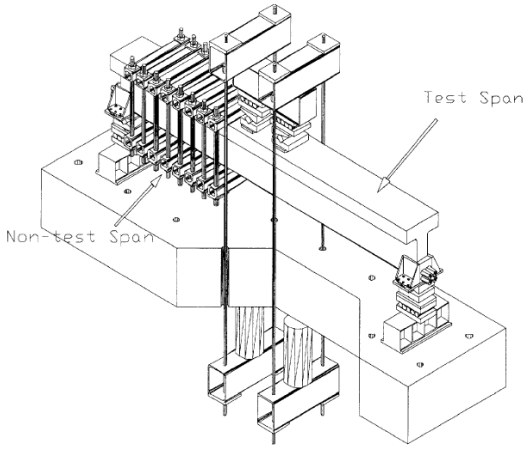

Figure 2.3 – Test Setup (Deniaud et al. 2001)

For the externally reinforced specimens, the FRP was extended underneath the flange to provide a minimum anchor of 4 inches (100 mm) and wrapped under the web forming a U-wrap.

www.manaraa.com

The investigation concluded that increasing the amount of internal reinforcement reduced the net increase of shear capacity due to the FRP laminates. For example, the CFRP laminates increased the shear capacity by 94% for the specimen with no steel stirrups but for the specimen with stirrup spacing of 15.7 inches (400 mm) the CFRP only increased the shear capacity by 78%. In the case where the stirrups were spaced 7.8 inches (200 mm) and external reinforcement was provided, the beam did not reach the maximum load of the control specimen. Therefore, FRP laminates are less effective when beams are heavily reinforced internally and in some cases can reduce the shear capacity by changing the critical shear path causing an even more sudden shear failure. The FRP changed the critical shear path by increasing the web crack angle in the same manner adding more internal reinforcement does. It was also found that the strain measured in the fibers that crossed a concrete crack was uniformly distributed among those fibers. Deniaud et al. (2001) observed that this differed from the linear strain distribution assumption made by others and previous research conducted by the authors. The failure modes of all the specimens were the same and resulted from debonding and peeling of the laminates. The debonding began where a web shear crack crossed a laminate and when further load was added peeling would occur resulting in total failure of the specimen. It was also observed that some of the internal stirrups had unexpectedly failed. It is believed that the reason for this is when the CFRP failed the energy that was released and transferred to the steel stirrups caused them to snap.

Bousselham et al. (2006) investigated the behavior of externally reinforcing RC T-beams in shear with CFRP laminates. The authors noted that some parameters that

www.manaraa.com

influence the shear resistance mechanism have not been sufficiently studied. These parameters are the shear steel reinforcement, or transverse steel, and shear span to depth ratio (a/d). The experimental program consisted of 22 tests performed on 11 full scale T-beams. This was accomplished by testing the specimens simply supported in three-point loading and having one of the ends of the beam overhung. This allowed for one beam end zone to be tested while the other end was overhung and unstressed. This is illustrated in Figure 2.4. Units are in millimeters.

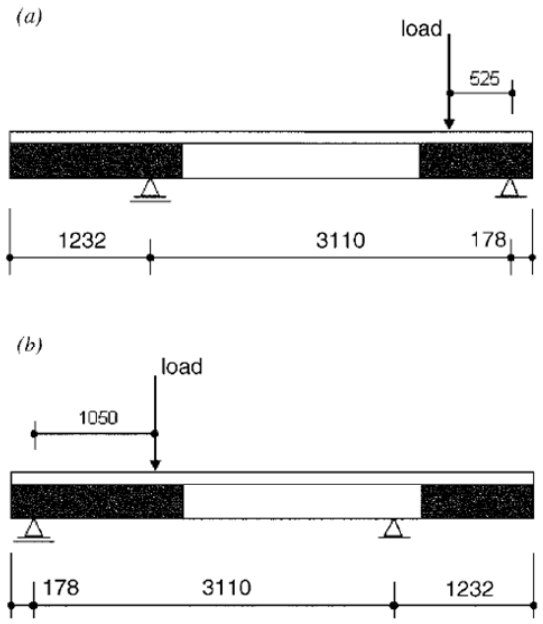

Figure 2.4 –Test Setup (Bousselham et al. 2006)

The total length of the beams is 14.8 feet (4520 mm) with a total depth of 16 inches (406 mm). The experimental program called for control specimens with no internal shear reinforcement, specimens with internal shear reinforcement spaced at d/2 and d/4 where d = 13.8 inches (350 mm), and specimens with the same increments of internal shear reinforcement but now externally reinforced with CFRP bonded layers of

www.manaraa.com

0.5, 1, and 2. These bonded layers represent a thickness of 0.002, 0.004, and 0.008 inches (0.06, 0.107, and 0.214 mm) respectively. The CFRP laminates are bidirectional, applied continuously over the test region in the shape of a U-wrap. Also, these specimens are split into two groups: deep beams and slender beams. The deep beams have an a/d of 1.5 and the slender beams have an a/d of 3.0. This test setup was a simple way to conduct slender and deep beam tests with the same specimen.

Overall, the contribution of the CFRP to the shear resistance was found to be greater for deep beams with no transverse steel than the corresponding slender beams. The gain in shear resistance for the deep beam was 62% and for the slender beam was 50%. When transverse steel is included, the total gain in shear resistance decreases drastically to an average of 15%. This behavior confirms the observations made in previous research studies such as Deniaud et al. (2001). The authors also noted that doubling the thickness of the CFRP did not lead to a significant increase in additional shear capacity as anticipated. For example, a specimen with no transverse steel and one layer of CFRP had a gain of 47.7% whereas a specimen with transverse steel and two layers of CFRP had a gain of 49.8%. However, even though no significant increase was observed, the authors noted that the gain in shear resistance due to the CFRP was dictated by the concrete strength rather than the FRP stiffness. Furthermore, the performance of the FRP was limited due to premature debonding because of the high FRP stiffness.

All of the beams tested failed in shear except for those that were slender beams with transverse steel spacing of d/4. It was observed that for the deep beams, a principal crack formed from the support to the load point, which is typical in deep beams, along

www.manaraa.com

with other fine cracks. For the slender beams, the cracking pattern depended on the amount of transverse steel but followed the general pattern from support to load point. Also, significant flexural cracking was observed in the slender beams. What varied the most was the angle and amount of the cracks. The specimens with transverse steel spacing of d/2 had cracks that were at a greater angle and widespread when compared to the control. The crack pattern for the slender beams allowed for more of the laminate to be engaged because it had to bridge wider and larger amount of cracks. Thus, the effectiveness of the laminate to bridge cracks and increase shear strength could be investigated.

For the specimens that had the continuous wrap, once the CFRP was carefully removed, it was observed that the concrete was completely pulverized due to the CFRP confining the concrete which subjected it to stresses well beyond its compressive unconfined strength. In the deep beams, one principal crack was also observed from the support to the load point. The authors concluded that neither the crack pattern nor the crack angle was modified due to the CFRP systems. Also, in respect to the strain in the internal steel reinforcement, it was observed that the internal shear reinforcement had much more strain when the CFRP was not present than when it was. Thus, the CFRP eased the strain in the steel. Finally, the authors compared the results to that of design codes and concluded that the prediction made by the codes did not capture major aspects such as the transverse steel, the FRP stiffness, and the ratio a/d.

Eshwar et al. (2008) investigated the performance of two anchor systems for externally bonded FRP laminates applied through wet layup. In the past, steel bolts and

www.manaraa.com

plates have been used to anchor the FRP laminates (Sato el al. 1997, Swamy et al. 1995 & Taljsten 1997). Steel anchors have been shown to be usually impractical for field applications due to the possibility of corrosion and stress concentrations. Therefore, the author investigated the validity of using an anchor system made of FRP material. The first anchor system was made by making a groove onto the specimen. Then, a GFRP bar is inserted with the wet layup laminate into the groove and filled with epoxy forming the anchor. The anchor was also tested using different groove sizes. The other anchor system used is a glass FRP (GFRP) spike. This spike was 4 inches (101.6 mm) long which had 2 inches (50.8 mm) that was pre-impregnated in resin. This spike is then inserted into a hole that is drilled through the laminate and concrete. The unsaturated end is then spread out onto the laminate and impregnated with resin (see Chapter 5 for detailed procedure). Figure 2.5 illustrates the first anchor system and Figure 2.6 shows a picture of the GFRP spike.

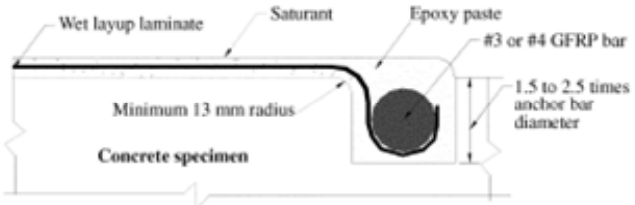

Figure 2.5 – End Anchor (Eshwar et al. 2008)

Figure 2.6 – GFRP Spikes (Eshwar et al. 2008)

www.manaraa.com

In total, sixteen plain concrete T-beams were cast and strengthened externally using CFRP wet layup laminate. The beams had a span of 42 inches (1050 mm) and total length of 48 inches (1200 mm). The external laminates had a width of 2 inches (50 mm). A groove with a depth of 2 inches (50 mm) was saw cut into the beam at midspan to ensure a crack would form at the specific location. A hinge 2 x 2 inches (50 x 50 mm) was also placed on the top midspan so that the distance between the internal compression and tension forces remain constant. To simulate a reentrant corner, a bump-out measuring 3 x 3 inches (76 x 76 mm) was cast 8 inches (200 mm) from the center of the beam. Specimens were then reinforced by placing the laminate and placing the end anchor either before or after the reentrant corner. The size of GFRP bar used in the anchor was 0.4 inches (10 mm). Spike anchors with the same diameter of the No. 3 bar were used. The spike anchors were tested to determine the shear load the spike could resist. This was done by placing RC blocks on both ends of a hydraulic jack. The blocks were then connected externally with two plies of CFRP laminate. The size of the laminate was 32 x 4 inches (800 x 100 mm). On one side, a spike was inserted at the center of the block and on the other side two spikes were inserted on each block with spacing of 2 inches (50 mm). An example of both setups is illustrated in Figure 2.7. All dimensions are in millimeters.

www.manaraa.com

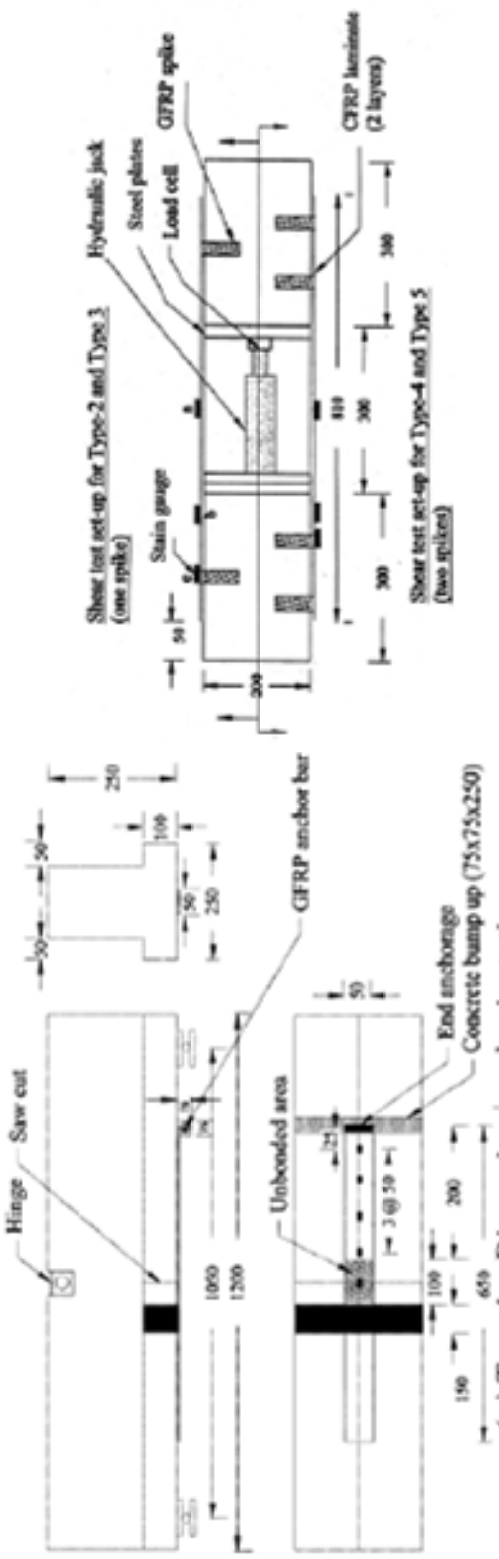

Figure 2.7 – Anchor Test Setup (Eshwar et al. 2008)

www.manaraa.com

The failure mode observed during testing was either anchor pullout or FRP rupture. The end anchor helped to prevent failure of the FRP system. Maximum strain levels at the midspan ranged from 9,000 to 12,000 με and due to the end anchorage, strain recorded at the ends were considerably higher with the increase in ultimate capacity. The location of the anchor also proved to have an influence on the capacity. Specimens that had anchors after the reentrant corner showed about 40% higher strength than those with the anchor before the reentrant corner. The author noted that a possible reason for this was the presence of stress concentrations caused by the laminate being inserted into the groove. Therefore, the author recommended that the minimum groove size range be 1.5 or 2.5 times the anchor bar diameter and minimum bar size of No. 3 GFRP. Also, the size of the groove influenced the ultimate capacity. Larger grooves reduced the stress concentration enabling the anchor to achieve higher capacities.

In the case of spike anchors, an increase of 25% in ultimate capacity was recorded for one spike placed at the center of the laminate. It was observed that the presence of the spike delayed the potential of a debonding failure. It was also noted that different embedment depths of the spike did not significantly increase capacity. This was not true for the specimens tested with two spikes. In this case, the embedment depth of 3 inches (75 mm) alone had an influence of 10% to the ultimate capacity when compared to a depth of 2 inches (50 mm). Overall the embedment depth had a negligible effect on the ultimate capacity. Failure of these specimens was due to debonding of the CFRP laminate with a thick layer of concrete attached. Specimens with multiple spike anchors had an increase in ultimate shear capacity of 200% when compared to single spikes.

www.manaraa.com

When comparing the strain recorded during testing to ACI 440.2R, the authors concluded that the bond reduction coefficient, K_v, can be reduced to 0.25 from 0.75 when using spike anchors for shear following the specifications provided by this paper. The author recommends using a minimum spike diameter of 0.4 inches (10 mm) and a minimum embedment depth of 2 inches (50 mm).

2.2.4 CONCLUSIONS

The research projects summarized in the previous sections cover different techniques and configurations of externally bonded CFRP to strengthen damaged or deficient specimens. The specimens tested ranged from rectangular RC beams to PC I-shaped beams. The techniques and configurations of CFRP used included fully and partially wrapped specimens with laminates which had widths that ranged from 2 inches (50 mm) to 10 inches (250 mm), placed at different angles, and strips of laminates that were applied vertically and diagonally with and without anchorage. The behavior of individual anchor systems was also investigated.

The research conducted by Deniaud et al. (2001) and Bousselham et al. (2006) used specimens that had internal shear reinforcement. In both research projects, the contribution of FRP to shear strength (V_f) decreases as the contribution of internal shear reinforcement (V_s) increases. This observation is similar to what other researchers have observed (Bousselham and Chaallal 2004, Khalifia and Nanni 2002, Pellegrino and Modena 2006). A possible explanation for this behavior is that as the internal shear reinforcement is increased, more strain is carried by the internal shear reinforcement

www.manaraa.com

reducing the amount that is carried by the FRP laminate, thus, reducing its shear contribution (Pellegrino and Modena 2006). This is based on the assumption that the internal shear reinforcement did not yield. Also, the total contribution of V_s and V_f can not exceed $4V_c$ (ACI 440.2r-08). The reason for this is because when the contribution of V_s, V_f, or the combination of both exceeds $4V_c$, crushing of the concrete compressive strut (web-crushing) occurs. This is observed in the aforementioned projects. As the internal shear reinforcement is increased, the total shear contribution approaches the limit; therefore, the contribution due to the external shear reinforcement is reduced. Recognizing these issues, the RC beams tested in this project did not have internal shear reinforcement because the intention of the project was to investigate the use of anchorage schemes to prevent premature debonding.

Deniaud et al. (2001) experimented with an anchorage scheme. This scheme consisted of extending the FRP laminate 4 inches (101.6 mm) underneath the beam. This, however, is not a very effective way to provide anchorage. The reason for this is because the laminate is being wrapped around an inside corner causing stress concentrations. The laminate underneath the flange does not experience a tensile force but rather a peeling force. This is because the tensile force in the laminate that is on the web pulls on the 4 inch (101.6 mm) piece that is underneath the flange causing it to peel off. General guidelines suggest that these types of details should be avoided. If these types of corners can not be avoided, then proper anchorage must be provided to ensure proper bond strength of the FRP laminate (ACI 440.2R-08). The laminate could be anchored by inserting it into the slab with a near surface mounted (NSM) bar (Khalifa et

www.manaraa.com

al. 1999). This peeling mechanism is illustrated in Figure 2.8. This is similar to what was observed by Hutchinson et al. (1999) and illustrated in Figure 1.2 for reentrant corners.

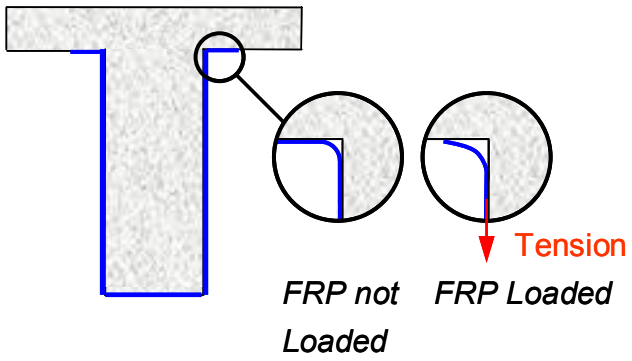

Figure 2.8 – Laminate Debonding at Inside Corner

In the research projects mentioned, failure mostly occurred due to debonding of the FRP system. The FRP was observed to fail in a brittle manner and in some cases caused failure of the internal shear reinforcement as a result of this sudden failure. The anchorage systems developed by Eshwar et al. (2008) showed that there are viable methods to anchor the FRP laminates and achieve greater capacities.

This research project being undertaken intends to not only further increase the amount of available data in shear strengthening of beams, but to develop and validate a system that utilizes available state of the art FRP technology and apply it to I-shaped beams. As seen in the research conducted by Hutchinson et al. (1999), a new mode of failure must be accounted for. Debonding of the vertical and diagonal CFRP laminates would begin at the location where the bulb meets the web. To mitigate this, mechanical anchorages were utilized in order to increase the efficiency of the laminates by

www.manaraa.com

preventing premature debonding, which led to failure, by means of a horizontal laminate or tubular steel section that were bolted onto the web. The research project to be undertaken builds upon the research by Hutchinson et al. (1999) and Eshwar et al. (2008) by first further investigating and validating the failure mode of the CFRP laminates applied to an I-beam that is deficient in its shear capacity. In many cases, flexure reinforcement is also added because the increase in shear strengthening can cause flexural failure. In this case, the specimens to be tested do not need flexural strengthening because the existing flexural capacity is significantly greater than the predicted shear capacity after strengthening. Thus, the experimental program is able to investigate the effectiveness of external shear reinforcement without the contribution of additional external flexural reinforcement. Furthermore, two different anchorage configurations are used. The first anchorage system to be used is a horizontal laminate that is applied along the joint of the bulb and web. The second is the use of glass FRP (GFRP) spikes inserted along the same joint. These two configurations allow for a shear strengthening system for I-shaped beams that is entirely composed of FRP technology rather than a combination of different materials.

2.3 DESIGN STANDARDS

The American Concrete Institute (ACI) has long established design and construction documents to guide in the design and construction of RC members. ACI has also expanded on its established documents by including a new guide for the design of RC and PC members strengthened with externally bonded FRP systems. This established guide is the ACI 440.2R-08 (ACI 2008). With an increase over the years in the use of

www.manaraa.com

FRP materials to repair and retrofit concrete structures, development of such a guide is ongoing around the world (ACI 440.2R-08). For simplicity, only documents from North America are used. Another such document that exists and has expanded to include the use of FRP materials is the Canadian Standards Association "Canadian Highway Bridge Design Code" (CAN/CSA-S6-06).

Before calculations can be formulated for the design of the FRP system, the characteristics of the specimen to be strengthened must be determined using ACI 318-05. Such characteristics are the flexural capacity and shear capacity due to concrete and stirrups, if applicable. Details into the calculations of such characteristics, specifically shear strength (V_c), for the specimens that will be tested in this project are outlined in Chapter 4. Once such characteristics are determined, design of the FRP system can be done using the ACI 440.2R-08.

The ACI 440.2R-08 not only lays out design procedures for FRP systems, but also gives background, typical material properties, construction guidelines, and guidelines for installation of the system. Such guidelines are exemplified for a beam with a rectangular cross section. When designing for shear strengthening, the guide suggests three reinforcement schemes. These schemes, illustrated in Figure 2.9, include full wrapping, 3-sided or U-wrapping, and 2-sided wrapping.

www.manaraa.com

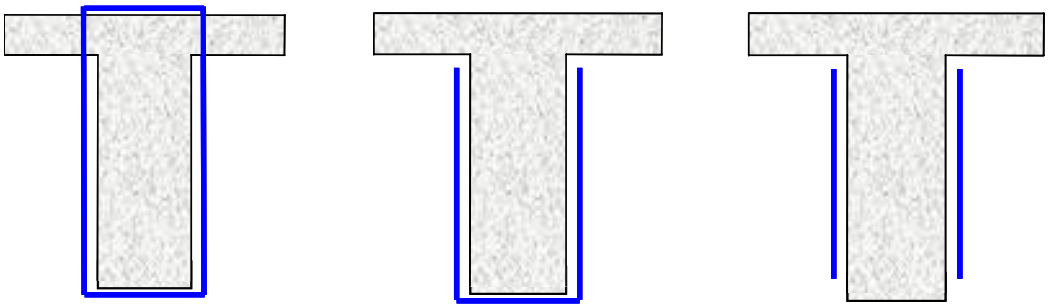

Figure 2.9 – Typical Shear Wrapping Schemes

According to the guide, the most efficient wrapping scheme is the full wrap but it is not always practical due to the presence of the slab. Therefore, it is recommended (although all three techniques have shown to improve shear strength) to use the U-wrap, followed by the 2-sided wrap in terms of efficiency. When using the U-wrap and 2-sided schemes, an area of concern is the bond performance because these systems are bond-critical applications. Delamination of the laminate has been observed to occur in the compression zone (top portion of beam) before the loss of aggregate interlock (ACI 440.2R-08). Another critical issue that affects the bond effect is the surface preparation (discussed in Chapter 5) and geometry of the specimen. The soundness and tensile strength of the concrete substrate limits the overall effectiveness of the bonded FRP system. The guide addresses these issues by applying a bond reduction factor and determining an effective bond length (furthered discussed in Chapter 4). Furthermore, it states that mechanical anchorage may be used as long as it is substantiated through testing. Effective strain in the FRP can not exceed 0.004 because failure would occur due to loss of aggregate interlock of the concrete. This has been observed to occur at fiber strains less than the ultimate fiber strain, therefore, the maximum strain used for design is

www.manaraa.com

limited (ACI 440.2R-08). As for changes in geometry such as inside corners and concave surfaces, special detailing must be made to ensure bonding of the system.

The CAN/CSA-S6-06 also addresses issues concerning FRP systems. In the case of using FRP materials for shear reinforcement, the code states that anchorage of the FRP laminate must be provided in the compression zone. This can be accomplished by running a horizontal FRP laminate or by embedding the vertical strips into the slab and anchoring them with an NSM bar (Khalifa et al. 1999). As an alternative to using anchorage, the code suggests fully wrapping the member.

2.3.1 CONCLUSIONS

Both the ACI 440.2R-08 and CAN/CSA-S6-06 provide guidelines and recommendations towards the design of externally bonded FRP systems. However, there are some issues that the documents addressed but did not elaborate on specifically. These issues are the types of effective anchorage schemes and the design of an FRP system on a member that has reentrant corners (i.e. I-shaped beam). ACI 440 says that anchorage can be used but it does not elaborate on the type of schemes. It also says that anchorage can be used as long as it is substantiated through testing. Furthermore, the guide just says that on the issue of reentrant or inside corners, special details must be made. In the case of theCAN/CSA-S6-06, the code states a specific method of providing anchorage by the use of a horizontal FRP laminate but does not elaborate on the issue of reentrant corners.

This research project intends to address these shortcomings. Testing of I-shaped specimens will address the issue of reentrant corners by characterizing the failure mode

www.manaraa.com

of the FRP system. The data collected will help in supporting ACI 440 that states that special attention needs to be given to reentrant corners in order to ensure bonding. In addition, testing of two different anchorage schemes will help in identifying viable anchorage techniques for FRP used to strengthen I-shaped beams. In essence, this research project aims at addressing the issue of reentrant corners and support design professionals by providing anchorage schemes and specifications that are viable in ensuring proper bonding.

www.manaraa.com

CHAPTER 3

CONSTRUCTION DETAILS AND MATERIAL PROPERTIES

3.1 OVERVIEW

This chapter provides test beam construction details including the materials used for manufacturing of the beams, by Precast Depot, and their properties. The CFRP material systems used to strengthen the beams, which were provided by BASF, are also detailed.

3.2 CONCRETE

The beam manufacturer used a nominal 4,000 psi (27.6 MPa) mix design that was supplied by a local vendor for construction of all specimens. The mix design used 4,000 psi (27.6 MPa) concrete based on one cubic foot (0.028 cubic meters), is shown in Table 3.1.

Table 3.1: Concrete Mix Design

Material	Quantity (per cubic foot/meter)
Type I Cement	470 lbs. (2.1 kN)
#67 Coarse Aggregate	1,580 lbs. (7.03 kN)
Natural Fine Aggregate	1,374 lbs. (6.1 kN)
Water	283 lbs. (1.26 kN)
Air Content Target %	4%
Air Entraining Agent	2.3 fluid oz. (68.01 ml)
Water Reducing Agent	18.8 fluid oz. (556 ml)

The coarse aggregate used in the mix design was limestone which is commonly used in Florida. In order to determine the compressive strength of the concrete, 2.75 x 5.5 inch (69.85 x 139.7 mm) cores were taken from each of the beams after testing. This was

www.manaraa.com

done so that the compressive strength at the time the beam was tested is known and more accurate comparisons can be made. Table 3.2 shows the compressive strength and the standard deviation of the cores tested.

Table 3.2: Core Compressive Strength

Specimen #	# of Cores	Average Strength (psi) [MPa]	STD (psi) [MPa]
B-1a	4	2,068 [14.3]	38 [0.26]
B-2a	5	1,850 [12.8]	150 [1.03]
B-2b	3	1,919 [13.2]	14 [0.1]
B-3a	5	1,850 [12.8]	82 [0.56]
B-4a	3	1,973 [13.6]	57 [0.39]

From this data, equivalent cylinder strengths are used in the analytical design calculations per Section 5.6.5 of ACI 318-05. The strength of concrete determined by the cores was significantly lower than what was expected. It is likely that the manufacturer added a significant amount of water to the mix lowering its compressive strength.

3.3 STEEL REINFORCEMENT

All of the beams were reinforced with two rows of four #7 (22.2 mm diameter) steel rebar in the tension region. 90 degrees bent #5 (15.9 mm diameter) steel rebar with a length of 8 in. (203.2 mm) and spaced at 12 in (304.8 mm) O.C. is used to insure load transfer between the flange and web of the beam. The flange is reinforced with 3 x 3 in. (76.2 mm x 76.2 mm) and 3/8 in. (9.53 mm) diameter steel wire mesh. Figure 3.1 shows a typical cross section of the beams being tested. Units are presented in inches. Full construction details are provided in Appendix A.

www.manaraa.com

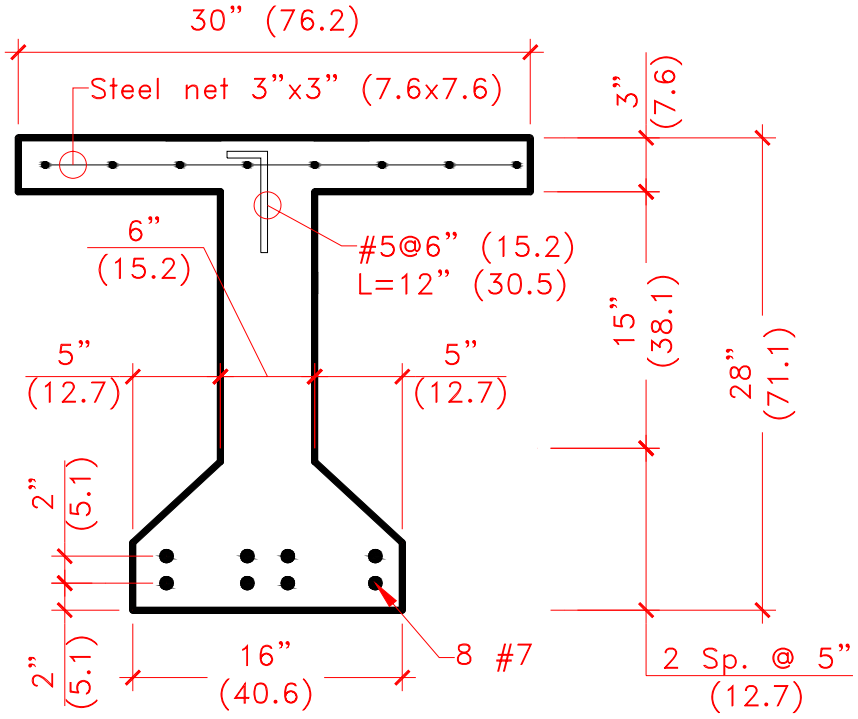

Figure 3.1 – Beam Cross Section
Note (SI conversion in cm)

3.4 FRP LAMINATE

The composite material system, provided by BASF, used for strengthening all the specimens in this research study consisted of MBrace CF 130 carbon fiber sheets that were impregnated with MBrace Saturant which is an epoxy encapsulating resin. Other materials used included MBrace Primer, and MBrace putty. The primer is used to enhance adhesion of the MBrace system to the concrete substrate. It penetrates the substrate's pores creating more surface area for bonding. Putty is used to fill any voids and smooth any offsets on the substrate. The saturant is used to impregnate the carbon fiber sheet and create a high strength laminate. It should be noted that the primer, putty, and saturant are two part chemicals and all are time-dependent once mixed so application was completed diligently and carefully. Procedures for installing the system are covered

www.manaraa.com

in Chapter 5. Table 3.3 shows the composite properties used for design and Table 3.4 shows the material properties as provided by the manufacturer. Coupon testing of the CFRP was not performed because its strength characteristics have been previously tested and validated (BASF 2008). Also, shear FRP reinforcement is not as sensitive to ultimate FRP strength as is flexural strengthening.

Table 3.3: Composite Properties

Material	Ultimate Tensile Strength (ksi) [GPa]	Nominal Thickness (in/ply) [mm/ply]	Tensile Modulus (ksi) [GPa]	Ultimate Rupture Strain
MBrace CF 130	550 [3.8]	0.0065 [0.165]	33,000 [227.5]	1.67%

Table 3.4: Material Properties

	Ultimate Strength (psi) [MPa]	Yield Strength (psi) [MPa]	Elastic Modulus (ksi) [MPa]	Rupture Strain
MBrace Primer	2,500 [17.24]	2,100 [14.5]	105 [724]	40%

	Ultimate Strength (psi) [MPa]	Yield Strength (psi) [MPa]	Elastic Modulus (ksi) [GPa]	Rupture Strain
MBrace Putty	2,200 [15.2]	1,800 [12.4]	260 [1.8]	7%

	Ultimate Strength (psi) [MPa]	Yield Strength (psi) [MPa]	Elastic Modulus (ksi) [GPa]	Rupture Strain
MBrace Saturant	8,000 [55.2]	7,900 [54.5]	440 [3.0]	3.50%

3.5 COMPOSITE ANCHORAGE

The materials used for anchorage consisted of CFRP laminates, properties previously discussed in Section 3.5, and glass FRP (GFRP) spikes. The spikes were

www.manaraa.com

made of glass fibers, provided by Fyfe Co. LLC, that were bundled together. Procedures to make the spikes are discussed in Chapter 5. The spikes were saturated with MBrace Saturant. Table 3.5 shows the material properties of the glass fibers (Fyfe 2008).

Table 3.5: Spike Anchorage Material Properties

Material	Ultimate Tensile Strength (ksi) [GPa]	Density (lb/in^3) [g/cm^3]	Tensile Modulus (ksi) [GPa]	Ultimate Elongation
Glass Fiber	470 [3.24]	0.092 [2.55]	10,500 [72.4]	4.50%

www.manaraa.com

CHAPTER 4

CALCULATION METHODOLOGY

4.1 OVERVIEW

Analytical calculations were performed following accepted design protocols as per ACI. These calculations were performed for a simply supported RC beam. Analytical calculations were also performed for the externally strengthened members. These calculations were not used in designing the RC beams and strengthening systems but rather the values obtained serve as the basis for predicting what results can be expected during testing. The calculations were first undertaken by using the nominal strength of concrete (f'_c) equal to 4,000 psi (27.6 MPa). After the core samples were tested and altered per Section 5.6.5 of ACI 318-05, the analytical calculations for each of the specimens were updated using the experimentally obtained compressive strengths. This strength is noted as f_c so that comparisons of the results can be made with respect to the difference in strength of concrete for each member. In this chapter, all analytical calculations and explanations as to the reasoning of how and why certain calculations were used are presented. See Appendix A for beam dimensions and notation. Results of these analytical calculations are presented in Chapter 7.

4.2 DESIGN AND ANALYSIS

4.2.1 FLEXURAL AND SHEAR STRENGTH

Before the design of the FRP system, analysis of the beams to be tested was conducted. As stated in Chapter 3, the ACI 318-05 was used as an analytical design

www.manaraa.com

guide for the RC beams. The beams were first checked to see if T- beam analysis is required. This was done by setting the tension force (area of tension steel and its strength) equal to the compression force (volume of the Whitney stress block) and solving for the location of the neutral axis. If the location of the neutral axis is greater than the depth of the flange, then the beam can be analyzed as a T-beam (illustrated in the following steps).

$$T = C \qquad (1)$$

$$A_s f_y = (0.85)(f'_c)(b_{eff})(a) \qquad (2)$$

$$a = (A_s f_y) / ((0.85)(f'_c)(b_{eff})) \qquad (3)$$

i.e. Control beam B-1a: a = 4.64" ≥ 3" Analyze as T-Beam

$$A_{sf} = \frac{0.85(f'_c)(b - b_w)(h_f)}{f_y} \qquad (4)$$

After this, the reinforcement ratio (ρ) was computed and compared with the maximum reinforcement ratio (ρ_{max}) in order to determine if the beam is over or under reinforced. This is important because an under-reinforced specimen is more desirable. In an under-reinforced member, flexure (or tensile) steel yields causing cracks to open in the flexure region and failure proceeds gradually as the steel yields. Also, the neutral axis moves towards the compression zone. In the case of an over-reinforced member, the flexure steel does not yield and the concrete reaches maximum strain causing sudden failure. The reinforcement ratio and ultimate moment capacity are calculated as:

$$\rho = A_s / ((b_w (d)) \leq \rho_{max} = 0.85\,(\beta_1)(f'_c / f_y)(\varepsilon_u / (\varepsilon_u + 0.004)) \qquad (5)$$

www.manaraa.com

$$M_u = A_{sf} f_y (d - (h_f / 2)) + (A_s - A_{sf})(f_y)(d - (a / 2)) \quad (6)$$

The final part of the analysis is the shear strength (V_c) contribution by the concrete. The shear strength was computed by referencing Section 11.3 of the ACI 318-05. This section covers shear strength provided by concrete for nonprestressed members that are only subjected to both shear and flexure. The basic expression used in calculating the shear strength is:

$$V_c = (1.9 (\sqrt{f'_c}) + 2500 \rho_w (V_u d) / M_u) b_w d \quad \text{Eq. (11-5)}$$

This equation is the basic expression and lower limit for shear strength of non-prestressed members that do not have internal shear reinforcement. The shear strength determined by this expression is affected by three variables: $\sqrt{f'_c}$, ρ_w, and $(V_u d) / M_u$. There has been a significant amount of research that indicates Eq. (11-5) overestimates the influence of f'_c and underestimates the influence of ρ_w and $(V_u d) / M_u$ (ACI 318-05 R11.3.2.1). It has also been noted that a change in f'_c (applicable for the range of f'_c = 2500 to 5000 psi) produced negligible variations in shear strength whereas a change in the amount of reinforcement and span length produced significant variations (Kani, 1966). V_c also depends on the depth of the specimen as it decreases as the depth increases. With this in mind, the ratio of a/d, shear span to member depth needs to be checked. The range of this ratio for which failure occurs due to diagonal (shear) cracks caused by reduced beam strength (failure occurs before full flexural strength is reached) is from a/d = 1.0 to 6.5. Outside the maximum of 6.5, failure occurs typically after the flexural capacity of the cross section is reached. It was also apparent that this range consisted of two different functions that intersected at a/d = 2.5. Thus, the laws that govern the strength of the beam are different for an a/d less than and greater than 2.5. Furthermore, Kani noted that

www.manaraa.com

the shear stress at failure, the area where failure occurred and the range for a/d was greatly reduced due to a low reinforcement ratio in the case of an under-reinforced member. This new range of a/d was reduced to 1.5 - 3.5. Since the specimens being tested have an a/d = 2.72, are under-reinforced and are without significant arching action, flexural failure is not expected and the beams should fail in shear. Therefore, Eq. (11-5) can be simplified to:

$$V_c = 1.9\ (\sqrt{f'_c})\ b_w d \text{ or } 2\ (\sqrt{f'_c})\ b_w d \qquad \text{Eq. (11-3)}$$

$$\text{by setting } 2500\ \rho_w\ (V_u d) / M_u = 0.1\ \sqrt{f'_c}$$

Eq. (11-3) is a format that is chosen from design. This equation can also be set to:

$$V_c = \beta\ (\sqrt{f'_c})\ b_w d$$

The coefficient of β is used in order to select a rational basis that is based on literature. Since Eq (11-3) is significantly conservative, this coefficient takes into account the inaccuracy of the design equation. Also, the coefficient of β is used because it allows V_c to be determined specifically for the beams being tested instead of using the general equation presented by the design guide. The coefficient β is the parameter that indicates the ability of the concrete section to transmit stresses across diagonal cracks. The value of β for the beams being tested was found to be approximately 2.80. This value was determined by using Kani's (1966) graph for test on size effect in shear which relates the reinforcement depth, d, to the normalized shear (V) with respect to strength of concrete, $\sqrt{f'_c}$, and to a/d. The value of d was set to 25 inches (635 mm), and a curve was drawn to represent a/d = 2.72. β was then found by interpolating the value at which d and a/d intersect each other on the graph and crosses the normalized shear axis. The value determined falls between the lower limit of 2.0 and the upper limit of 3.5 set by ACI 318-

www.manaraa.com

05. This graph is shown in Figure 4.1, which was adapted from Kani (1966) and illustrated by Collins and Kutchma (1999).

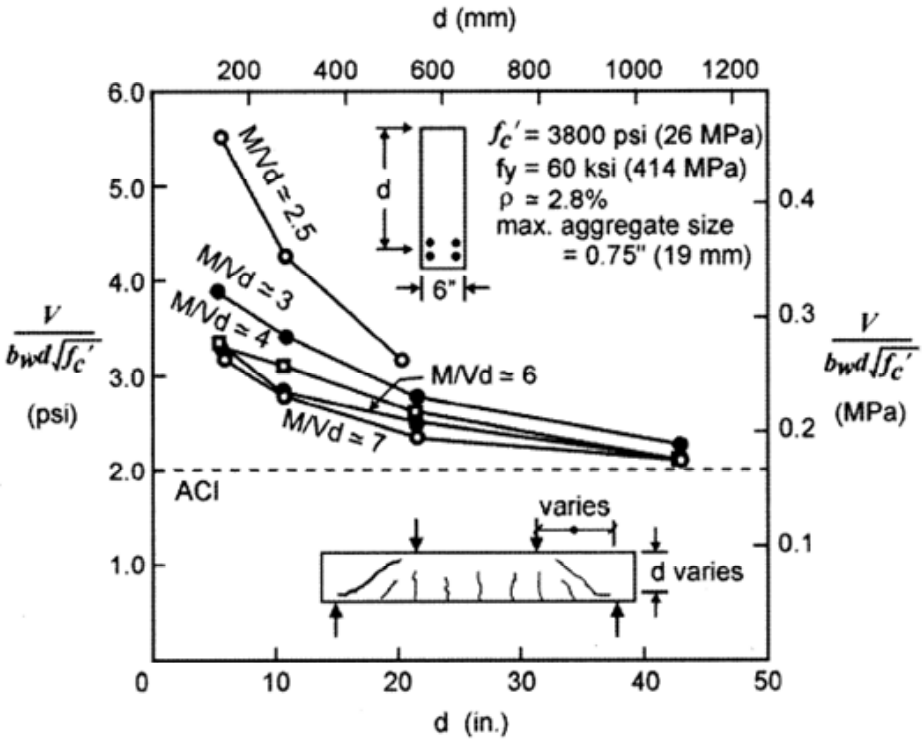

Figure 4.1 – Kani's Test on Size Effect in Shear (Collins et al. 1999)

4.2.2 EXTERNAL REINFORCEMENT

As previously stated, the contribution to shear strength due to the CFRP system was computed by following the ACI 440.2R-08. The first step in the analytical design process is to establish the material properties. These properties are:

rupture strain - $\varepsilon_{fu} = C_E \varepsilon_{fu}^*$ Eq. (9-4)

modulus of elasticity - $E_f = f_{fu} / \varepsilon_{fu}$ Eq. (9-5)

tensile strength of shear reinforcement - $f_{fe} = \varepsilon_{fe} E_f$ Eq. (11-5)

www.manaraa.com

Eq. (11-5) is the tensile strength of the FRP shear reinforcement at nominal strength which is proportional to the level of strain that can be developed in the FRP shear reinforcement. Depending on the type of wrapping, different levels of strain in the reinforcement can be achieved. This is due to the fact that certain wrapping schemes tend to debond, or delaminate, sooner than others. This can be easily seen in the case of complete wrapping and U-wrapping. The complete wrap achieves higher strain than the U-wrap because the laminates are overlapped creating a strong bond. Failure is most likely to occur due to FRP rupture as opposed to delamination because the bond between the overlapped laminates is much stronger than the bond between the FRP laminate and concrete at the termination end, or open end as in the case of the U-wrap. Thus, the tensile strength is dependent on the strain and wrapping schemes. The strain in the shear reinforcement can be found by:

$$\textit{for completely wrapped members;}\quad \varepsilon_{fe} = 0.004 \leq 0.75\,\varepsilon_{fu} \qquad \text{Eq. (11-6a)}$$

$$\textit{for U-wrap and 2-sided wrapped members;}\quad \varepsilon_{fe} = K_v\,\varepsilon_{fu} \leq 0.004 \qquad \text{Eq. (11-6b)}$$

$$\textit{where}\ K_v = \frac{k_1 k_2 L_e}{468\,\varepsilon_{fu}} \leq 0.75 \qquad \text{Eq. (11-7)}$$

As can be seen in the above equations, the strain is limited to 0.004 or 0.4% of the ultimate strain in the FRP. The reason for this is because failure due to loss of aggregate interlock has been observed at FRP strains less than the ultimate FRP strain. Therefore, in order to avoid this mode of failure, a limit of 0.004 has been set. Furthermore, Eq. (11-6b) is reduced by a bond-reduction coefficient, K_v, because as stated earlier, U-wrapping and 2-sided wrapping have been observed to delaminate. This coefficient is

www.manaraa.com

dependent on two modification factors, k_1 and k_2, which account for the strength of concrete and the type of wrapping scheme, respectively, and the active bond length, L_e, which is the length that the majority of bond stress is maintained. The active bond length is basically the same as the development length that is found for internal reinforcing steel. These variables are found by using Eqs. (11-8), (11-9), and (11-10) in the ACI 440. Once these calculations are completed, the shear strength provided by the FRP reinforcement can be found. This contribution is found by:

$$V_f = \frac{A_{fv}(f_{fe})(\sin\alpha + \cos\alpha)d_{fv}}{s_f} \quad \text{Eq. (11-3)}$$

$$\textit{where } A_{fv} = 2nt_fw_f \quad \text{Eq. (11-4)}$$

Eq. (11-4) is the cross sectional area of the FRP sheet where n is the total number of plies, t_f is the thickness of the ply, and w_f is the width of the ply. In Eq. (11-3), the angle is the angle which the laminate is oriented, d_{fv} is the effective depth of the FRP and s_f is the center to center spacing of the laminates. The total nominal shear strength is the total of the shear strength contribution due to concrete, internal steel, and FRP multiplied by strength reduction factors as shown in Eq. (11-2) of the design guide. The calculations were repeated using the two sided wrap instead of the U-wrap.

www.manaraa.com

CHAPTER 5

ATTACHMENT OF EXTERNAL REINFORCEMENT

5.1 OVERVIEW

Before the external reinforcement can be attached, the specimen's surface needs to be treated. The specimens were first sandblasted. This was done on the web, bulb, and underside of the beam. The specimens were sandblasted to a minimum concrete surface profile (CSP) 3 as defined by the International Concrete Repair Institute (ICRI) surface profile chips (ICRI 2008). Once this was completed, the corners along the bottom edge of the bulb were rounded to a minimum 0.5 inch (13mm) radius so that stress concentrations on the CFRP laminates could be avoided. After the corners have been rounded, the external reinforcement can be attached.

5.2 ATTACHMENT PROCEDURE FOR CFRP LAMINATES

1. **Measurement and Placement of the CFRP Laminates.** The spacing between laminates for all the reinforced specimens B-2a, B-2b, B-3a, and B-4a (figures presented later in the chapter) and the width of the actual laminate is ten inches. The first laminate is placed fourteen inches from the end of the beam. This allowed for sufficient space between the first laminate and the support of the beam. In order to get the length of the CFRP laminates, a string was strung around the cross section of the beam.

2. **Prepping the Surface.** Before the impregnating resin could be applied, the concrete surface of the beam needs to be primed. As stated in Chapter 3, the

www.manaraa.com

primer used is a two part MBrace Primer. The mixing ratio for the primer is 3:1 (Part A to Part B) by volume. The two parts are mixed in a bucket for three minutes. After mixing, the primer was placed within the marked substrate of the beam by using paint rollers. The primer was allowed to cure for half an hour. Next, the MBrace Putty was mixed. The ratio for the putty is also 3:1 (Part A to Part B) by volume. After three minutes of mixing time, the putty was spread onto the substrate, where the primer was previously placed, covering any voids and offsets with a plastic spatula. The putty was allowed to cure for one hour. The beam is now ready for impregnation of the CFRP sheets. Figures 5.1 and 5.2 show the application of the primer and putty.

Figure 5.1 – Application of Primer

Figure 5.2 – Application of Putty

3. **Impregnating CFRP Sheets.** Once the primer and putty has set, the MBrace Saturant can be applied. The mixing ratio is also 3:1 (Part A to Part B) by

www.manaraa.com

volume. After mixing the saturant for three minutes in a bucket, a thick enough layer that does not run is rolled onto the substrate, where the primer and putty was placed, with a painting roller. The pre-cut CFRP sheet is then placed starting from one side of the beam and stretching it all the way around. Then, a roller with grooves is used to remove any air voids. Then, another layer of saturant is rolled over the sheet. Again, the roller with the grooves is used to remove any air voids. Figures 5.3 through 5.5 show the application process of the CFRP sheets and Figure 5.6 shows the reinforcement schematic for beams B-2a and B-2b.

Figure 5.3 – Application of Saturant

www.manaraa.com

Figure 5.4 – Application of Sheet

Figure 5.5 – Removement of Air Voids

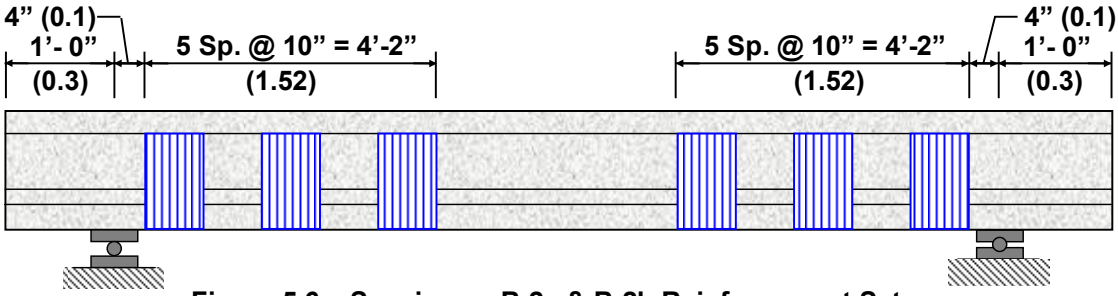

Figure 5.6 – Specimens B-2a & B-2b Reinforcement Setup
Note (SI conversion in m)

5.3 APPLICATION OF ANCHORAGE

The anchorage used on two of the specimens tested, B-3a and B-4a, consisted of two different types of configurations: 1) a horizontal CFRP laminate and 2) GFRP Spikes. On the first specimen, after the shear reinforcement was applied, a horizontal CFRP laminate was placed over the CFRP laminates used for shear reinforcement. The same procedure, as discussed in Section 4.4, was used to attach the horizontal laminate for anchorage. The laminate was placed from the edge of the beam (horizontally) with

www.manaraa.com

half of the sheet on the web and the other half on the bulb. The laminate has a width of 10 inches (254 mm) and a total length of 6 feet 4 inches (1.93 m). Figure 5.7 illustrates the horizontal laminate configuration.

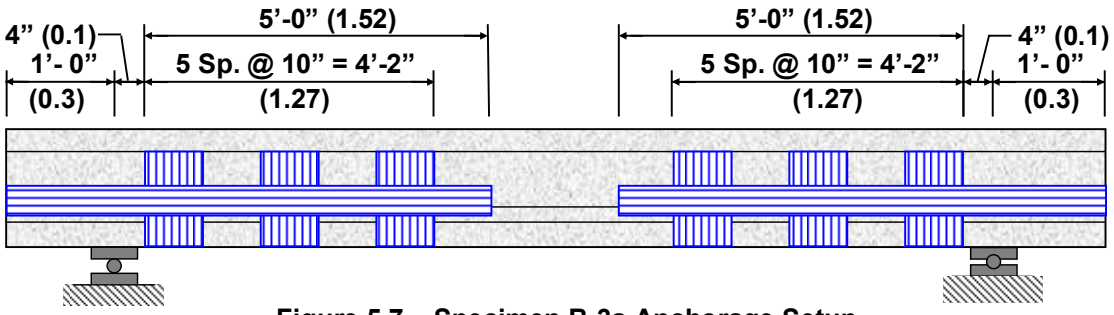

Figure 5.7 – Specimen B-3a Anchorage Setup
Note (SI conversion in m)

The second anchorage configuration consisted of inserting GFRP spikes through the CFRP laminates used for shear reinforcement. This time, the laminates were bonded to the sides of the beam rather than all the way around forming a U-wrap. The spikes were made with a total length of 4 inches (101.6 mm) and a diameter of ½ inch (12.7 mm) (75% of final diameter) before being saturated with resin and a final saturated diameter of 11/16 inch (17.46 mm). Of the 4 inches (101.6mm), only 2 inches (50.8 mm) was saturated and cured before installation. To achieve the desired diameter and length, the bundle of fibers was first passed through a wooden block with a ½ inch (12.7 mm) diameter hole. Then, 2 inches (50.8 mm) were covered with tape so that only half the length of the fibers would be saturated as shown in Figure 5.8.

www.manaraa.com

Figure 5.8 – Prepping of Glass Fibers

The loose end of the fibers was then saturated using MBrace Saturant and passed through a wooden block with an 11/16 inch (17.46 mm) diameter hole in order to achieve a uniform diameter. The spikes were then hung instead of being placed on a table in order to avoid the saturated end from flattening out. After curing for 24 hours, the tape was removed and any deformities such as loose fibers or excess resin that had dripped and cured were removed with a blade. Figure 5.9 shows an example of a finished GFRP spike.

Figure 5.9 – Finished GFRP Spike

www.manaraa.com

After the CFRP laminates have cured on the specimen, a 3/4 inch (19.05 mm) diameter hole with a depth of 2-1/4 inches (57.15 mm) was drilled into each sheet. The hole was located in the center of the sheet (or 5 inches from the edge of the sheet) and as close as possible to the bottom of the web, where the web meets the bulb. This achieves a spacing of 20 inches (508 mm) per spike. The hole was then thoroughly cleaned by scrapping the hole with a steel wire brush and then using a manual air pump to blow out any debris. This was done several times to get the hole as clean as possible to ensure the resin bonds to the concrete. The hole was then filled, about 50%, with MBrace Saturant and the spike was inserted in a twisting manner. This allows the resin to fully coat the spike and inside part of the hole. The unsaturated or flared end of the spike is then spread out evenly onto the web and bulb and saturated with resin. It should be noted that installation of the spike was rather difficult. The reason for this was due to the low viscosity of the resin used. Since the hole drilled was perpendicular to the face of the web, the resin would easily flow out making it difficult to fill the hole entirely. This not only caused voids in the hole but also caused the fibers in the flared end to clump up and sag due to the resin flowing out. Figures 5.10 & 5.11 illustrate the GFRP configuration and the installation location of the GFRP spikes.

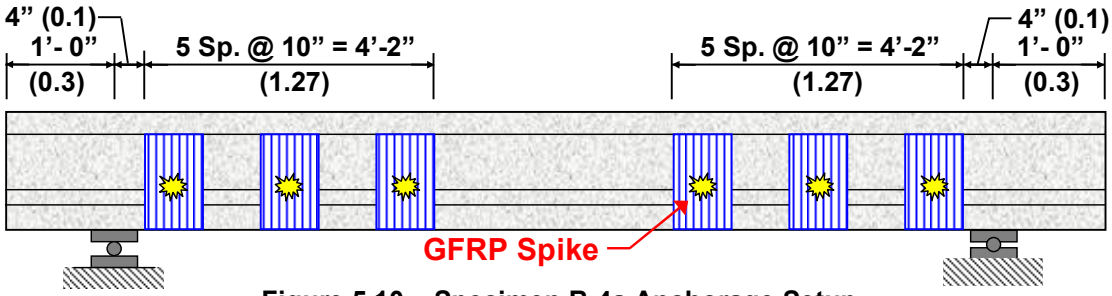

Figure 5.10 – Specimen B-4a Anchorage Setup
Note (SI conversion in m)

www.manaraa.com

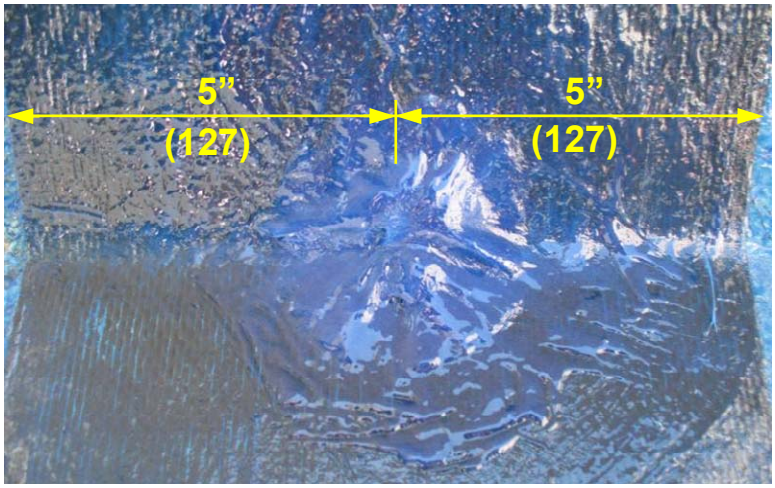

Figure 5.11 – Typical GFRP Spike Location
Note (SI conversion in mm)

www.manaraa.com

CHAPTER 6

TESTING OF FULL SCALE I-BEAMS

6.1 OVERVIEW

The experimental setup shown in Figure 6.1 consisted of placing the simply supported beam in four-point bending through two load points equally spaced from the supports of the beams. The constant moment span was 3 feet 4 inches (1.02 m) and the shear span was 5 feet 8 inches (1.73 m). The beam rested on supports that were placed one (1) foot from the ends of the beam. Each support consisted of a nominal 8 x 8 x 16 inch (20.3 x 20.3 x 40.6 cm) CMU block filled with concrete and reinforced with a #3 (9.53 mm dia.) rebar in each cell, two ½ inch (12.7 mm) steel plates, a 1-1/2 inch (38.1 mm) steel rod, and two ¼ inch (6.4 mm) pieces of plywood placed between the bottom steel plate and CMU block and the other between the top steel plate and the beam. The total clear span of the beams was 14 feet 8 inches (4.5 m).

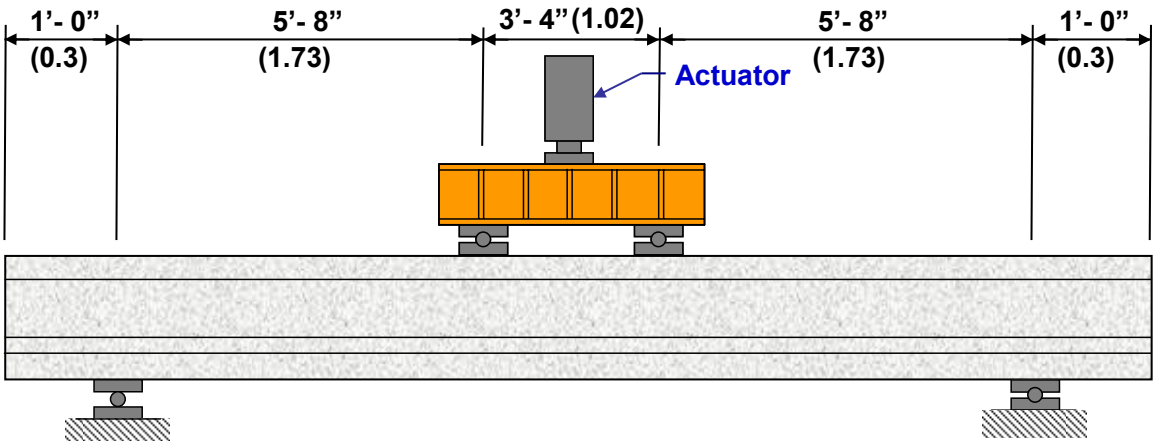

Figure 6.1 – Experimental Setup
Note (SI Conversion in m)

www.manaraa.com

The test was performed using a Baldwin Testing frame with a 200 kip (889.6 kN) actuator (a single load applied onto a spreader beam) at a rate of deflection of 0.05 inches (1.27 mm) per minute. Test data was recorded from the following sensors:

a) FRP Strain gauges: nine 120 ohm gauges placed on three strips of FRP (three gauges per strip) spaced 2 inches (50.8 mm) from where the web meets the flange and 6 inches (152.4 mm) thereafter. This is illustrated in Figure 6.2.

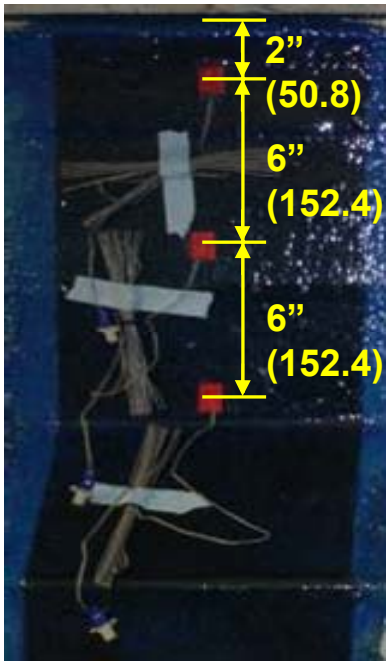

Figure 6.2 – Strain Gauge Spacing
Note (SI conversion in mm)

b) PI-Gauges: five 120 ohm gauges placed at the midspan. Gauges were placed at top and bottom center, 2-1/2 inches (63.5 mm) from the bottom of the bulb, and spaced 5 inches (127.0 mm) apart on the web with the first gauge starting at 15 inches (381.0 mm) from the bottom. This is illustrated in Figure 6.3.

www.manaraa.com

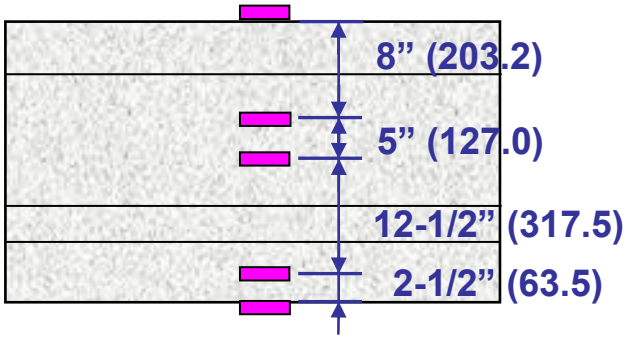

Figure 6.3 – Pi-Gauge Spacing
Note (SI conversion in mm)

c) DCVTs: two DCVTs were used to measure the deflection at midspan and two DCVTs were used to measure settlement of the supports.

d) Load: three independent readings were taken. One reading was taken at the loading point from the Baldwin Testing frame and the other two were taken at the loading sections on the beam.

Figure 6.4 shows a side view of an actual specimen ready for testing.

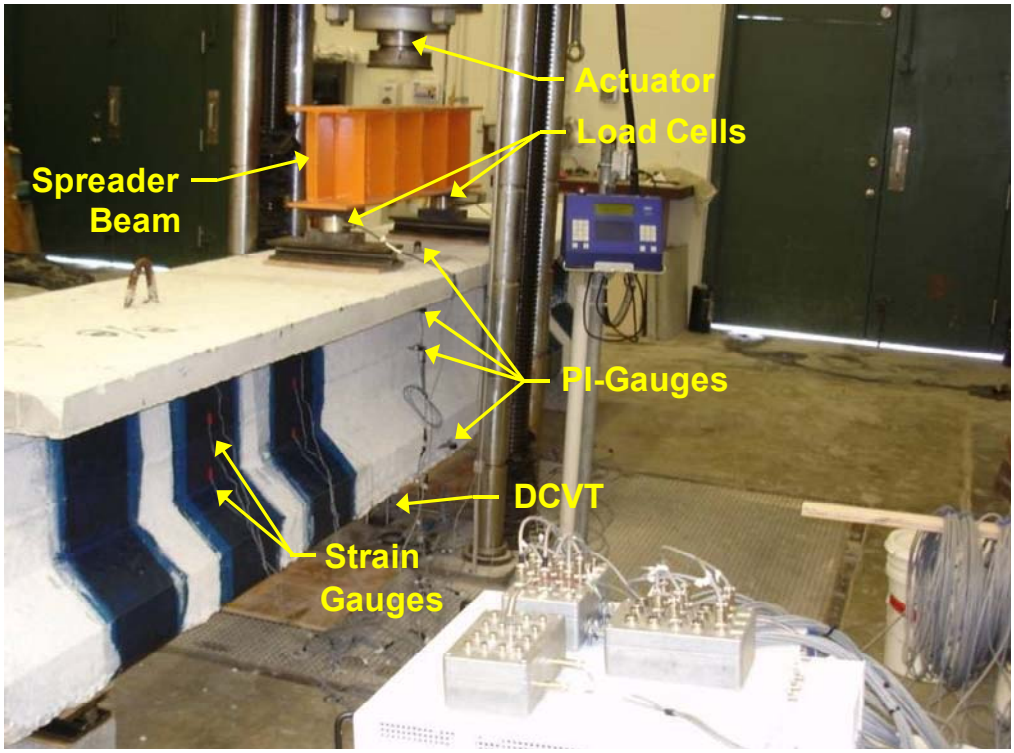

Figure 6.4 – Beam B-2a Test Setup

www.manaraa.com

6.2 TEST PLAN

The test plan consisted of testing a total number of five specimens. The first specimen to be tested was a control specimen followed by two specimens externally reinforced with CFRP laminates. The next two specimens to be tested had the same external reinforcement setup but now include the use of two different anchorage schemes. Table 6.1 shows the test matrix for the research project.

Table 6.1 Test Matrix

Specimen #	# of Plies	Type of Anchorage	Specimen Purpose
B-1a	None	None	Control
B-2a	1	None	Investigate the effect of a bulb on CFRP laminates
B-2b	1	None	Investigate the effect of a bulb on CFRP laminates
B-3a	1	1 Ply horizontal CFRP laminate along the web	Investigate the effect of a bulb on CFRP laminates with anchorage
B-4a	1	GFRP Spikes	Investigate the effect of a bulb on CFRP laminates with anchorage

6.3 CONTROL BEAM TEST

The first specimen to be tested was control beam B-1a. The loading was applied in three cycles at a rate of 0.05 inches (1.27 mm) per minute. The first cycle consisted of loading the beam to a load that was before the expected cracking moment and then unloading to about 3 kips (13.3 kN). The second cycle loaded the beam until cracking was observed. Once a crack was observed, the loading was stopped so that the cracks could be marked. Then, the beam was once again unloaded to about 3 kips (13.3 kN).

www.manaraa.com

The final cycle loaded the beam until failure. The loading was stopped periodically to mark the progression and development of new cracks but never unloaded.

6.4 CFRP STRENGTHENED BEAM TESTS

The next specimen to be tested was beam B-2a which has three strips with single ply of CFRP on both sides of the beam. The loading was applied in five cycles at a rate of 0.05 inches (1.27 mm) per minute. The first two cycles were stopped at loads that were before the expected cracking moment and then unloaded to a load of about 3 kips (13.3 kN). The third cycle was stopped when cracking was first observed. Once the cracks were marked, the beam was unloaded to the same load of about 3 kips (13.3 kN) and loaded once again. The fourth cycle was stopped and unloaded to the same load as the other cycles when significant cracking was observed. The final cycle applied loading until failure of the specimen.

The next specimen to be tested in the group was beam B-2b, which has identical external reinforcement as B-2a. The only difference between beams B-2a and B-2b is the amount of loading cycles. The number of cycles used to load beam B-2b was the same as B-1a. The same loading rate and criteria were also used in stopping, unloading, and marking of the cracks in each cycle. Figure 6.5 shows marking of cracks during a loading cycle.

www.manaraa.com

Figure 6.5 – Beam B-2b Test

6.5 CFRP STRENGTHENED BEAM TESTS WITH ANCHORAGE

The final two specimens to be tested are beams B-3a and B-4a which have the same amount of reinforcement as beams B-2a and B-2b but now include anchorage. The criterion for stopping and marking of the cracks was the same as all the other tests. The total number of loading cycles achieved for beam B-3a was four and for beam B-4a was five.

www.manaraa.com

CHAPTER 7

RESULTS OF FULL SCALE I-BEAM TESTS

7.1 OVERVIEW

The following chapter presents the data collected for all of the five specimens tested and a discussion of this data. As stated earlier, the first specimen to be tested was control beam B-1a. The purpose of the control beam was to characterize the behavior of an un-reinforced specimen and to setup a benchmark in which all the other specimens would be compared against. The purpose of the next two specimens to be tested, beams B-2a and B-2b, was to characterize and validate expected results, which will be specified in the following sections, of reinforcing a bulb-T type beam with external CFRP laminates. The purpose of the final two specimens to be tested, beams B-3a and B-4a, was to validate the use of two different anchorage schemes for external CFRP laminates used as shear reinforcement.

In Table 7.1, a summary of the theoretical results that were calculated using the methodology in Chapter 4 is given, in Table 7.2, a summary of the experimental results is given, and in Table 7.3, a summary of the normalized results is given. In Table 7.1, V_M is the shear load due to the ultimate moment capacity. In Table7.2, V_w is the shear due to the self weight of the specimen and V_{exp} is the maximum shear load that was achieved during the test. This was read from the load cell on the side of the beam which failed. The reason for this was because of the difference in relative stiffness between the left and right side of the beam. V_r is the total shear resistance of the specimen being tested which is the sum of V_w and V_{exp}. The ultimate moment, M_u, given is the total shear resistance

www.manaraa.com

multiplied by the shear span and the maximum deflection, Δ_{max}, is the net deflection between the midspan and settlement of the support. In Table 7.3, the values of V_r are normalized with respect to the beams strength of concrete, f_c, $\Delta_{V,t}$ is the theoretical shear strength difference between the control and externally strengthened specimens, and $\Delta_{V,exp}$ is the experimental shear strength difference between the control and externally strengthened specimens.

Table 7.1 Theoretical Results

Specimen #	V_c (kips) [kN]	$V_{f,U\text{-}wrap}$ (kips) [kN]	$V_{f,side\ wrap}$ (kips) [kN]	V_{tot} (kips) [kN]	V_M (kips) [kN]
B-1a	20.7 [92.1]	-	-	20.7 [92.1]	96.1 [427.3]
B-2a	19.6 [87.2]	13.0 [57.8]	6.8 [30.2]	32.6 [145.0]	94.9 [422.1]
B-2b	20.0 [89.0]	13.3 [59.2]	6.9 [30.7]	33.3 [148.1]	95.3 [423.8]
B-3a	19.6 [87.2]	13.0 [57.8]	6.8 [30.2]	32.6 [145.0]	95.0 [422.6]
B-4a	20.2 [89.9]	13.5 [60.1]	7.1 [31.6]	33.7 [149.9]	95.6 [425.2]

Table 7.2 Test Results

Specimen #	V_w (kips) [kN]	V_{exp} (kips) [kN]	V_r (kips) [kN]	M_u (kip-ft) [kN-m]	Δ_{max} (in) [mm]
B-1a	2.2 [9.8]	47.9 [213.1]	50.1 [231.9]	295.4 [401.2]	0.67 [17.02]
B-2a	2.2 [9.8]	45.3 [201.5]	47.5 [211.3]	269.3 [365.5]	0.33 [8.38]
B-2b	2.2 [9.8]	47.8 [212.6]	50.0 [222.4]	283.5 [384.8]	0.36 [9.14]
B-3a	2.2 [9.8]	67.4 [300.0]	69.6 [309.8]	394.6 [535.9]	0.68 [17.3]
B-4a	2.2 [9.8]	61.4 [273.1]	63.6 [282.9]	360.6 [489.4]	0.62 [15.75]

www.manaraa.com

Table 7.3 Normalized Results

Specimen #	$\Delta_{V,t}$ (kips) [kN]	$\Delta_{V,exp}$ (kips) [kN]	Normalized V_r
B-1a	-	-	6.77
B-2a	13.0 [57.8]	-2.6 [-11.6]	6.79
B-2b	13.3 [59.2]	-0.1 [-0.44]	7.02
B-3a	13.0 [57.8]	19.5 [86.7]	-
B-4a	13.5 [60.1]	13.5 [60.1]	-

As can be seen in Tables 7.2 and 7.3, beams B-2a and B-2b did not have an affect on the shear strength. However, the CFRP laminates did stiffen the beams and reduced the maximum deflection by an average of 48% of that of the control beam. Beams B-3a and B-4a, which had a horizontal laminate and GFRP spikes, respectively, as anchorage had the greatest increase of maximum shear strength. Also, it can be observed in Table 7.3 that the experimental strengthening in B-3a was about 50% greater than that of the theoretical strengthening and in B-4a both values are the same. The normalized V_r values in Table 7.3 are also presented in Figure 7.1. As can be seen in the figure, the specimens were about 2.4 to 2.5 times that of what was found for $\beta = 2.80$ (Chapter 4). The V_r values of B-3a and B-4a were not normalized because there was contribution of the external strengthening system to the shear strength therefore comparisons could not be made with respect to β, whereas, in B-2a and B-2b the external strengthening system did not have any contribution to the shear strength, thus, the normalized values could be compared to β.

By looking at the crack pattern of all the beams (crack patterns are presented later in the chapter), it is possible that there could have been a contribution to shear strength due to some arching caused by the formation of a compressive strut. It has been shown

www.manaraa.com

that the arching behavior in a concrete member can significantly contribute to the overall strength of the member (Thorburn et al. 2001). In some cases, the concrete member can achieve up to 4 times the design standards by utilizing the arching behavior (Robbins 2003). Another possibility could have been the contribution of the bulb section. Preliminary analyses were performed using a rectangular section that did not account for the remaining bulb section. The area of the rectangular section used in the preliminary analyses was 150 in^2 (967.74 cm^2) and the area of the bulb section that was neglected was about 75 in^2 (483.87 cm^2). The area neglected is 50% that of the rectangular section. This area could have been large enough to have had a contribution to the shear strength. Shear stress analysis of the cross section of the beam showed that the maximum stress in the bulb area was about 25% of that of the maximum shear stress in the web. The additional area of the bulb allows the shear stress to be distributed across a larger area which allows the cross section to carry a higher load (Nilson et al. 2004).

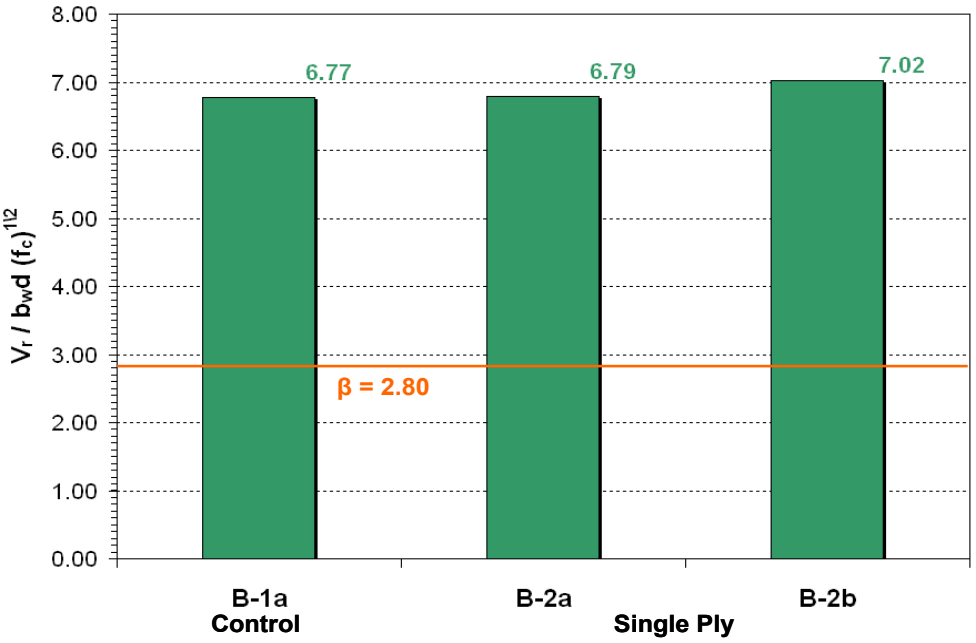

Figure 7.1 – Normalization of Results

www.manaraa.com

In Figure 7.2, the load – deflection plot of each of the specimens along with their respective f_c is shown. It can be observed that all of the plots closely overlap (due to the similarity in relative stiffness) each other up to the range of about 22 kips (97.8 kN) and net deflection of 0.15 inches (3.81 mm) and four of the five plots closely overlap each other up to the range of 30 kips (133.4 kN) and 0.2 inches (5.08 mm). After this common point, the four reinforced specimens began to show greater stiffness per load applied when compared with the control specimen, B-1a. It was not the intention of this project to provide ductility. Shear failure still occurred.

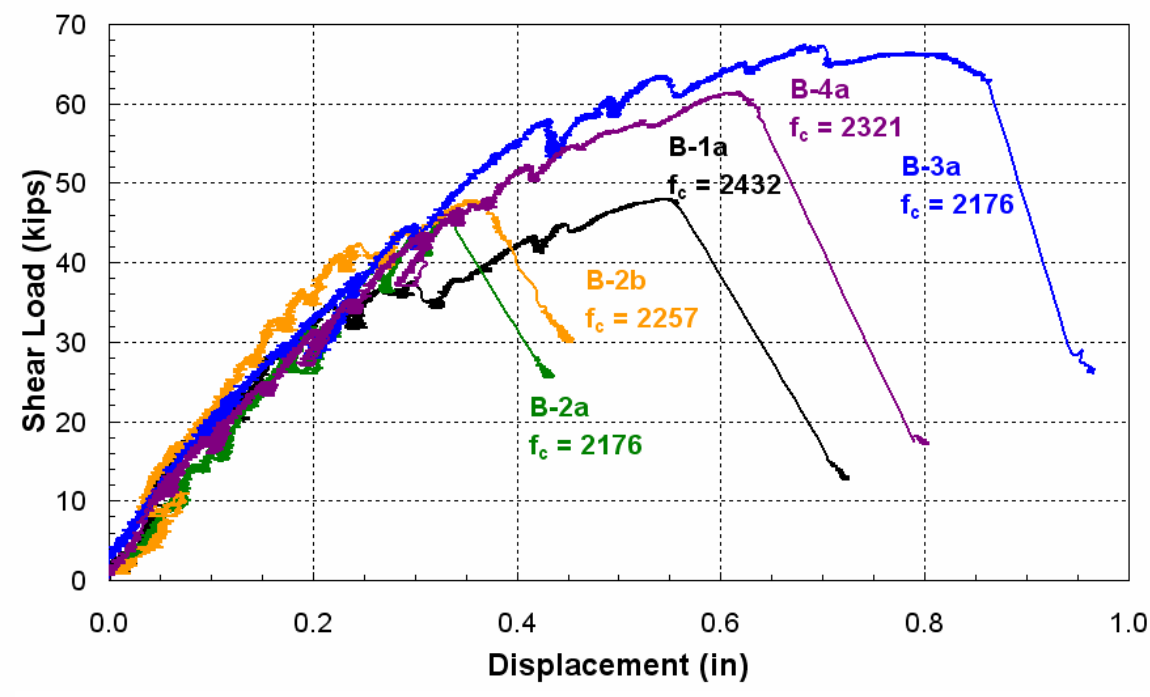

Figure 7.2 – Load-Deflection for Specimens Tested

7.2 BEAM B-1a RESULTS

Although some low cracking sounds could be heard towards the end of the first cycle, cracking was first observed during the second loading cycle at a load of 18 kips (80.1 kN). This was higher than the theoretical cracking shear load of 14 kips (62.3 kN),

www.manaraa.com

about 28% greater. The cracks were mostly located in the middle third, or flexure region, of the beam. Some shear cracks and flexure-shear cracks were also observed on the two outside thirds of the beam at this same loading. The flexure cracks were observed to stop propagating at about 20 kips (89.0 kN). In other words, the flexure cracks stabilized and only shear cracks were forming and propagating ensuring a desirable shear failure would occur rather than a flexural failure. At around 35 kips (155.7 kN), significant cracking was being observed in the shear region of both sides of the beam. The pattern of the shear cracks were observed to follow a similar path to the loading point stopping right where the flange meets the web. As the loading continued, few cracks were observed forming and propagating but the existing cracks were increasing in width. Failure finally occurred at a shear load of 47.9 kips (213.1 kN) with formation of a ¾ inch (19.05 mm) wide shear crack and crushing of the flange at the loading point where the shear crack passed through.

In Figure 7.3, the load-deflection diagram clearly shows every time a major crack formed. Figure 7.4 shows the crack pattern of the beam and Figures 7.5 and 7.6 shows the specimen once it has failed. See Appendix B for the map of sensors and the pi-gauges strain data at midspan.

www.manaraa.com

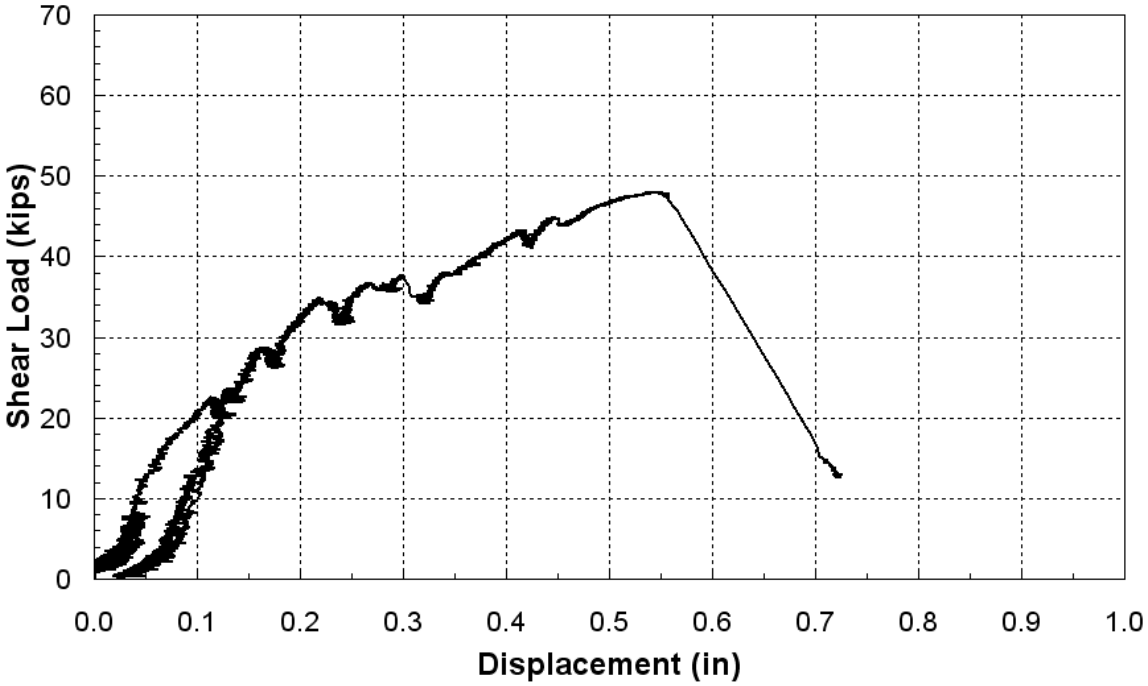

Figure 7.3 – B-1a Load - Deflection

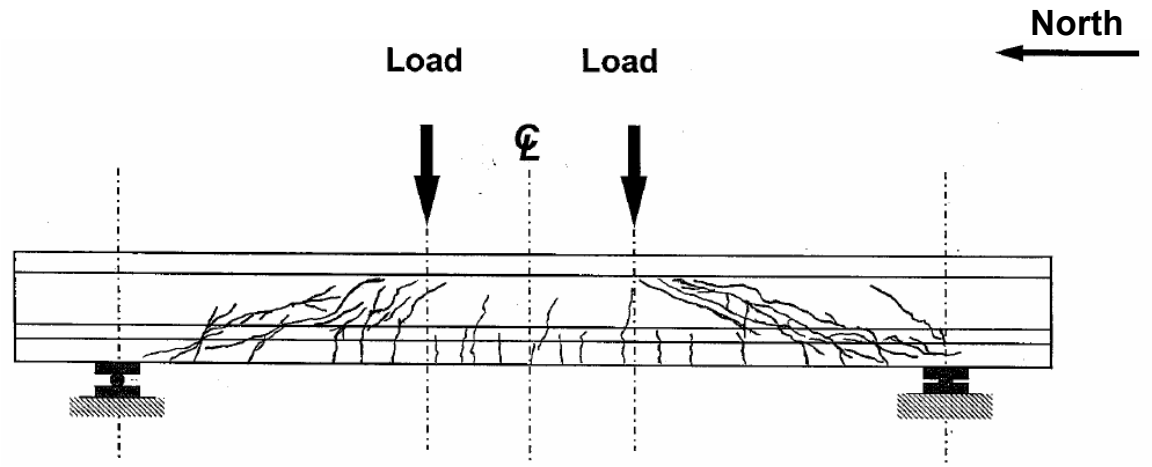

Figure 7.4 – B-1a Crack Pattern

www.manaraa.com

Figure 7.5 – B-1a

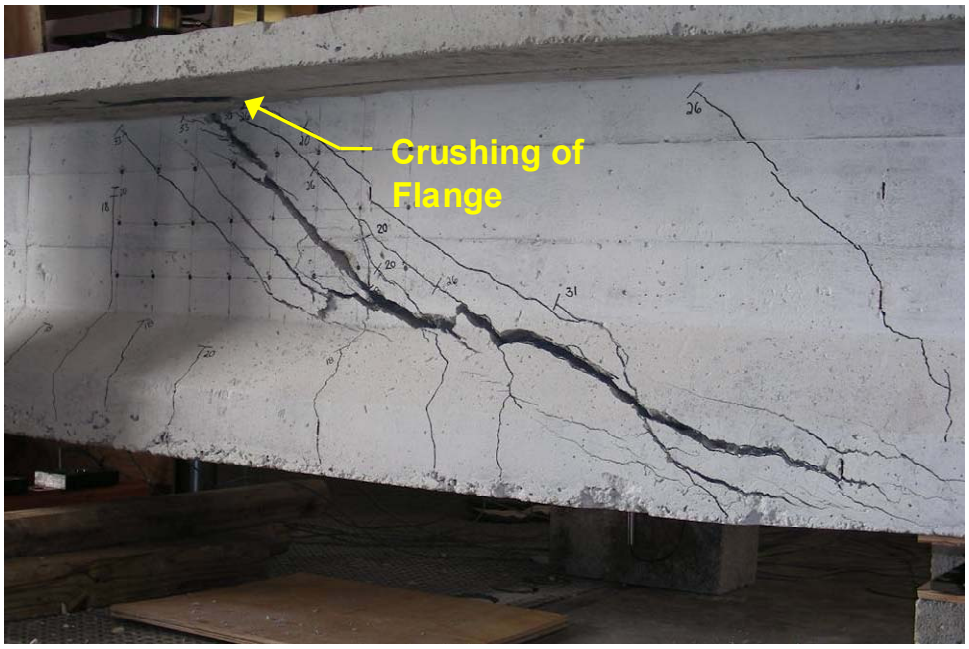

Figure 7.6 – B-1a Failed Section

www.manaraa.com

7.3 BEAM B-2a RESULTS

Cracking for beam B-2a was first observed at a load of 14.5 kips (64.5 kN). This was slightly less than the calculated cracking shear load of 15.1 kips (67.2 kN), about 4%. It was also observed that fewer cracks had formed in the middle third of the beam when compared to the control beam B-1a. At a load of 24 kips (106.8 kN), flexure-shear cracks were observed to form. The flexure cracks in the middle third of the beam were observed to finally stabilize at a load of 27 kips (120.1 kN). At this same loading, a principal shear crack was observed intersecting the CFRP laminates. The only other significant shear cracking observed was at a load of 35 kips (155.7 kN). Failure of the beam finally occurred at a load of 45.3 kips (201.5 kN) due to failure of the laminate and a 3/8 inch (9.5 mm) shear crack that passed through the two laminates closest to the loading point and terminated before reaching the laminate near the support. The maximum shear capacity achieved was slightly lower than the control specimen, about 5%. However, when the maximum shear loads are normalized with respect to f_c, the specimen had a slight increase to that of the control specimen, by a factor of 0.02 (values obtained in Figure 7.1) or 0.3%. Furthermore, the maximum midspan deflection was about 51% less than the control. Figure 7.7 shows the load-deflection diagram.

www.manaraa.com

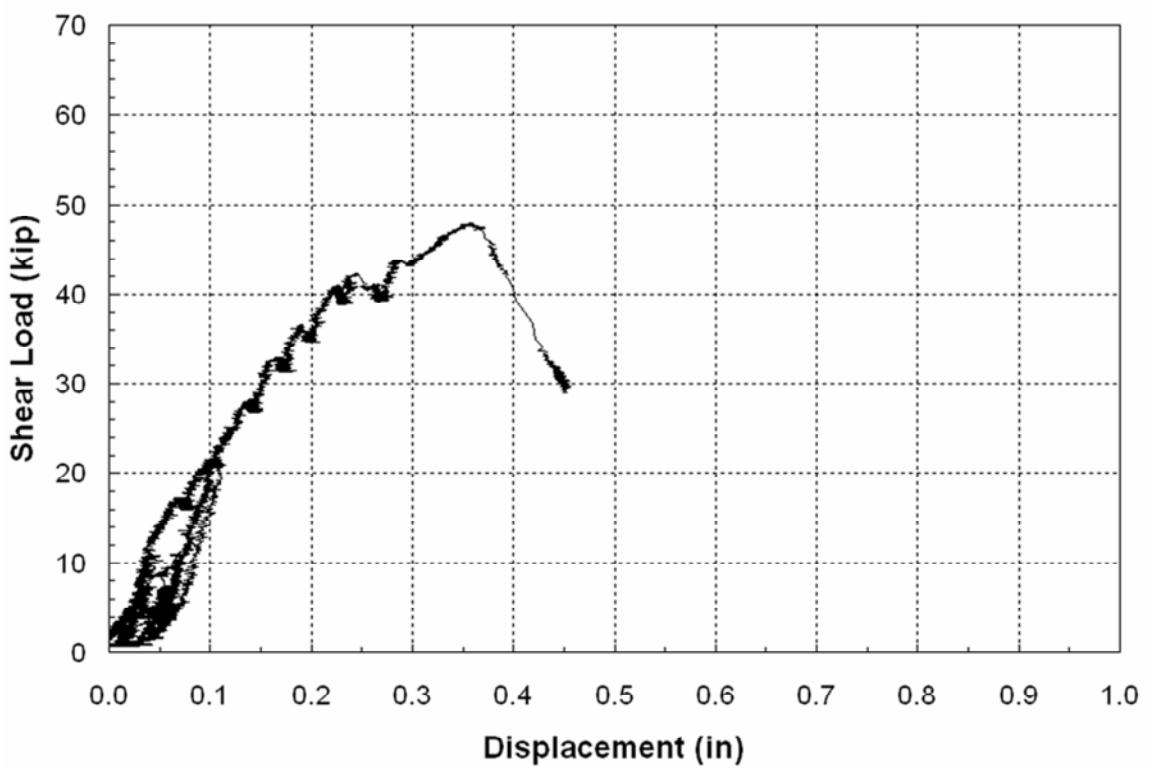

Figure 7.7 – B-2a Load - Deflection

The reduction in deflection is due to the high stiffness characteristic of the CFRP. Also, the laminates acted as a form of confinement which in a sense "hold" the beam and keep it from severely deflecting. Failure of the laminate occurred due to straightening of the center laminate followed simultaneously by peeling of the laminate closest to the loading point. As described in Chapter 1, this straightening was caused by a peeling force which acts perpendicular to the laminate. In the area where the laminate peeled, a layer of about ½ inch (12.7 mm) of concrete was observed to have been peeled off along with the laminate. This failure illustrates that the reinforcement is bond critical and that failure occurs in the concrete substrate and not in the CFRP laminate. These failure modes are illustrated in Figures 7.8, 7.9 and 7.10.

www.manaraa.com

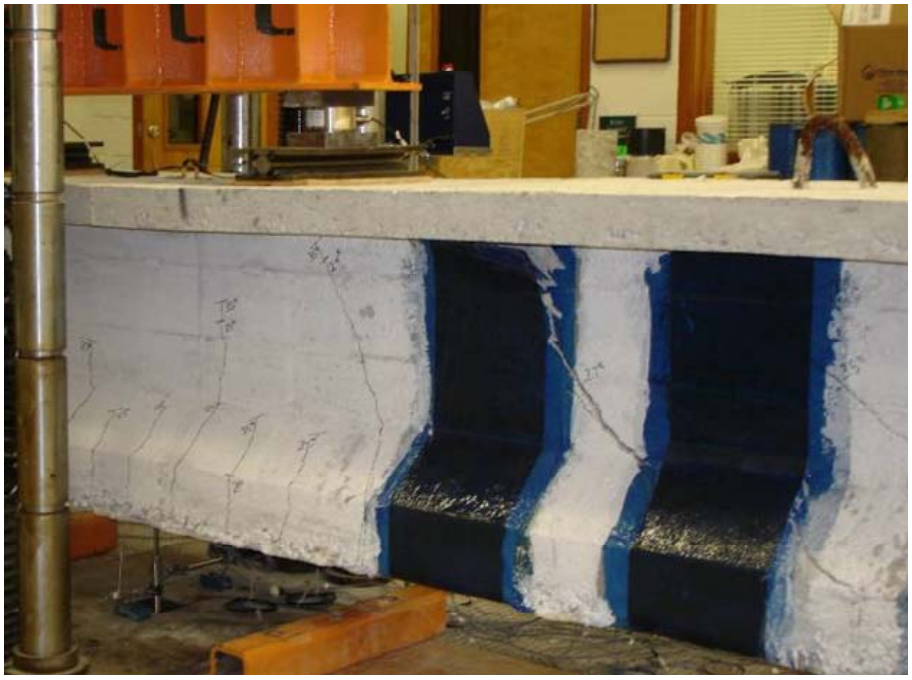

Figure 7.8 – B-2a Failed Section

Figure 7.9 – B-2a Peeling of Laminate

www.manaraa.com

Figure 7.10 – B-2a Straightening of Laminate

Also, it was observed that B-2a had significantly less cracks than that of B-1a but the cracks that did form had the same pattern to those of B-1a. This confirms with what was noted in previous research that the use of FRP does not alter the general crack pattern. This is evident when the crack patterns of both specimens are compared. Figure 7.11 shows the crack pattern for B-2a.

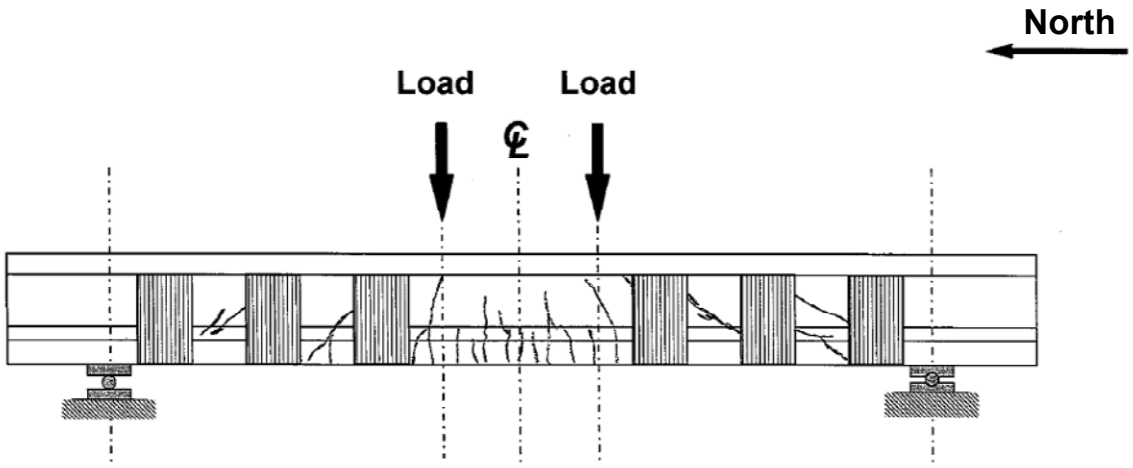

Figure 7.11 – B-2a Crack Pattern

www.manaraa.com

Strain data in the CFRP laminates was also recorded and is shown in Figures 7.12 through 7.14. The first significant increase in strain occurred at a load of about 26 kips (115.7 kN). This was due to the laminates bridging a shear crack that was observed intersecting it. This crack would later develop into the principal shear crack that would lead to failure of the specimen. Up to this loading point, the CFRP laminates had no contribution to the shear capacity. As the loading increased, widening and formation of new shear cracks occurred resulting in an increase in strain because more of the laminate was engaged. As can be seen in the figure, B0 did not record any significant levels of strain because as expected, B0 was outside the area where the principal shear crack had formed. B1 recorded higher levels of strain than in all of the gauges, except for A3, that were in the failed section side. This was because B1 was at the location where the laminate was bridging a shear crack whereas in the failed section, the gauges were not at the exact location where the laminates bridged the shear cracks, thus, recording less strain. Gauges A1, A2, A4, A5, and B2 all exhibited similar behaviors in recording strain. This was due to a similar crack pattern on both sides of the beam which caused the laminates to engage. The levels of strain in A2 and B2 were a result of the peeling stress that was caused by the reentrant corner. This would later lead to straightening of the laminates and ultimately failure of the specimen. Both A3 and B1 had the highest levels of strain which were about 1256 and 796 με, respectively. The high level of strain in A3 was due to peeling of the laminate. These levels of strain were much less than the limit of 4000 με that is set by ACI 440.2R-08. The strengthening system only achieved about 31% of the allowable strain. Thus, the strengthening system proved to be inefficient because it did not utilize as much of the available strain as possible. This was

www.manaraa.com

due to premature debonding of the laminate that was initiated at the location of the reentrant corner. See Appendix B for the map of sensors and for the strain in pi-gauges located at the midspan.

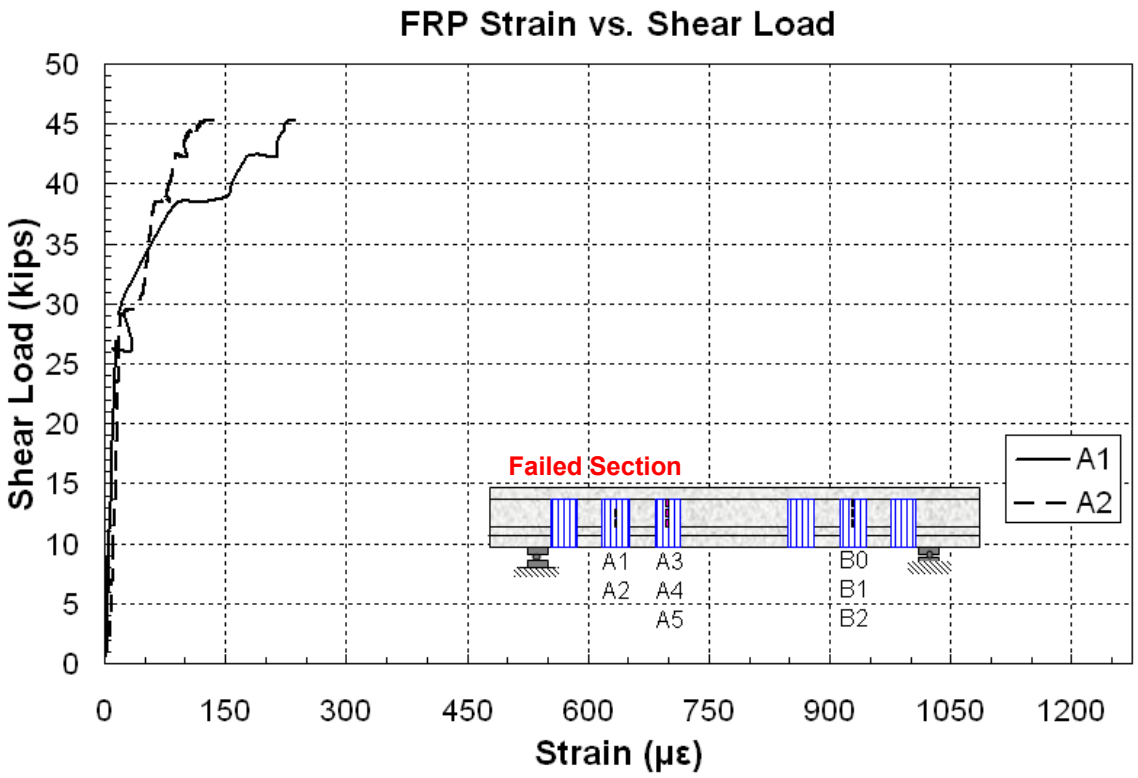

Figure 7.12 – B-2a Strain in CFRP (Gauges A1 & A2)

www.manaraa.com

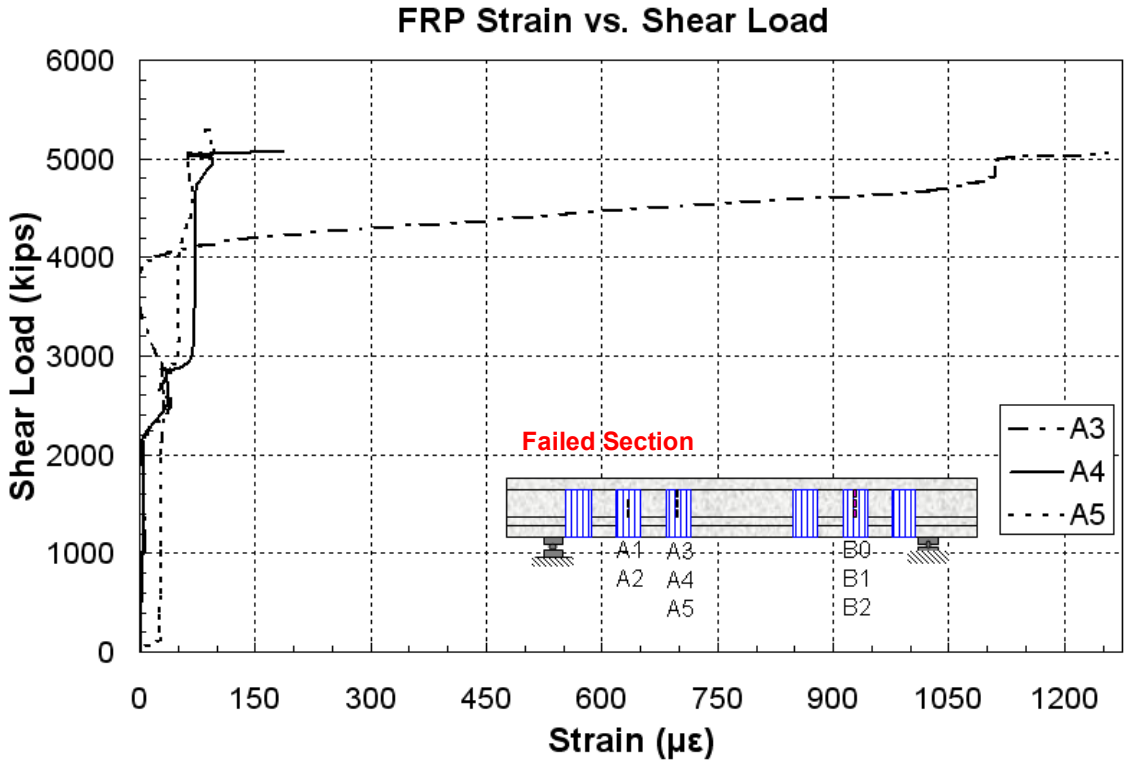

Figure 7.13 – B-2a Strain in CFRP (Gauges A3, A4, & A5)

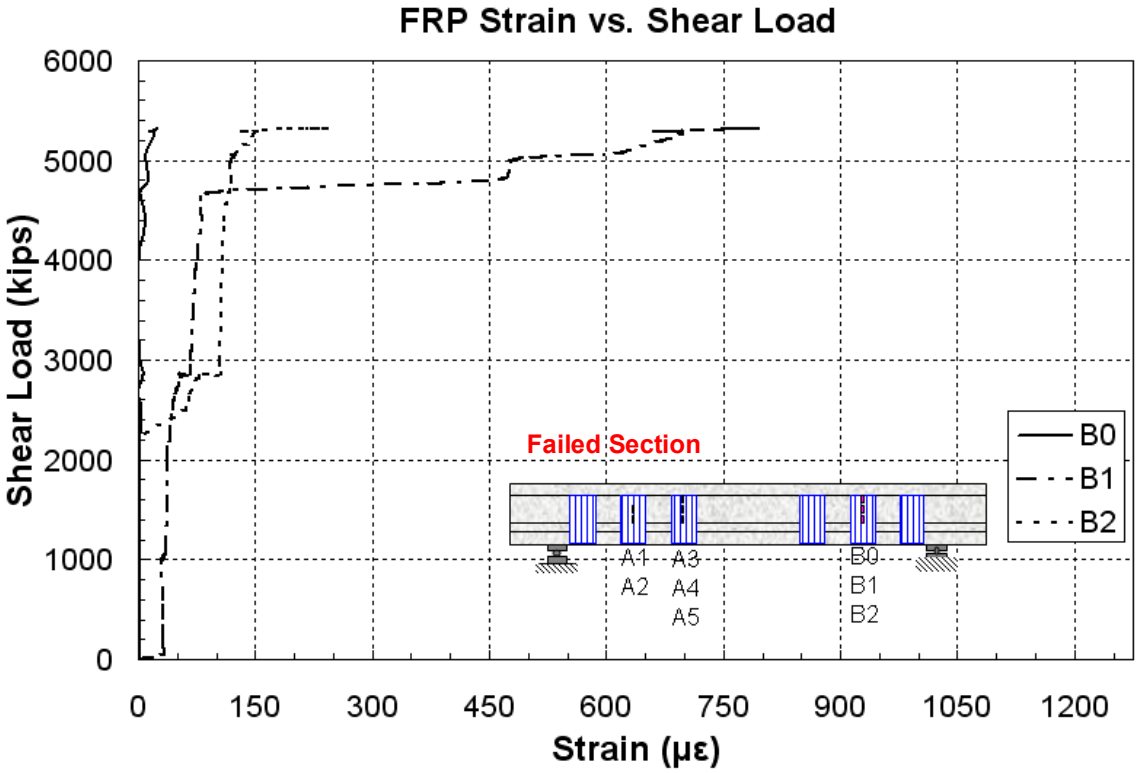

Figure 7.14 – B-2a Strain in CFRP (Gauges B0, B1, & B2)

www.manaraa.com

7.4 BEAM B-2b RESULTS

Beam B-2b was the second specimen to be tested in order to verify the effectiveness CFRP laminates have on I-shaped beams. The first flexural cracks were observed, as usual, in the middle third of the beam at a load of 15 kips (66.7 kN) and the first shear cracks, in the web, were observed at a load of 22 kips (97.8 kN). Stabilization of the flexure cracks were also observed at 22 kips. Failure of the specimen finally occurred at a load of 47.8 kips (212.6 kN). As the loading reached the maximum capacity, significant amounts of cracking were being heard and it was decided to stop loading the specimen so that cracks could be marked. Once stopped, the cracking sounds continued until suddenly failure occurred. It was determined that the sounds being heard were that of the laminates straightening and debonding. This mode of failure shows that the CFRP laminates stored a great deal of energy that eventually led to failure even though no additional external loading was being applied. The maximum capacity of beam B-2b is roughly the same capacity achieved as the control (only 0.2% difference). However, when the maximum shear loads are normalized with respect to f_c, the specimen overachieved by a factor of 0.27 (values obtained in Figures 7.1) or 3.7%. The maximum deflection achieved was about 46% less than that of the control. The reduction in deflection due to the CFRP stiffness and it "holding" the specimen together once again confirms what was determined in the previous test and past research. Figure 7.15 shows the load-deflection diagram.

www.manaraa.com

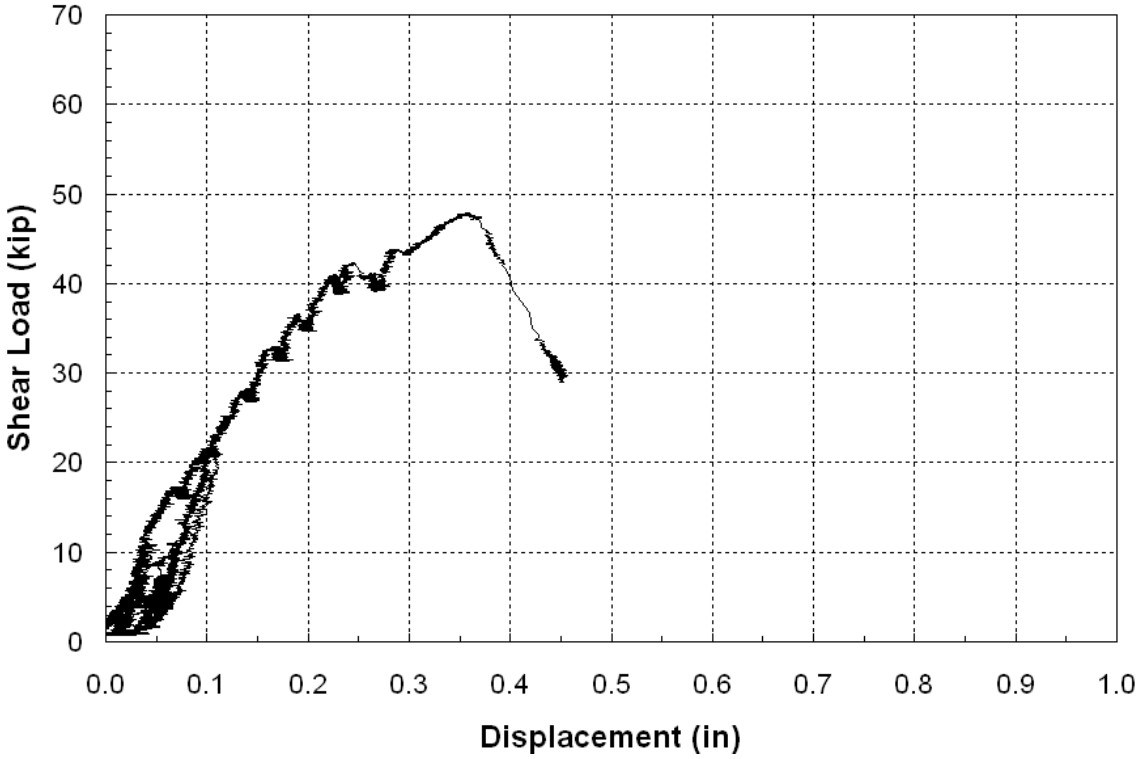

Figure 7.15 – B-2b Load - Deflection

Failure of the specimen was due to straightening and peeling of the laminates and a principal shear crack that had a width of approximately 3/8 inch (9.5 mm). Minor differences in the amount of cracks that had formed were observed between specimens B-2a and B-2b. However, there was a main difference in the crack pattern. The principal shear crack passed through all three of the laminates and terminated before reaching the support. This caused straightening of the two laminates closest to the support. Figure 7.16 shows the failed section of the specimen and Figure 7.17 shows the crack pattern.

www.manaraa.com

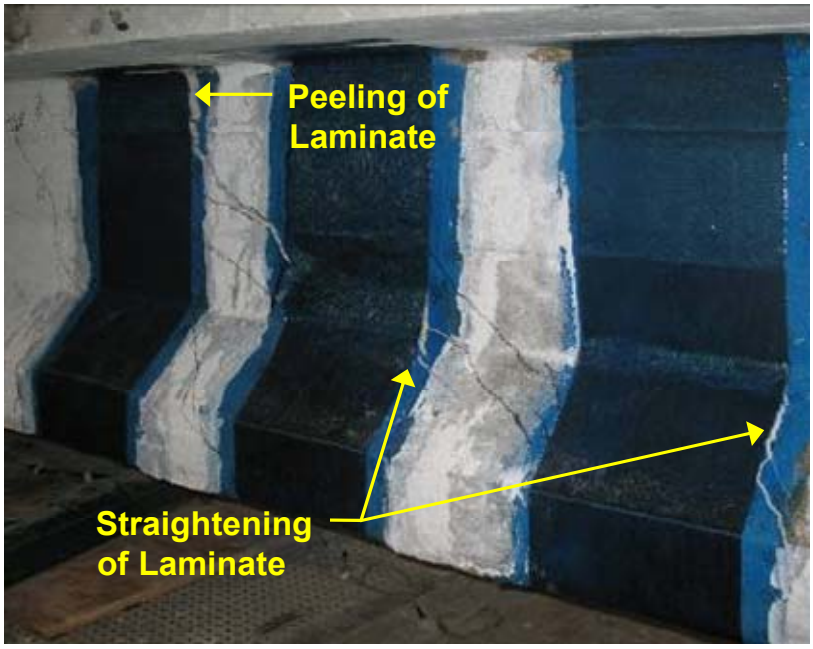

Figure 7.16 – B-2b Failed Section

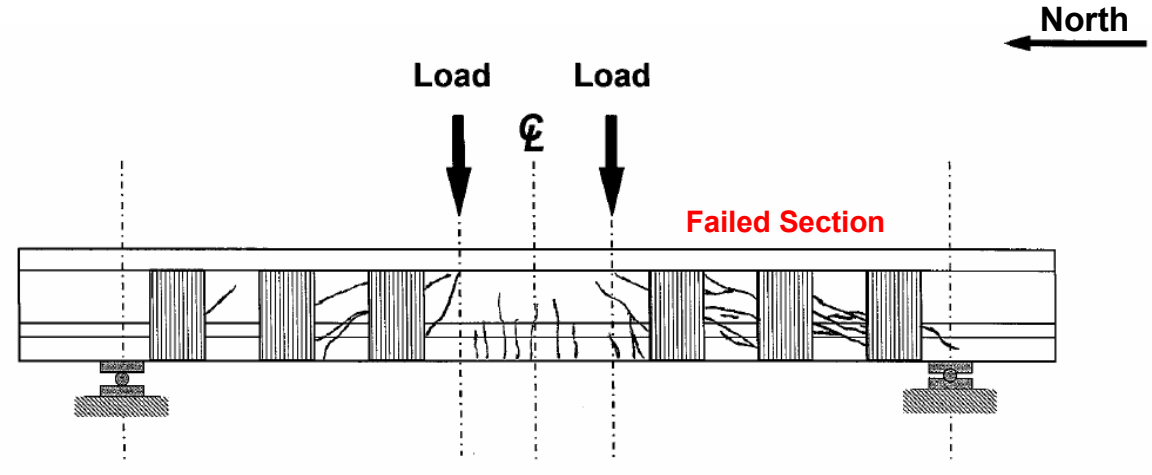

Figure 7.17 – B-2b Crack Pattern

Significant levels of strain were first observed at a shear load of about 28 kips (124.5 kN). This was due to shear cracks that had just formed and were observed intersecting the laminates. Similarly to beam B-2a, the CFRP laminates had no contribution to the shear strength up to this loading point. As the loading increased, the level of strain in A3, A4, and B1 increased linearly at a high rate. This was due to widening of the shear cracks that had intersected the laminates and the close proximity of

www.manaraa.com

the gauges to the area where the laminates bridged the shear cracks. At a load of about 35 kips (155.7 kN), the strain in A2 began to increase drastically. This was due to the laminate bridging a crack that had propagated through the laminate around the area of the reentrant corner. At about 37 kips (164.6 kN), the strain in B2 began to increase drastically. This was also due to the laminate bridging a shear crack that had propagated through it. Popping and cracking sounds along with some small amounts of the laminate bulging were observed and signified the beginning stages of debonding and straightening. As stated earlier, the straightening was due to the peeling stress caused by the reentrant corner. As in beam B-2a, B0 did not record any significant levels of strain because it was outside the area where the principal shear crack had formed. The highest levels of strain achieved were 1360, 1474, and 1368 με by gauges A2, A3, and A4, respectively. This was expected because the gauges were in the failed section side and as can be seen in Figure 7.17, there were a significant amount of shear cracks that were bridged by the laminates. Furthermore, this can be seen in Figure 7.21 which shows the strain progression in each of the laminates instrumented. In the figure, the path of the principal shear crack can be observed by the strain that was recorded.

Similarly to beam B-2a, the maximum levels of strain achieved were much less than the limit of 4000 με and supported what was found in the B-2a test that the strengthening system proved to be inefficient. The highest strain achieved was about 37% of that of the limit. Figures 7.18 through 7.20 show the strain plots. See Appendix B for the map of sensors and for the strain in pi-gauges located at the midspan.

www.manaraa.com

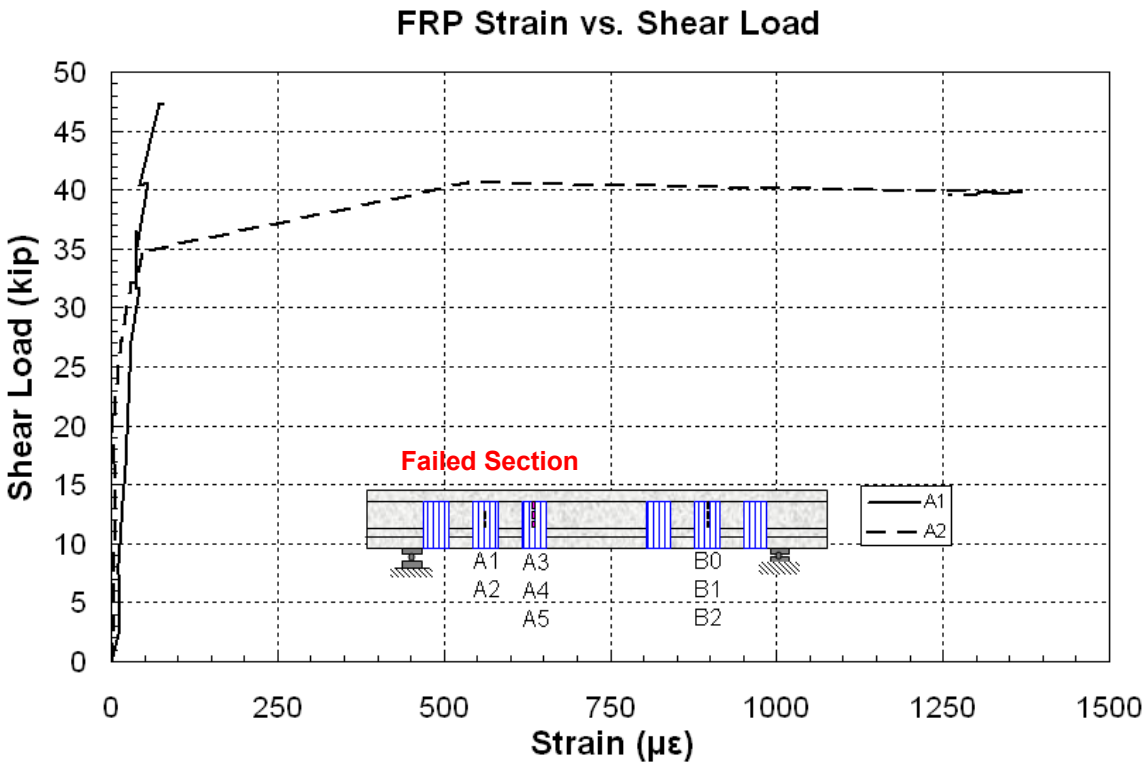

Figure 7.18 – B-2b Strain in CFRP (Gauges A1 & A2)

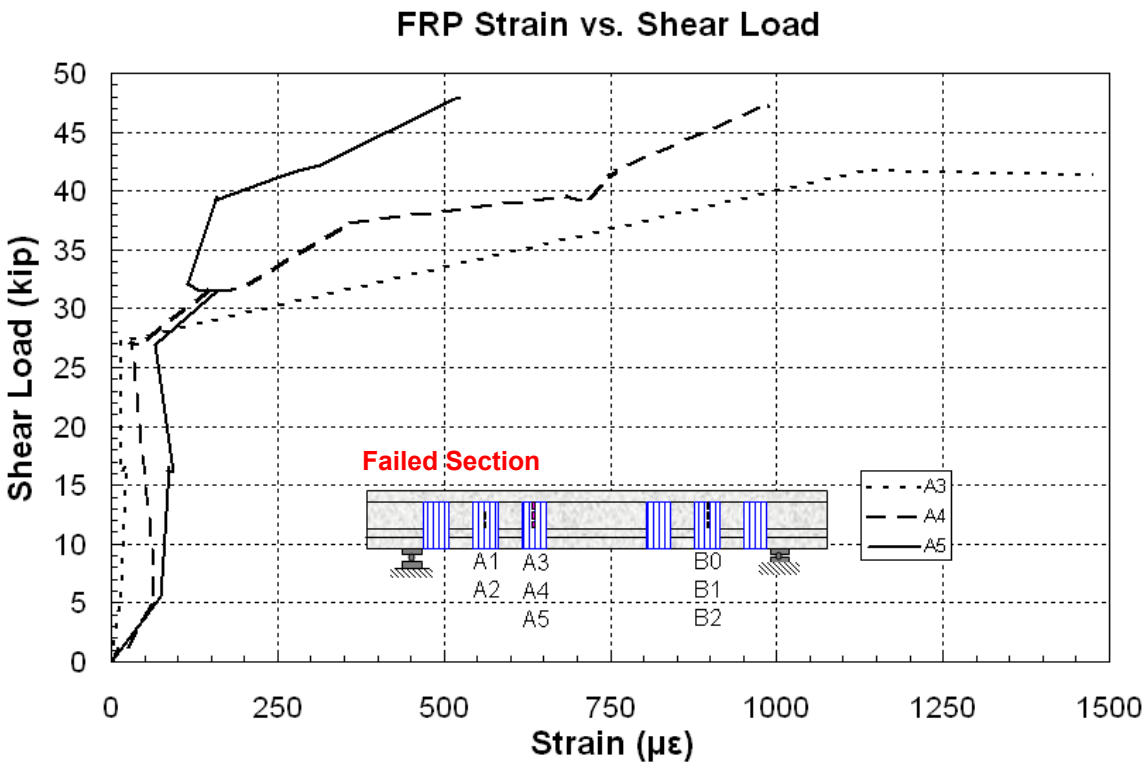

Figure 7.19 – B-2b Strain in CFRP (Gauges A3, A4, & A5)

www.manaraa.com

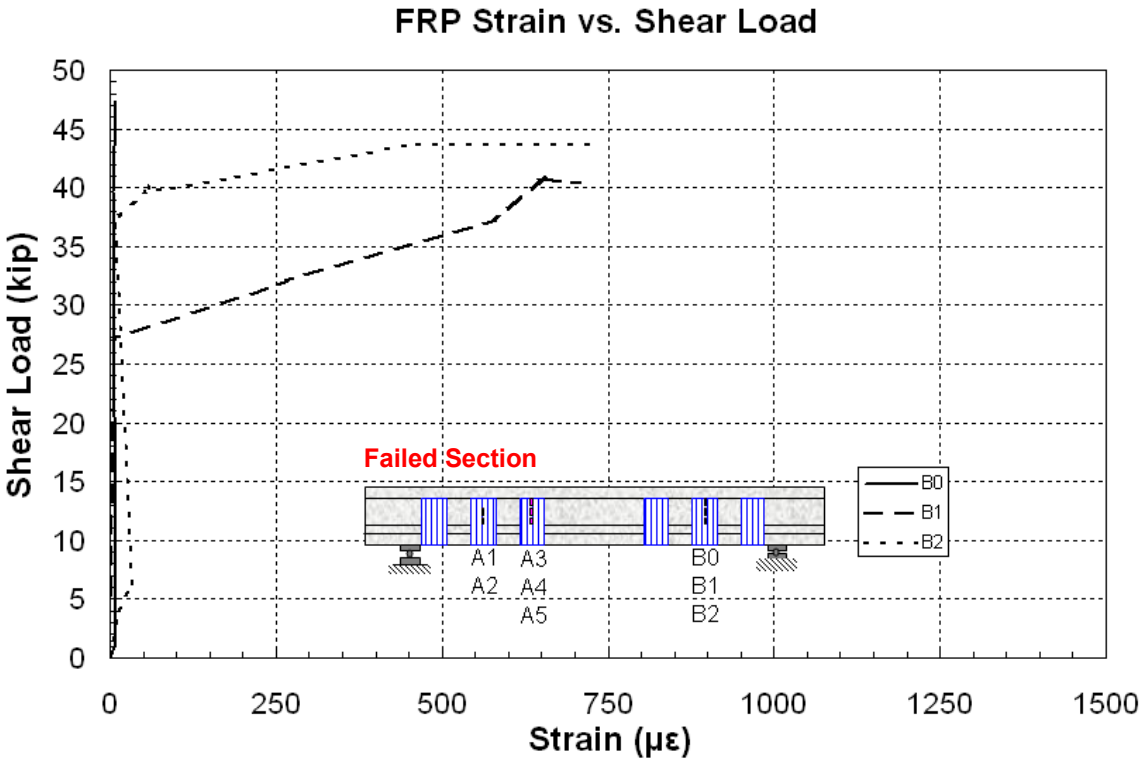

Figure 7.20 – B-2b Strain in CFRP (Gauges B0, B1, & B2)

www.manaraa.com

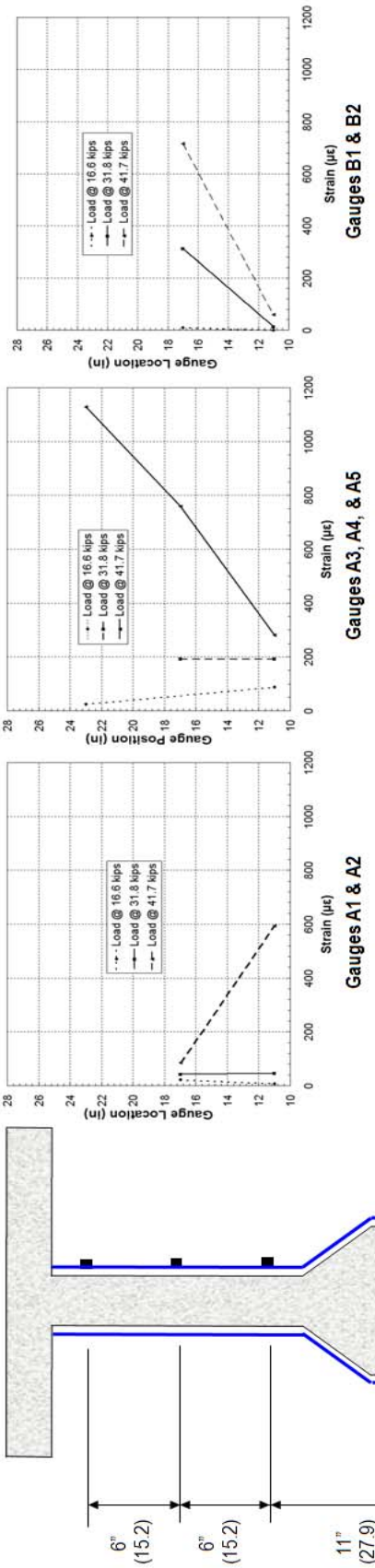

Figure 7.21 – B-2b Strain Progression
Note (SI Conversion in cm)

www.manaraa.com

7.5 BEAM B-3a RESULTS

Beam B-3a was the first specimen tested with anchorage that utilized a horizontal laminate. The first flexure cracks were observed at a load of 20 kips (88.9 kN). Although cracking could be heard in the shear region of the beam, the first shear cracks were not observed until a load of 32 kips (142.3 kN). This was because more of the surface area of the beam was covered with the laminates thus the cracks could not be observed. However, as the loading continued to increase, cracks were observed in the horizontal laminate used as anchorage. Since the fibers in the laminate are unidirectional and were not oriented perpendicular to the shear cracks, a splitting or pulling apart effect was observed in the horizontal laminate. This is illustrated in Figure 7.22.

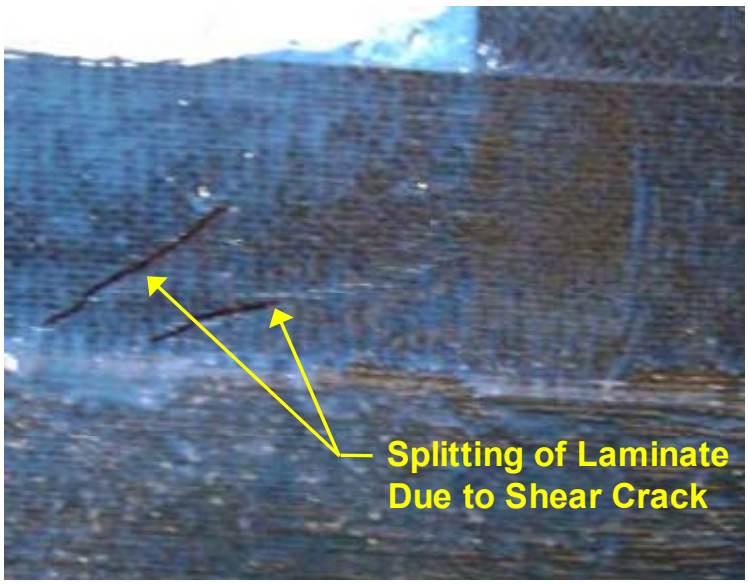

Figure 7.22 – Cracks in Laminate

Stabilization of the flexure cracks was observed at a load of about 52 kips (231.3 kN). At this same loading, multiple shear cracks were observed intersecting the laminates on both sides of the beam. On the right side of the beam (farthest side from the lab doors) two

www.manaraa.com

principal shear cracks were observed intersecting the center laminate. These two cracks would eventually lead to failure of the beam. Failure of the beam occurred at a shear load of 67.4 kips (299.8 kN) and a maximum deflection of 0.68 inches (17.3 mm). This was an increase in shear strength (with respect to the control) of about 41% and an increase in deflection of about 1.5%. When the normalized values are compared, the beam had an increase in shear strength of about 47%. When beam B-3a is compared to the normalized values of B-2a and B-2b, B-3a achieved a higher shear load of about 47% and 42%, respectively, over the other beams (an average of 44%). Figure 7.23 shows the load-deflection diagram and Figure 7.24 shows the crack pattern.

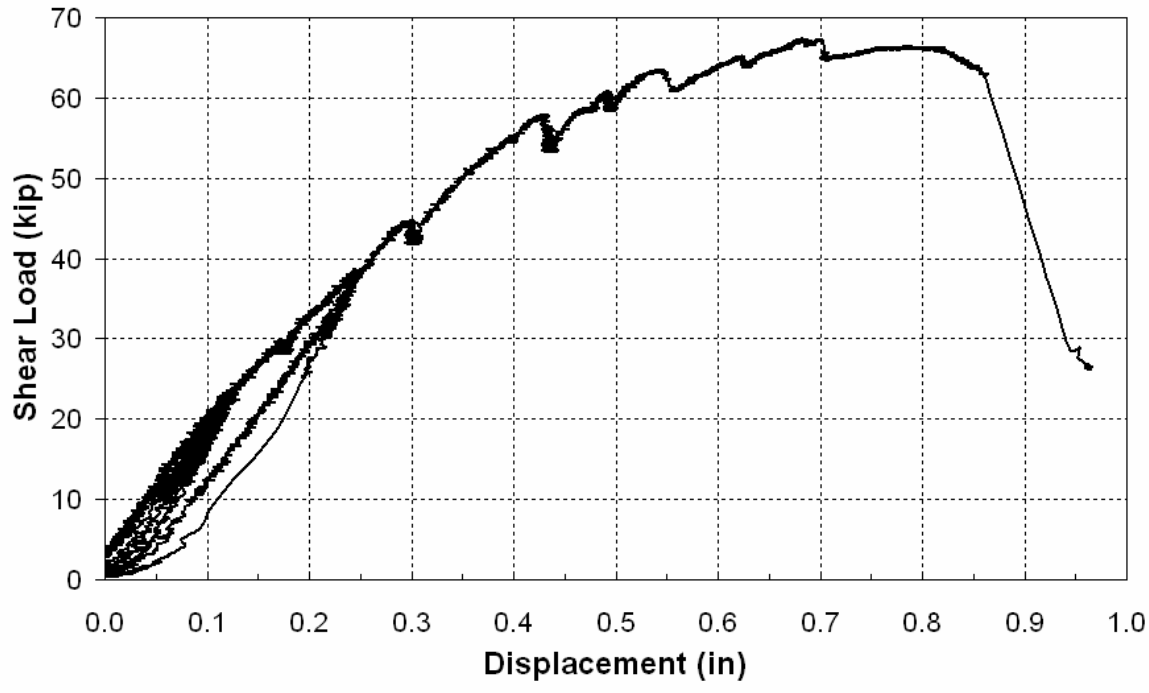

Figure 7.23 – B-3a Load - Deflection

www.manaraa.com

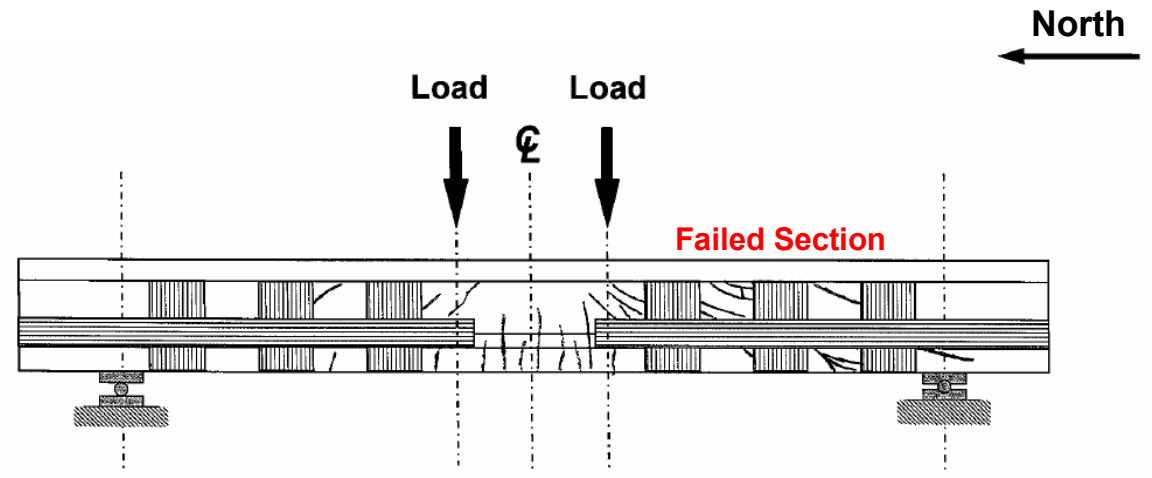

Figure 7.24 – B-3a Crack Pattern

Failure of the beam occurred once delamination of the horizontal laminate took place, resulting in straightening of the vertical laminates. As the load was approaching its peak, a significant amount of cracking sounds could be heard. This was due to the laminates beginning to debond. Once the loading reached its peak, the horizontal laminate debonded simultaneously with the vertical laminates resulting in failure of the beam. This gives reason to believe that the horizontal laminate kept the vertical laminates from prematurely debonding allowing a higher shear capacity to be achieved. The horizontal laminate had duel functionality. It not only had an anchor effect but also a crack bridging effect as it was observed to bridge shear cracks that had formed. This contributed to the total shear resistance because it provided resistance to the horizontal component of the principal stress that the vertical laminates could not provide as effectively. The horizontal laminate is the controlling factor because once it debonds, failure of the entire strengthening system and consequently the beam occurs.

www.manaraa.com

As the shear cracks continued to grow and debonding began in the horizontal laminate, the strength could be observed to decrease somewhat and then increase a small amount until complete debonding and failure occurred. This can be seen in Figure 7.23 within the deflection range of 0.5 and 0.7 inches (12.7 and 17.8 mm). Splitting of the horizontal laminate was also observed. This was due to the fact that the fibers in the horizontal laminate were unidirectional which does not allow it to resist shear forces that are perpendicular to the fiber orientation. Figures 7.25 through 7.27 show the beam after failure.

Figure 7.25 – B-3a Failed Section 1

www.manaraa.com

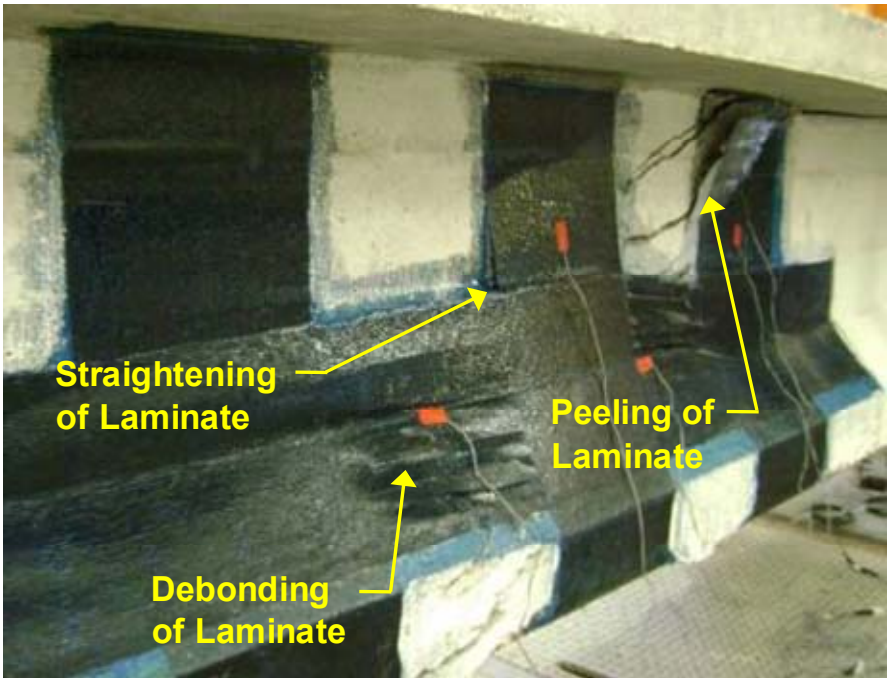

Figure 7.26 – B-3a Failed Section 2

Figure 7.27 – Close-up of Horizontal Anchorage

www.manaraa.com

Increases in the levels of strain were first observed at a load of about 42 kips (186.8 kN). Strain gauges A4 and B1 showed the largest increase in strain at this loading due to shear cracks that were observed intersecting the laminates. At a load of about 56 kips (249.1 kN), levels of strain in gauges A3 and A5 increased dramatically. The increase of strain in A3 was due to several shear cracks that were intersecting the laminate at this location and the increase of strain in A5 was because the horizontal laminate engaged the vertical laminate. At this point, the CFRP system began contributing to the shear capacity by: 1) bridging of shear cracks by the vertical laminate and 2) bridging of shear cracks and anchorage of the vertical laminates by the horizontal laminate. It can be argued that the horizontal laminate not only prevented premature debonding of the vertical laminate but also allowed for redistribution of the strain from the vertical laminate to the horizontal one. This is because the horizontal laminate not only anchors the vertical laminates but also provides external reinforcement over a greater area of the concrete substrate. This can be observed by comparing the strain plots of beams B-2a and B-2b to that of B-3a. The strain plots for B-3a are presented in Figures 7.28 through 7.30. The first significant levels of strain in B-2a and B-2b were observed to occur about 10 kips (44.5 kN), or about 25%, lower than that of B-3a. This redistribution of strain is similar to what was observed in other research projects for beams that had both internal and external shear reinforcement (i.e. Hutchinson et al.1999, Deniaud et al. 2001, Bousselham et al. 2004).

Gauge A2 did not record any significant levels of strain and the negative strain recorded was due to failure of the laminate which is illustrated in Figure 7.22. The

www.manaraa.com

sudden decrease in A5 was due to debonding of the horizontal laminate. This debonding led to failure of the specimen. The highest levels of strain achieved were 2192 and 2019 με by gauges A3 and A5, respectively. Peeling of the laminate occurred at the location of A3. These levels of strain were about 55% and 51% that of the limit of 4000 με. The efficiency of the strengthening system in B-3a was about 16-22% better than that of B-2a and B-2b which resulted in a shear capacity increase of about 47%. The different locations of the gauges on the horizontal laminate allowed for certain observations to be made. Gauge A5 was placed on the horizontal laminate and close (about ≥ 1 inch (25.4 mm)) to the vertical laminate whereas gauge A2 was placed on the horizontal laminate midway between both vertical laminates. The close proximity of A5 to the vertical laminate allowed A5 to record strain levels as the vertical laminate engaged the horizontal one. This also allowed for the determination of when the horizontal laminate begins to engage and prevent debonding. Figure 7.31 shows the progression of strain in the laminates. See Appendix B for the map of sensors and for the strain in pi-gauges located at the midspan.

www.manaraa.com

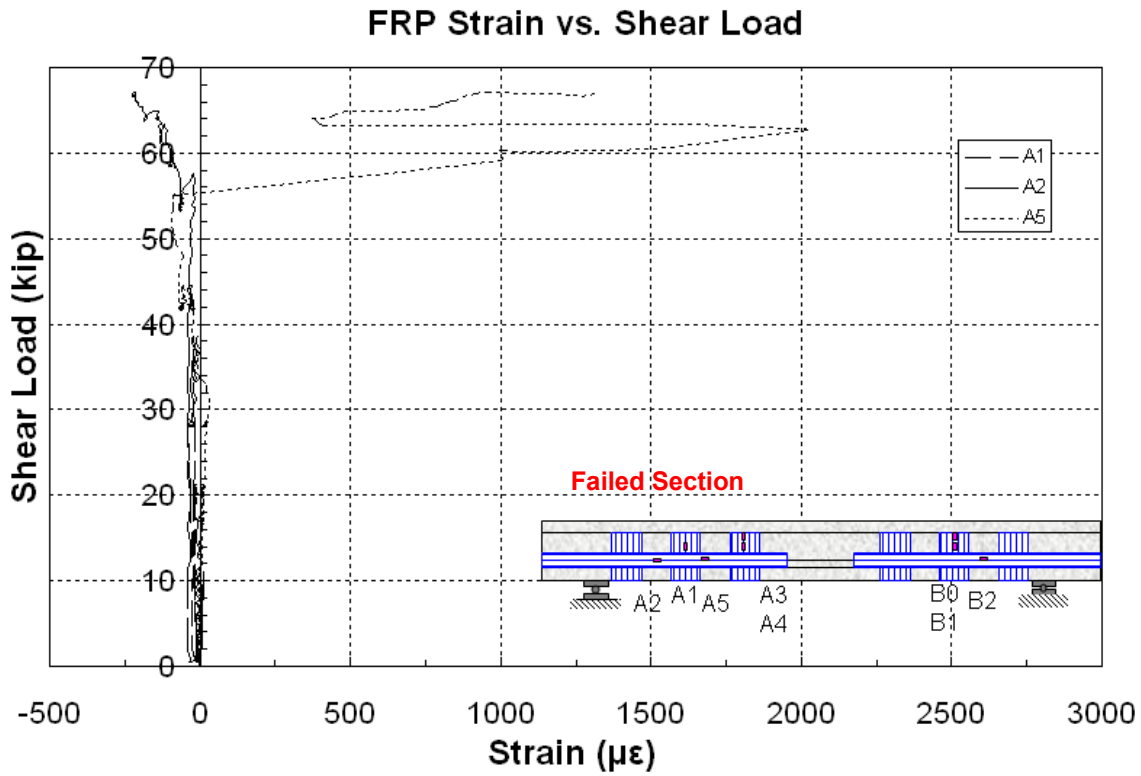

Figure 7.28 – B-3a Strain in CFRP (Gauges A1, A2, & A5)

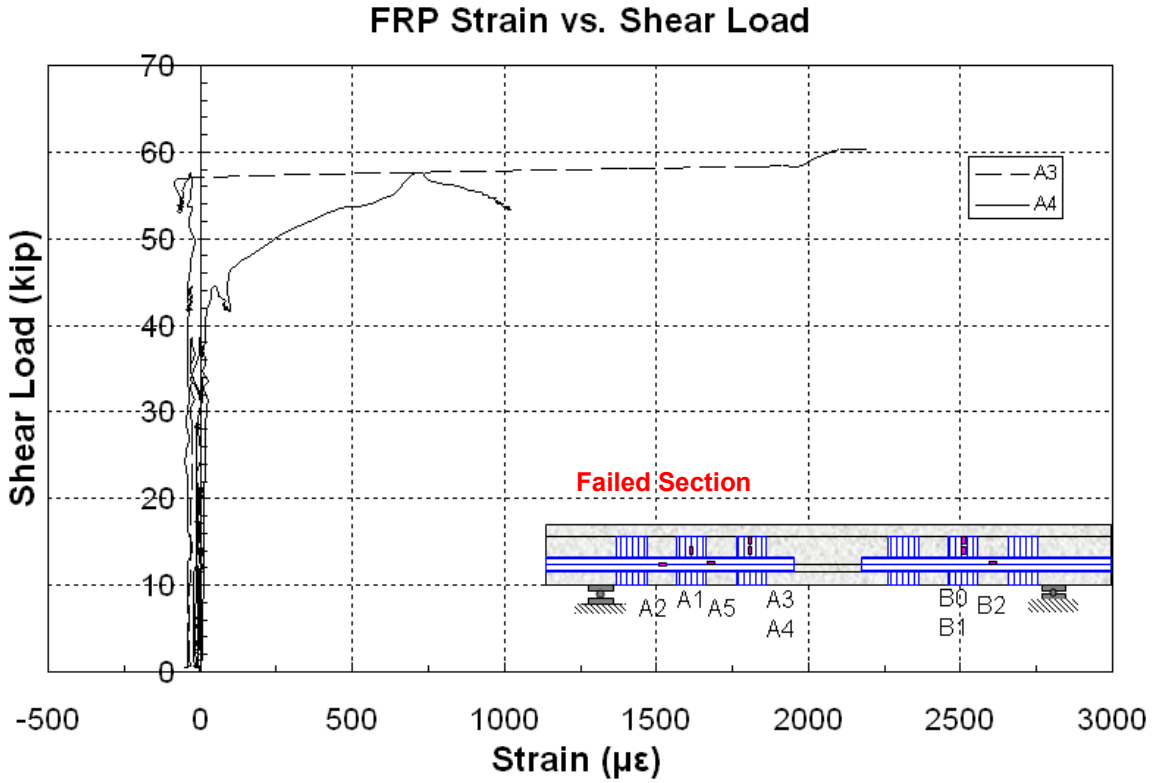

Figure 7.29 – B-3a Strain in CFRP (Gauges A3 & A4)

www.manaraa.com

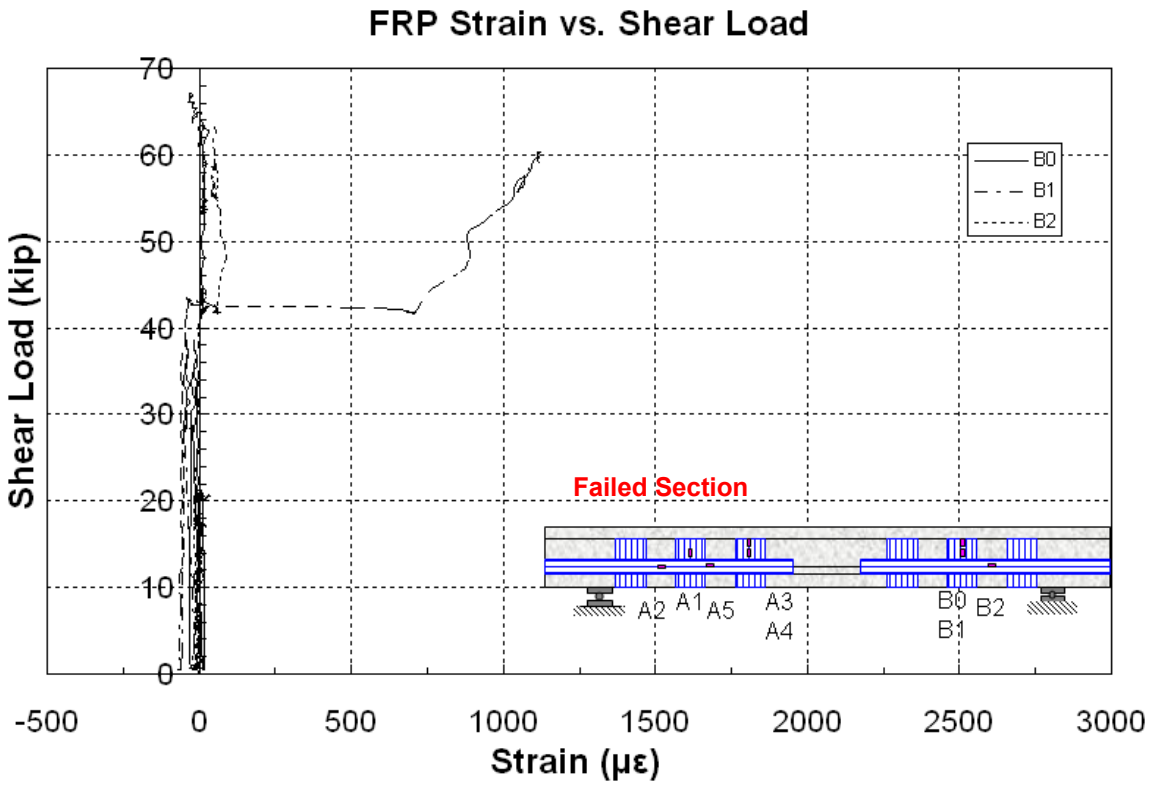

Figure 7.30 – B-3a Strain in CFRP (Gauges B0, B1, & B2)

www.manaraa.com

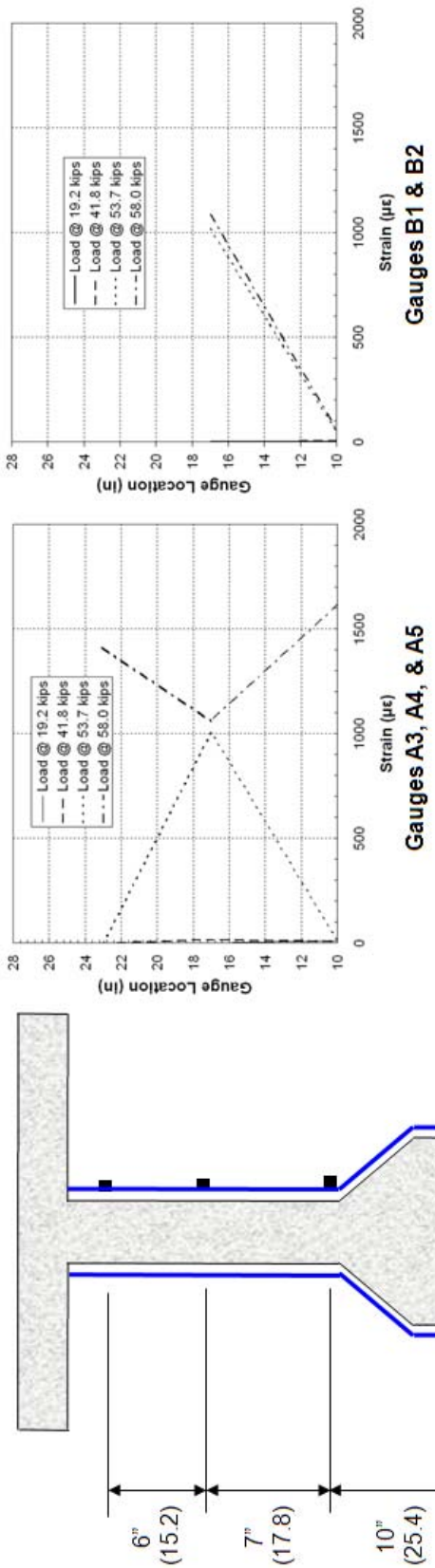

Figure 7.31 – B-3a Strain Progression Note (SI Conversion in cm)

www.manaraa.com

7.6 BEAM B-4a RESULTS

Beam B-4a used GFRP spikes as anchorage and was the last specimen tested. The first flexure cracks were observed at a load of 17 kips (75.6 kN) and the first flexure-shear cracks were observed at a load of 25 kips (111.2 kN). The first shear cracks that intersected the laminates occurred at a load of 32 kips (142.3 kN). Stabilization of the flexure cracks was observed at a load of 44 kips (195.7 kN), which is about 15% lower than beam B-3a. Very few shear cracks (that could be observed) formed after this loading until failure. Failure of the specimen occurred at a load of 61.4 kips (273.1 kN) and maximum deflection of 0.62 inches (15.7 mm). This is an increase in shear strength of about 28.2% and a decrease in maximum deflection of about 7.5%. When compared to the normalized values, the beam had an increase of shear load of about 30.1%. When compared to specimens B-2a and B-2b, B-4a had an increase in shear strength of about 29.8 and 25.5%, respectively (an average of 27.7%). When compared to B-3a, B-4a only achieved about 88.5% in shear strength of what was achieved with B-3a. Figure 7.32 shows the load-deflection diagram.

www.manaraa.com

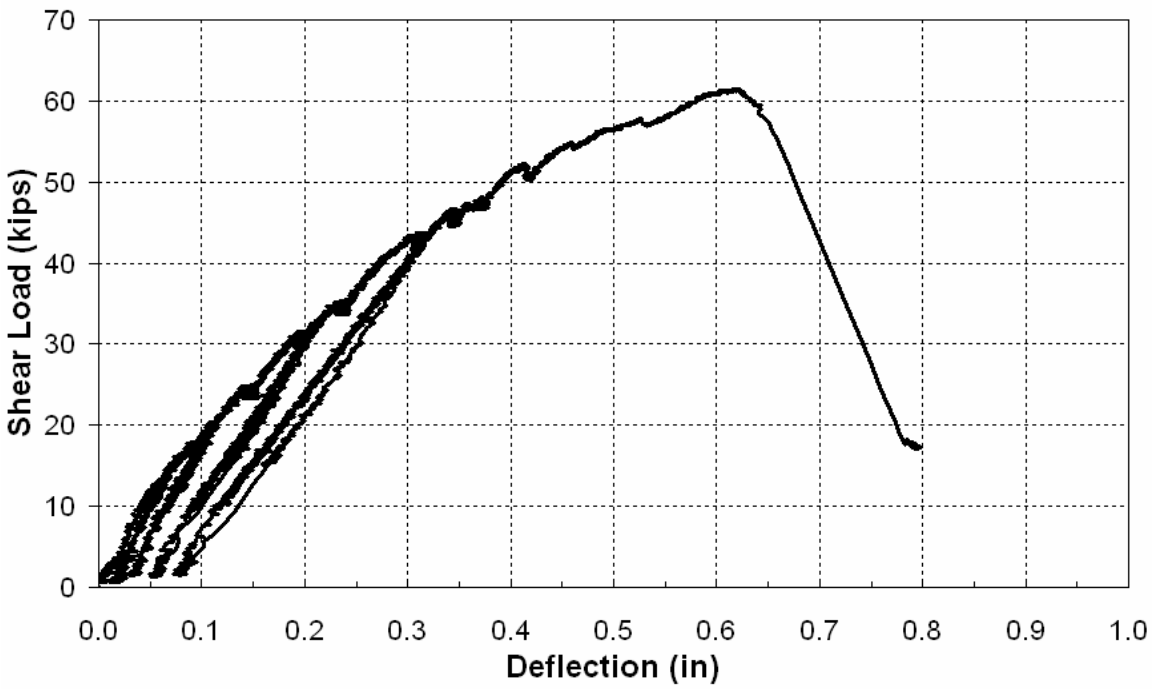

Figure 7.32 – B-4a Load - Deflection

Failure of the specimen occurred due to straightening of the laminate and rupture of the GFRP spike at the flared end. During the test, straightening of the laminate was observed to have initiated along its edge and continued until it reached the general area of the GFRP spike. This was observed in both sides of the beam. Failure finally occurred once the maximum strain in the spike was reached causing it to rupture. Splitting, or tearing, of the two laminates closest to the loading point was also observed along with rupture of the spike. The reason for this was because since the spike ruptured at the flared end, part of the spike stayed attached to the laminate keeping it from debonding whereas the parts that broke free allowed the laminate to debond. This shows that failure of the laminate (and as a result the beam) is dependent on the rupture strength of the spike at the flared end. Figure 7.33 shows the crack pattern and Figures 7.34 through 7.36 illustrate the failure mode encountered.

www.manaraa.com

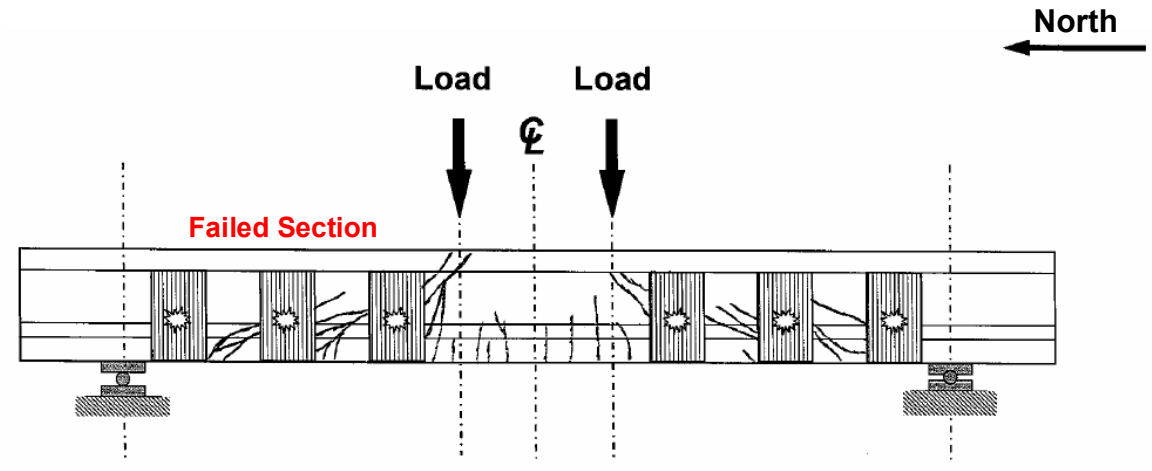

Figure 7.33 – B-4a Crack Pattern

Figure 7.34 – B-4a Failed Section

www.manaraa.com

Figure 7.35 – B-4a Failed Laminate

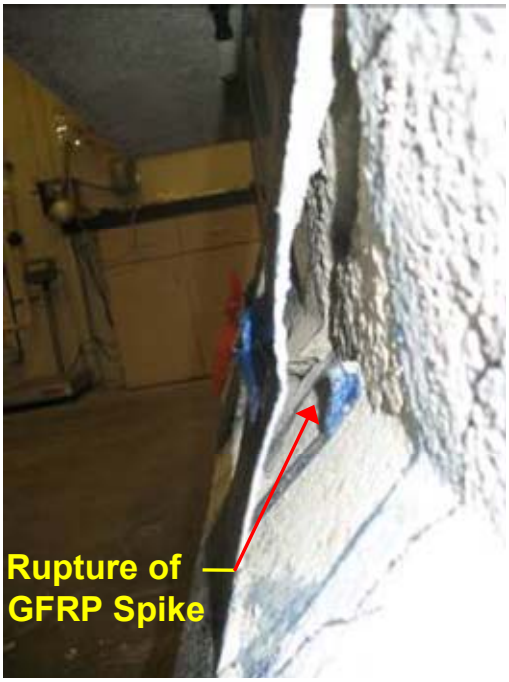

Figure 7.36 – B-4a Spike Failure

A significant increase of strain in the laminates was first observed at a load of about 35 kips (155.7 kN). A key difference between the strain plots of B-4a, which are shown in Figures 7.37 through 7.39, and the others was that the last loading-unloading cycle could be observed in the strain plot. This cycle occurred at a time when the laminates had engaged by bridging of the shear cracks. When the loading was released to about 2 kips (8.9 kN), the strain did not return to zero which showed the laminate was now engaged and contributing to the shear strength of the beam. As expected, strain gauges A0 and B0 had no significant increase in strain because the gauges were outside of the area where the principal shear cracks would have formed. The increase of strain in A1, A3, A4, and B1 was due to shear cracks that were observed intersecting the laminates at these locations.

www.manaraa.com

The highest level of strain achieved was about 5813 με by A5. A possible explanation for this is that the gauge was placed on the flared end of the spike, thus, recording the strain in the spike. The next group of gauges that achieved high levels of strain was A4 and B2 with strain levels of 1342 and 1309 με, respectively. The strain in A5 was about 145% of that of the limit of 4000 με. The strain in A4 and B2 was about 34% of that of the limit. If A5 is disregarded due to the location of the gauge (as previously stated), the laminates still were not very efficient and had about the same efficiency as B-2a and B-2b. It can be argued that the laminates did not have a significant increase in strain, even though a higher shear capacity was achieved, because the strain was redistributed to the GFRP spikes. This was due to the GFRP spike engaging when the laminates had debonded preventing complete debonding and failure of the system, thus, improving the overall contribution of the FRP system (Eshwar et al. 2008). Figure 7.40 shows the strain progression in the CFRP laminates. See Appendix B for the map of sensors and for the strain in pi-gauges located at the midspan.

www.manaraa.com

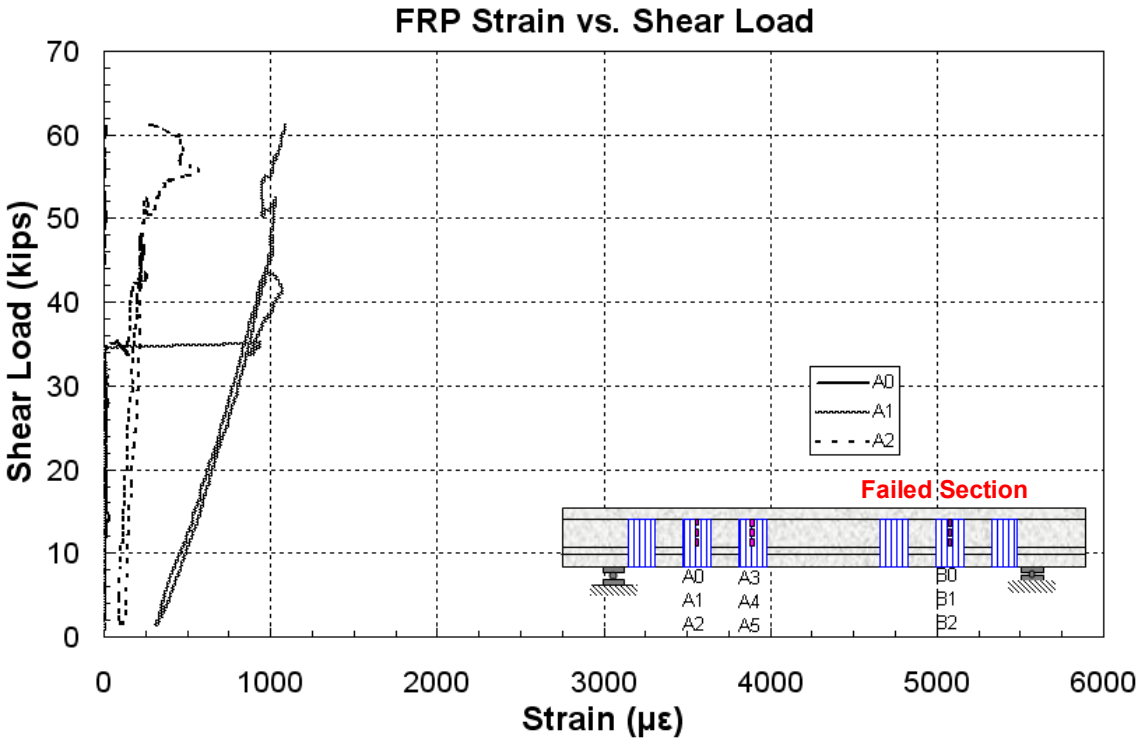

Figure 7.37 – B-4a Strain in CFRP (Gauges A0, A1, & A2)

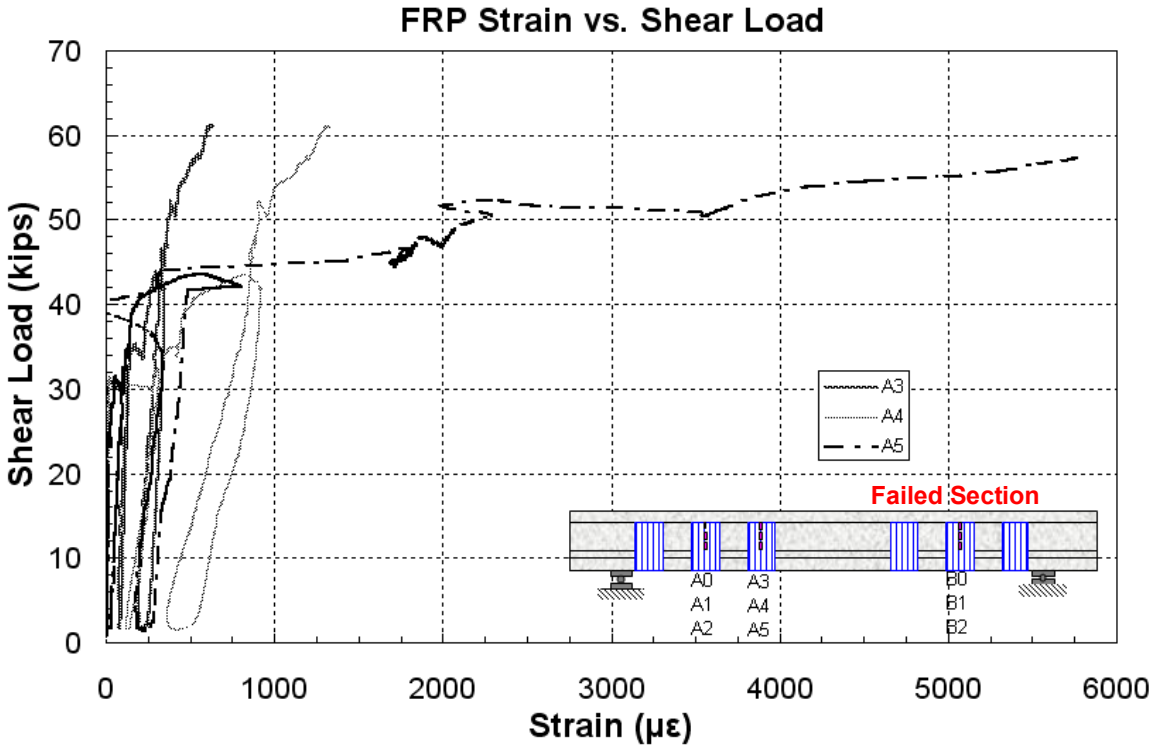

Figure 7.38 – B-4a Strain in CFRP (Gauges A3, A4, & A5)

www.manaraa.com

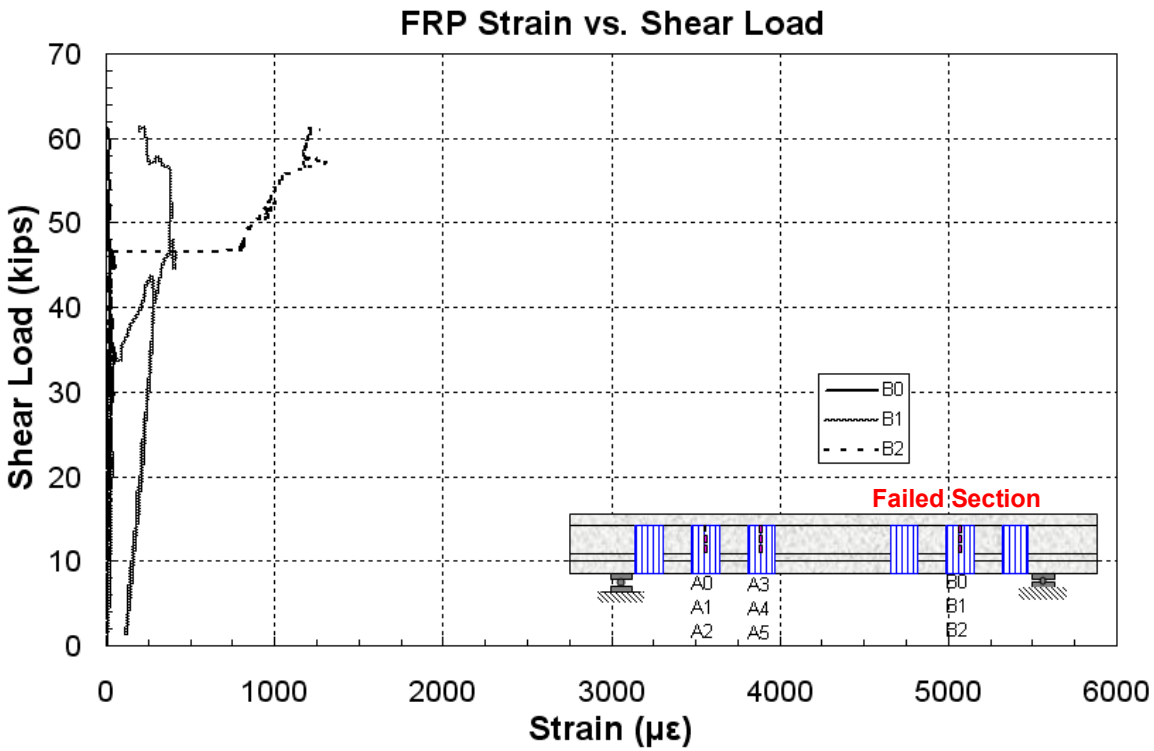

Figure 7.39 – B-4a Strain in CFRP (Gauges B0, B1, & B2)

www.manaraa.com

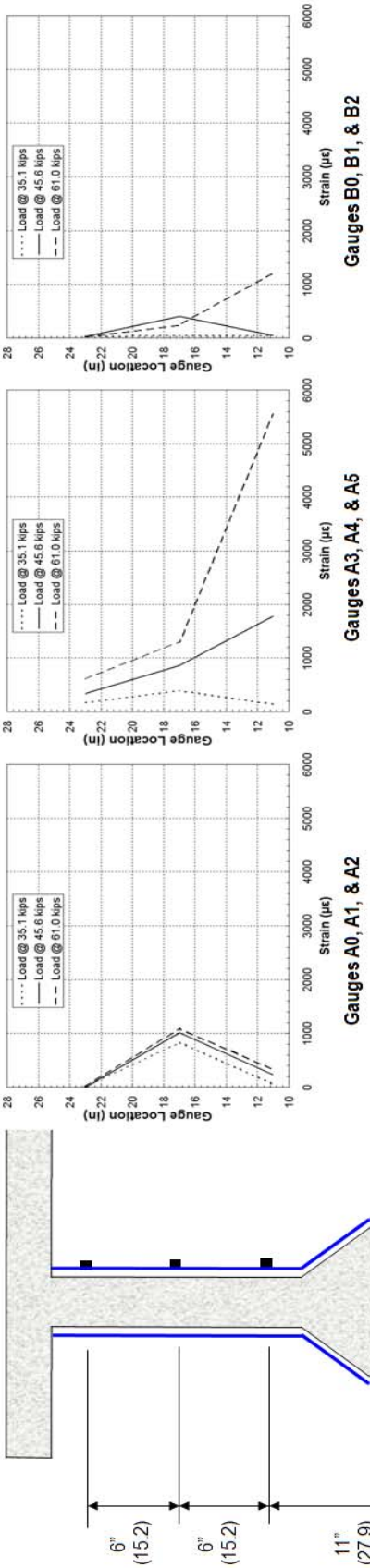

Figure 7.40 – B-4a Strain Progression
Note (SI Conversion in cm)

www.manaraa.com

CHAPTER 8

CONCLUSIONS

The tests conducted in this research projected provided valuable information into the behavior of I-section beams reinforced with CFRP laminates. More importantly, the tests demonstrated anchorage schemes that can aid in preventing premature debonding of the laminates. The data collected from the tests led to the following conclusions:

1. **Comparison to design guidelines:** The test results obtained showed that the behavior of the CFRP strengthening system with no anchorage was not captured by the ACI 440.2R-08 due to the presence of the bulb. The use of an anchorage system showed that the CFRP laminate strengthening system can attain a shear contribution similar to what is predicted by the ACI 440.2R-08 guidelines. However, the ACI 440.2R-08 does not have design guidelines for determining the shear contribution of a FRP system that utilizes anchorage schemes.

2. **Single-ply CFRP Reinforcement:** As seen in the tests of beams B-2a and B-2b, the use of single-ply CFRP laminates did not provide significant increases in strength. On average, the shear strength was increased by only 2%. This insignificant increase in strength was due to the fact that the laminates would debond prematurely. The debonding would occur due to a peeling stress that acts perpendicular to the laminate, thus, causing premature failure. Furthermore, strain in the laminates was significantly lower than the allowed limit per ACI 440.2R-08, thus, the laminates were inefficient. The laminates

www.manaraa.com

did, however, reduce the maximum net deflection of the beams by an average of 48% due to bridging of the shear cracks.

3. **Single-ply CFRP Reinforcement with Horizontal Laminate as Anchorage:** Beam B-3a achieved an increase of shear strength of about 47% which is the highest of all the beams tested with external shear strengthening. When compared to the beams that had no external anchorage, B-3a achieved a higher average normalized shear strength of 47%. Strain in the laminates was about 53% lower than the limit but had an increase of about 16-22% when compared to beams B-2a and B-2b. Failure of the beam occurred once the horizontal laminate debonded. Splitting of the horizontal laminate was observed due to the fact that the fibers were unidirectional and could not resist shear forces that were perpendicular to the fiber orientation.

4. **Single-ply CFRP Reinforcement with GFRP Spikes as Anchorage:** Beam B-4a had an increase in shear strength of about 30%. When compared to the beams that had no external anchorage, B-4a had a higher average shear strength of about 28%. When compared to B-3a, B-4a only achieved about 88% in shear strength. Again, strain in the laminates were significantly lower (about 34%) than the limit. However, strain recorded at the flared end of the spike achieved 145% that of the limit. The laminate was observed to have completely debonded at the reentrant corner until it was engaged by the GFRP spike. Failure of the beam occurred once the GFRP spike reached its ultimate

www.manaraa.com

rupture strength. Therefore, strengthening and failure of the FRP system was dependent on the GFRP spikes.

5. **Design Recommendations:** Further testing is needed to validate appropriate specifications for the anchorage schemes used. The results obtained are only preliminary in determining an appropriate anchorage system and are not sufficient in determine accurate design methodologies.

6. **Overall Performance:** Both anchorage schemes performed well in preventing premature debonding of the vertical laminates. Both schemes are practical solutions that can be applied with ease in the field. Since both systems performed relatively the same, other parameters must be taken into account when selecting the appropriate system. These parameters are: cost of materials, aesthetics, labor, etc. The horizontal laminate is much simpler to install because it does not require additional equipment or labor but is much less aesthetically pleasing and costs a little more due to the amount of extra CFRP used. The aesthetics can be solved by painting over the laminates but this adds to the cost as well. The use of spikes costs less in terms of materials but requires additional labor for drilling and prepping of the holes. Also, as stated earlier, the placement of the spike was rather difficult due to the low viscosity of the resin. The resin would easily flow out of the hole causing air voids. Furthermore, time and extra care must be taken to locate internal reinforcement ensuring that they will not be damaged during drilling adding to the labor cost. In the case of the horizontal laminate, this concern is

www.manaraa.com

eliminated. The designer must take these parameters into account to ensure the feasibility of a cost effective and viable external reinforcement.

www.manaraa.com

CHAPTER 9

RECOMMENDATIONS FOR FUTURE RESEARCH

The research has shown that the use of horizontal CFRP laminates and GFRP spikes are viable options for preventing premature debonding of CFRP shear reinforcement in bulb-shaped beams. In order to further develop and refine these methods, research recommendations have been made:

1. Exact tests of the two anchorage schemes should be done again in order to further validate the effectiveness and consistency of the anchorage schemes. These additional tests would allow a design professional to determine what additional shear strength can be expected from the use of these anchorage schemes.

2. Since premature debonding of the CFRP laminates was observed due to the bulb, section enlargement with a single-ply and no anchorage should be investigated. The section enlargement removes the constraints of the bulb by filling the web area where the laminates will be bonded to with concrete. This creates a rectangular section at these locations and removes the peeling stresses caused by the reentrant corner. Since the ACI 440.2R-08 design guidelines use a rectangular cross section as its basis, better comparisons of the efficiency of the strengthening system between theoretical and experimental results can be made.

www.manaraa.com

3. Splitting of the horizontal laminate was observed due to shear forces and the fact that the fibers were unidirectional and not in the direction of the force. Therefore, bi-directional laminates should be investigated in order to determine if this splitting effect and debonding of the laminate can be further reduced. Furthermore, the bi-directional laminate can improve the efficiency of the strengthening system by providing resistance to the two component stress caused by a shear crack that was illustrated in Figure 1.1, thus, increasing the shear capacity.

4. Since debonding was observed to occur until it reached the GFRP spike, the use of multiple spikes is suggested in order to further delay debonding of the laminate. Furthermore, since failure was dependent on the rupture strength of the GFRP spike, the use of multiple spikes to delay failure by redistribution of strain between each spike can be investigated.

5. An inclined angle for the drilled hole should be investigated in order to determine if this is a feasible way to prevent the resin from flowing out and causing the formation of air pockets that can adversely affect its strength by decreasing the surface area that is bonded. Perhaps a resin with a higher viscosity could also be used.

www.manaraa.com

REFERENCES

1. Bakis, C. E.; L. C. Bank; V. L. Brown; E. Cosenza; J. F. Davalos; J. J. Lesko; A. Machida; S. H. Rizkalla; and T. C. Triantafillou (2002). "Fiber-Reinforced Polymer Composites for Construction--State-of-the-Art Review." *ASCE Journal of Composites for Construction: 150th Anniversary Paper, Vol. 6, No. 2, pp. 73-87.*

2. National Cooperative Highway Research Program Report 549 (2005), "Simplified Shear Design of Structural Concrete Members," Published by the Transportation Research Board, Washington, DC.

3. Nilson, Arthur H.; David Darwin; and Charles W. Dolan (2004). "Design of Concrete Structures 13th ed." Published by The McGraw-Hills Companies, Inc., 1221 Avenue of the Americas, New York, NY 10020.

4. Khalifa, Ahmed; William J. Gold; Antonio Nanni; and Abdel Aziz M.I. (1998). "Contribution of Externally Bonded FRP to Shear Capacity of RC Flexural Members." *ASCE Journal of Composites for Construction, Vol. 2, No. 4, pp. 195-202.*

5. Chaallal, O.; M. J. Nollet; and D. Perraton (1998). "Shear Strengthening of RC Beams by Externally Bonded Side CFRP Strips." *ASCE Journal of Composites for Construction, Vol. 2, No. 2, pp. 111-113.*

6. Triantafillou, Thanasis C. (1998). "Shear Strengthening of Reinforced Concrete Beams Using Epoxy-Bonded FRP Composites." *ACI Structural Journal, V. 95, No. 2, pp. 107-115.*

7. Hutchinson, R. L. and S. H. Rizkalla (1999). "Shear Strengthening of AASHTO Bridge Girders Using Carbon Fiber Reinforced Polymer Sheets." *ACI Special Publication 188-80, pp. 945-958.*

8. Deniaud, Christophe and J. J. Roger Cheng (2001). "Shear Behavior of Reinforced Concrete T-Beams with Externally Bonded Fiber-Reinforced Polymer Sheets." *ACI Structural Journa,. V. 98, No. 3, pp. 386-394.*

9. Bousselham, Abdelhak and Omar Chaallal (2006). "Behavior of Reinforced Concrete T-Beams Strengthened with Carbon Fiber-Reinforced Polymer-An Experimental Study." *ACI Structural Journal, V. 103, No. 3, pp. 339-347.*

10. Eshwar, Nagaraj; Antonio Nanni; and Timothy J. Ibell (2008). "Performance of Two Anchor Systems of Externally Bonded Fiber-Reinforced Polymer Laminates." *ACI Materials Journal, V. 105, No. 1, pp. 72-80.*

www.manaraa.com

11. Sato, Y.; H. Katsumata; and Y. Kobatake (1997). "Shear Strengthening of Existing Reinforce Concrete Beams CFRP Sheet." *Proceedings of the Third International Symposium on Non-Metallic (FRP) Reinforcement for Concrete Structures (FRPRCS-3), Japan Concrete Institute, Sapporo, Japan, Vol. 1, pp. 507-514.*

12. Swamy, R.N. and P. Mukhopadhyaya (1995). "Role and Effectiveness of Non-Metallic Plates in Strengthening and Upgrading Concrete Structures." *Non-Metallic (FRP) Reinforcement of Concrete Structures, E&FN Spon, London, pp. 473-482.*

13. Taljsten, B. (1997). "Strengthening of Beams by Plate Bonding." *Journal of Materials in Civil Engineering, Vol. 9, No. 4, pp. 206-212.*

14. Bousselham, Abdelhak and Omar Chaallal (2004). "Shear Strengthening RC Beams with FRP: Assessment of Influencing Parameters and Required Research." *ACI Structural Journal, Vol. 101, No. 2, pp. 219-227.*

15. Khalifa, Ahmed and Antonio Nanni (2002). "Rehabilitation of Rectangular Simply Supported RC Beams with Shear Deficiencies using CFRP Composites." *Journal of Construction and Building Materials 16, pp. 135-146.*

16. Pellegrino, Carlo and Claudio Modena (2006). "FRP Shear Strengthening of RC Beams: Experimental Study and Analytical Modeling." *ACI Structural Journal, Vol. 103, No. 5, pp. 720-728.*

17. Khalifa, Ahmed, Tarek Alkhrdaji, Antonio Nanni, and Scott Lansburg (1999). "Anchorage of Surface Mounted FRP Reinforcement." *Concrete International, Vol. 21, No. 10, pp. 49-54.*

18. ACI 318-05 (2005), "Building Code Requirements for Structural Concrete and Commentary (318R-05)," Published by the American Concrete Institute, Farmington Hills, MI.

19. ACI 440.2R-08 (2008), "Guide for the Design and Construction of Externally Bonded FRP Systems for Strengthening Concrete Structures," Published by the American Concrete Institute, Farmington Hills, MI.

20. CAN/CSA-S6-06 (2006), "Canadian Highway Bridge Design Code," Published by the Canadian Standards Association, Mississauga, Ontario, Canada, pp. 722-724.

21. Kani, G. N. J. (1966). "Basic Facts Concerning Shear Failure." *ACI Journal Proceedings, V. 63, No. 6, pp. 675-692.*

22. Collins, Michael P. and Daniel Kuchma (1999). "How Safe are Our Large, Lightly Reinforced Concrete Beams, Slabs, and Footings?" *ACI Structural Journal, V. 96, No. 4, pp. 482-490.*

23. BASF Construction Chemicals, LLC (2008). Building Systems, 889 Valley Park Drive Shakopee, MN 55379. www.buildingsystems.basf.com

www.manaraa.com

24. Fyfe Company LLC (2008). 6310 Nancy Ridge Drive, Suite 103 San Diego, CA 92121. www.fyfeco.com

25. International Concrete Repair Institute, Inc. (2008). 3166 S. River Road, Suite 132 Des Plaines, IL 60018. http://www.icri.org/publications/bulletin.asp

26. Thorburn, J. and A. A. Mufti (2001). "Design Recommendations for Externally Restrained Highway Bridge Decks." *ASCE Journal of Bridge Engineering, Vol. 6, No. 4, pp. 243-249.*

27. Robbins, V. W. (2003). "Design of a Steel Free Bridge Deck System." Center for Transportation Research and Education, The Bridge Engineering Center at Iowa State University, 2901 S. Loop Dr., Suite 3100 Ames, IA 50010.

www.manaraa.com

APPENDIX A

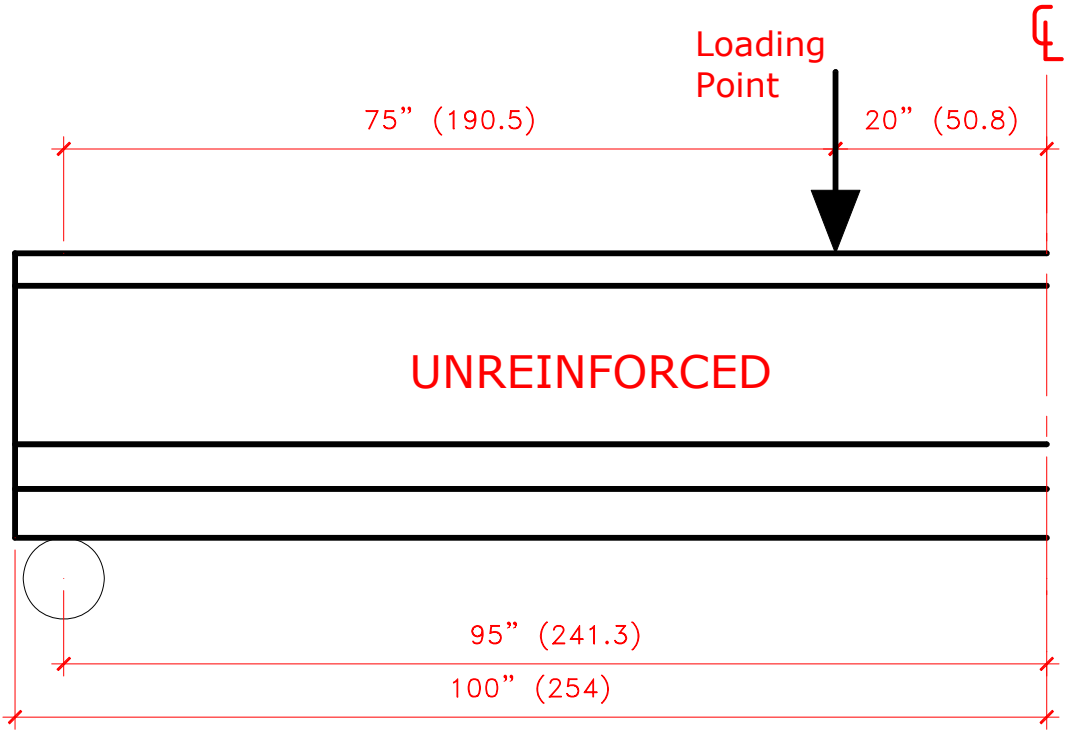

Figure A.1 – Beam Elevation
Note (SI conversion in cm)

www.manaraa.com

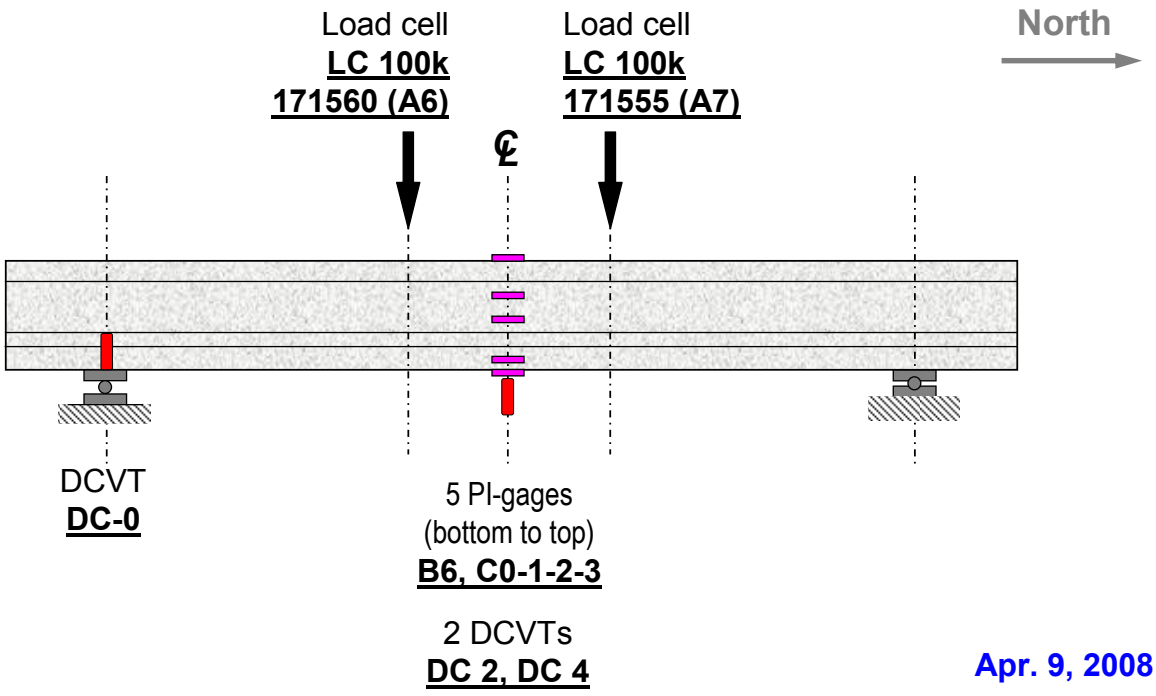

Figure B.1 – B-1a Map of Sensors

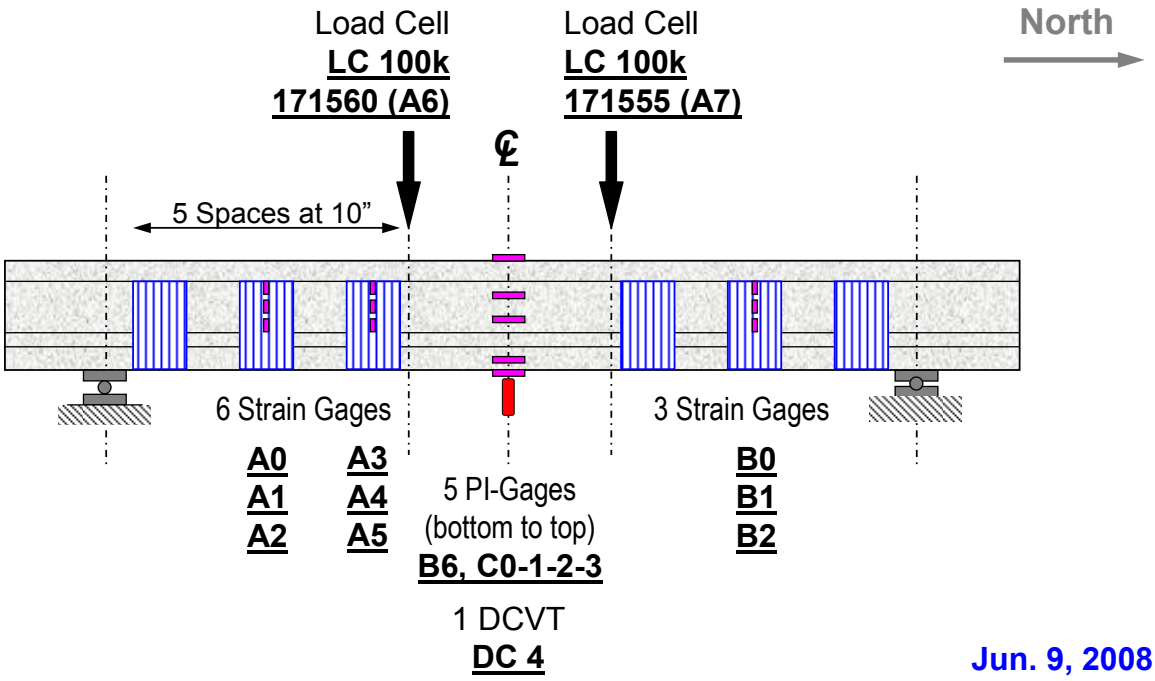

Figure B.2 – B-2a & B-2b Map of Sensors

www.manaraa.com

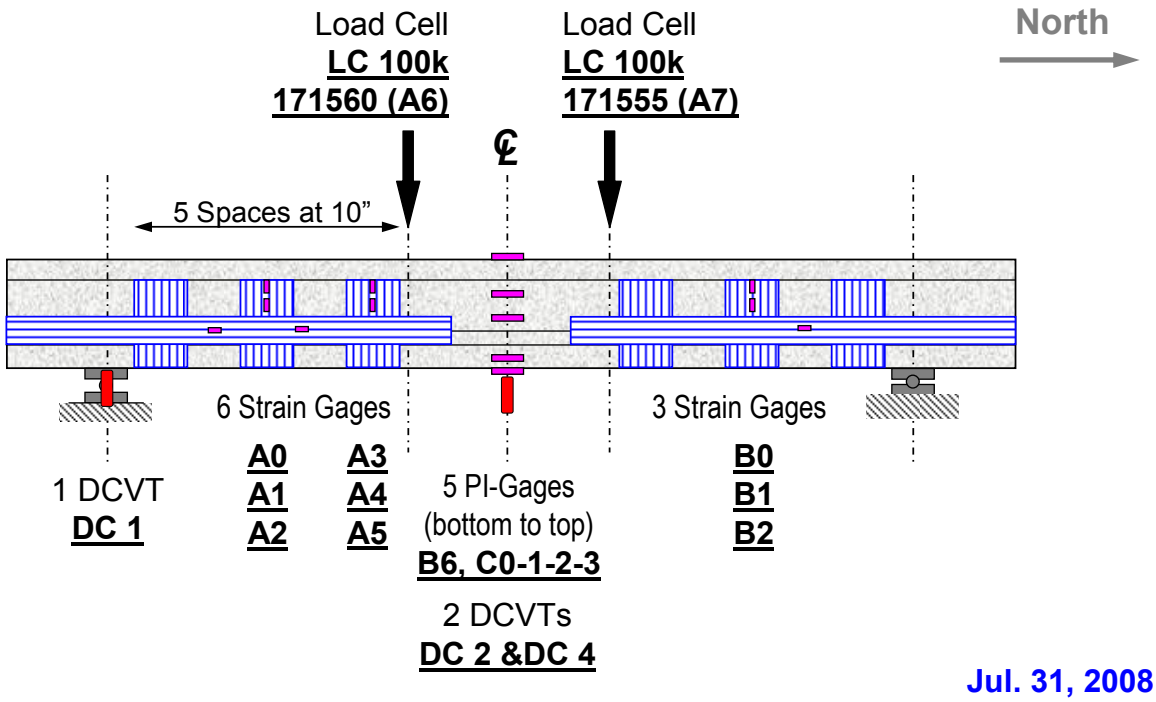

Jul. 31, 2008

Figure B.3 – B-3a Map of Sensors

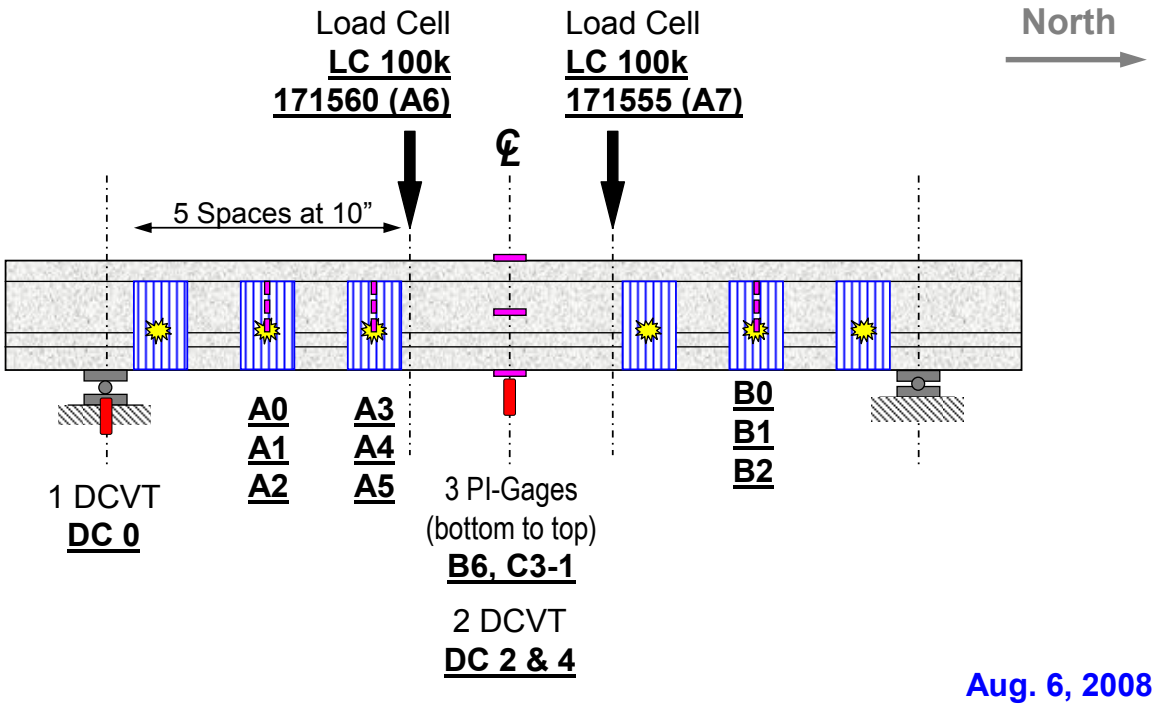

Aug. 6, 2008

Figure B.4 – B-4a Map of Sensors

www.manaraa.com

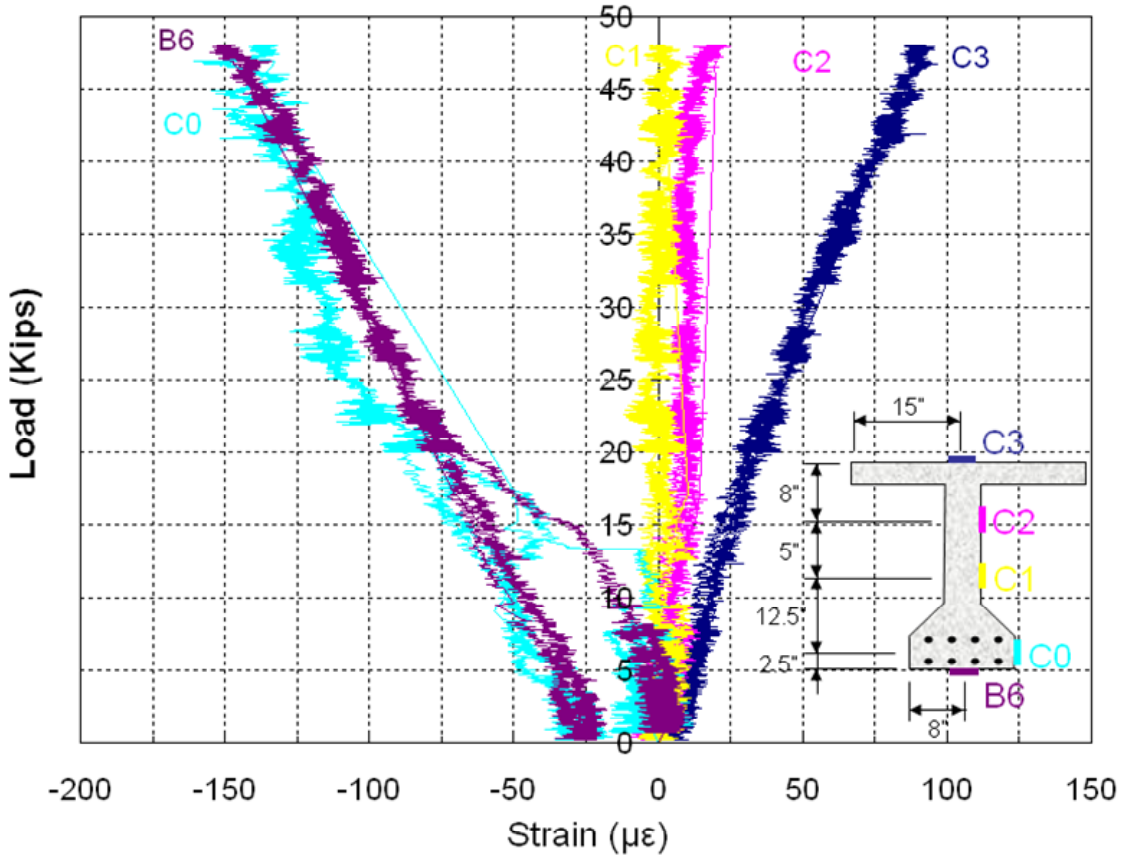

Figure B.5 – B-1a Pi-Gauge Strain Data

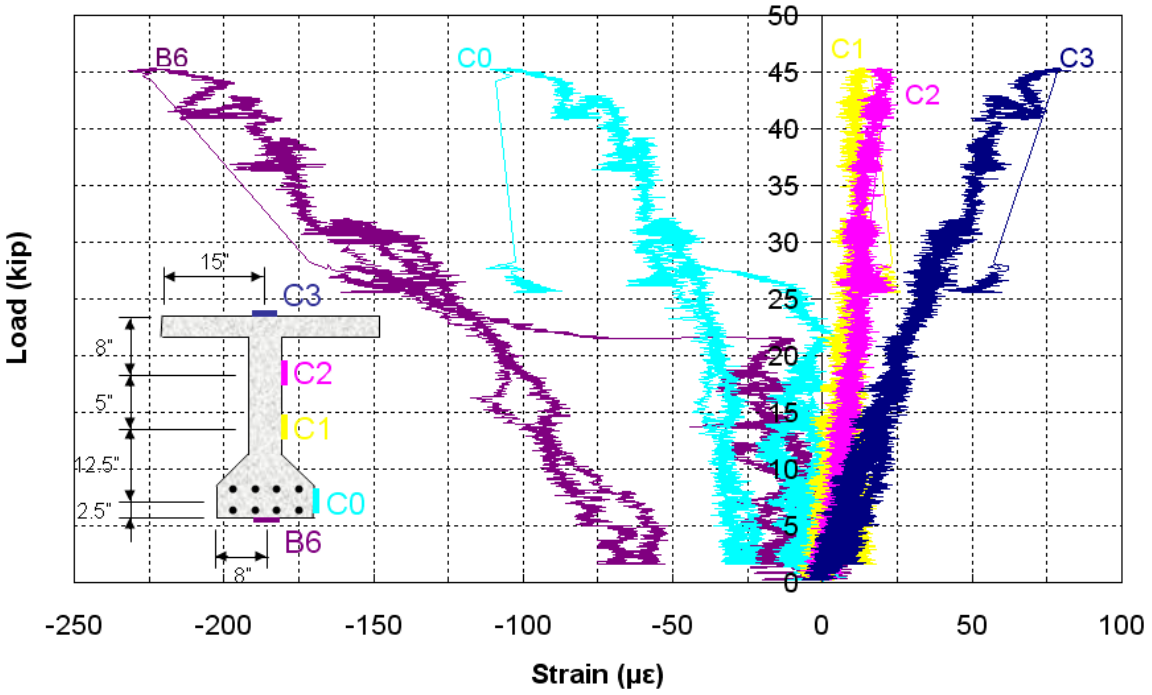

Figure B.6 – B-2a Pi-Gauge Strain Data

www.manaraa.com

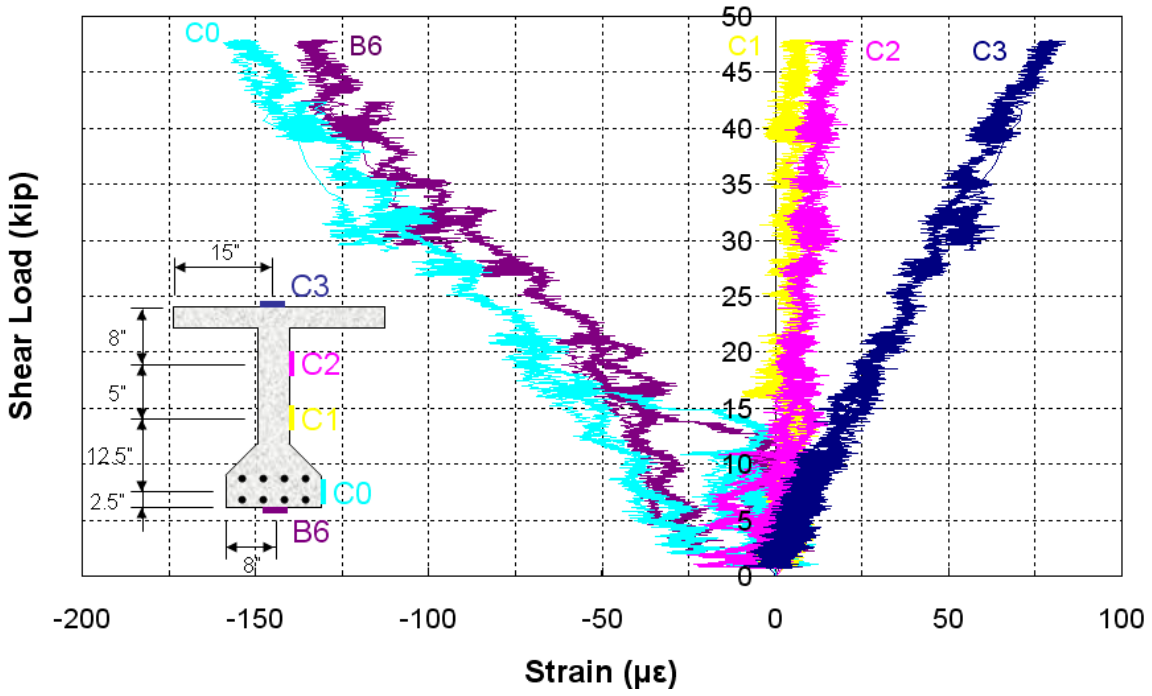

Figure B.7 – B-2b Pi-Gauge Strain Data

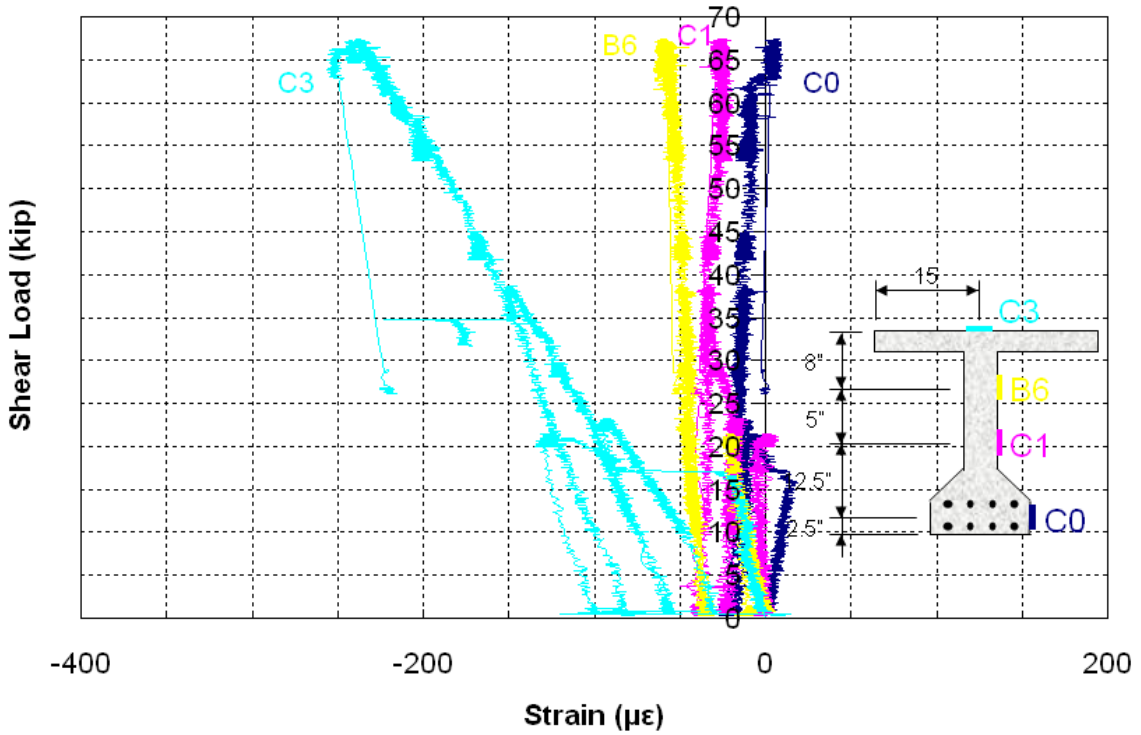

Figure B.8 – B-3a Pi-Gauge Strain Data

www.manaraa.com

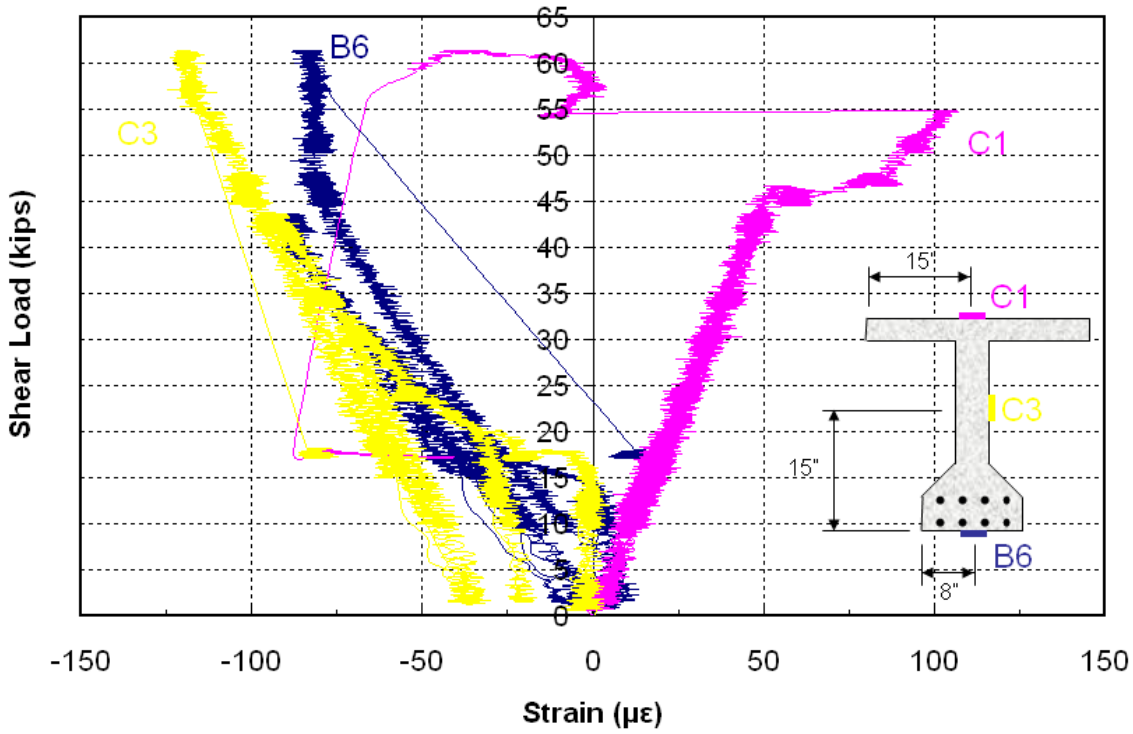

Figure B.9 – B-4a Pi-Gauge Strain Data

www.manaraa.com